

Nonequilibrium dynamical mean field theory

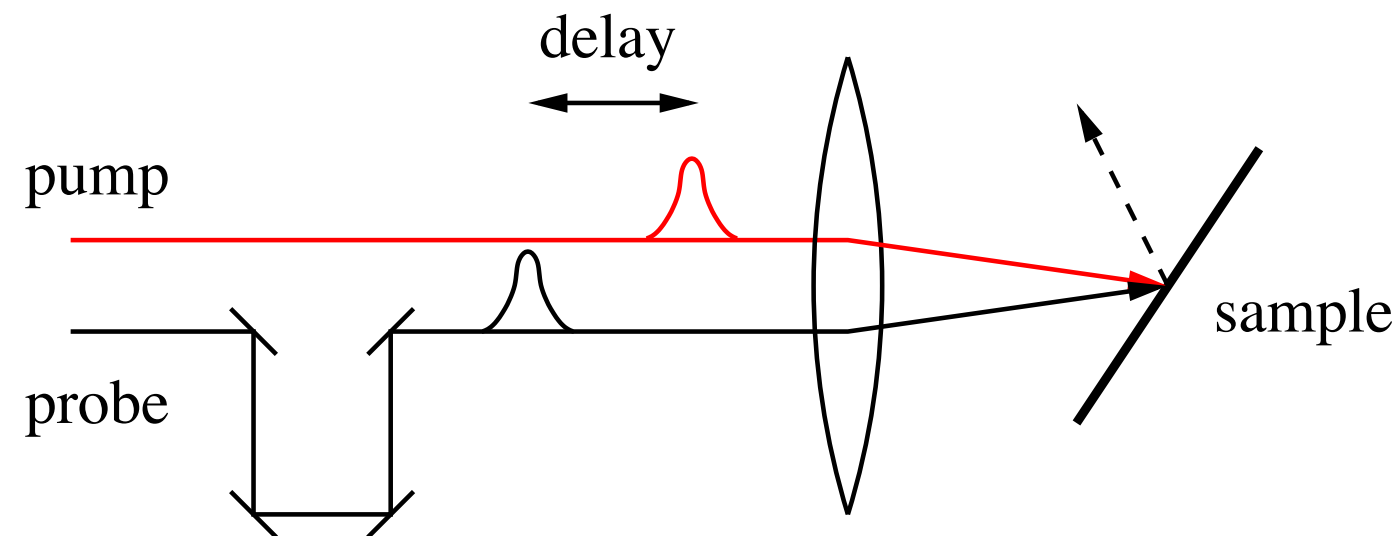
Philipp Werner

University of Fribourg

Motivation

Ultrafast pump-probe spectroscopy

- Time resolution: ~ 10 fs \rightarrow measures excitation and relaxation processes on the intrinsic timescale of the electrons



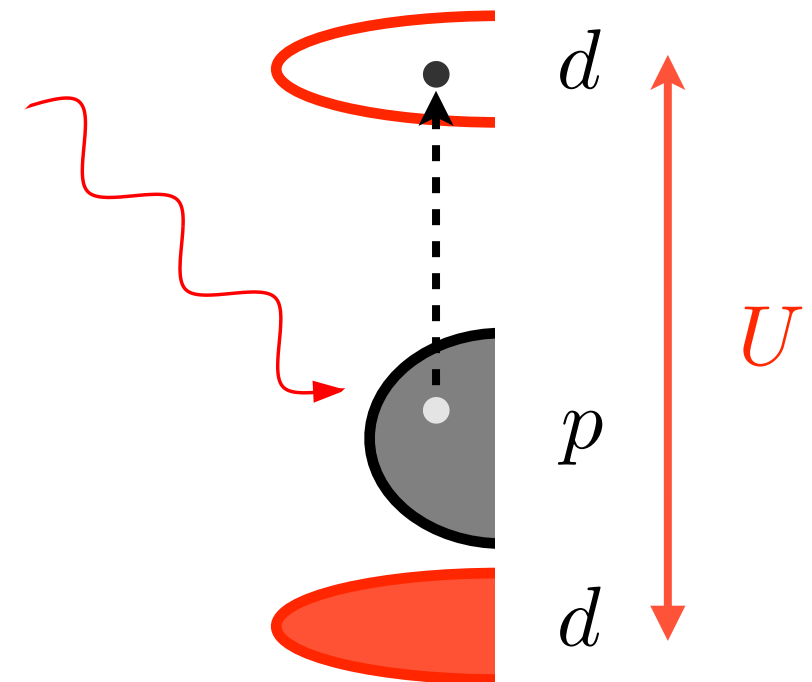
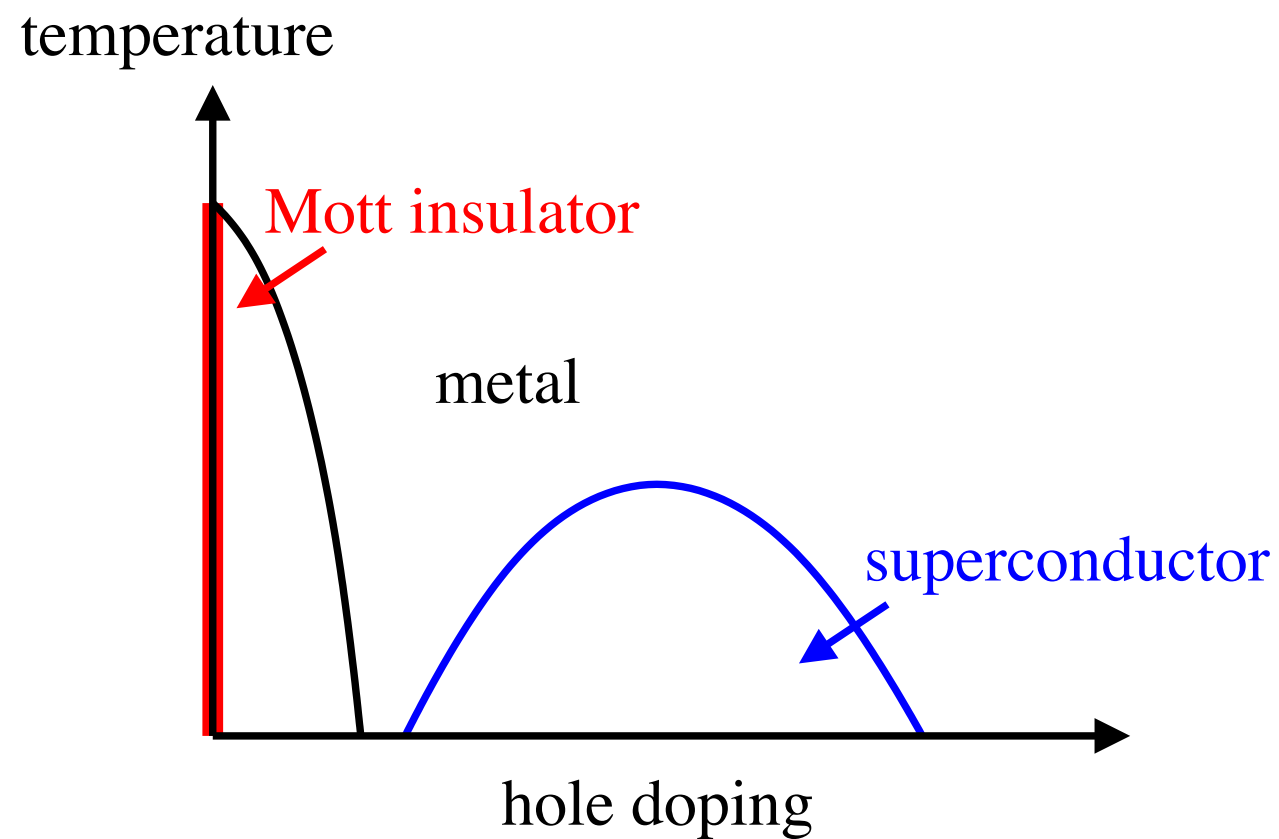
- Pump pulse drives system out of equilibrium
- Time evolution measured by subsequent probe pulses
- Possibility to “disentangle” competing effects on the time-axis

Motivation

“Tuning” of material properties by external driving

- Ultra-fast insulator-metal transition (“photo-doping”)

Iwai et al. (2003)

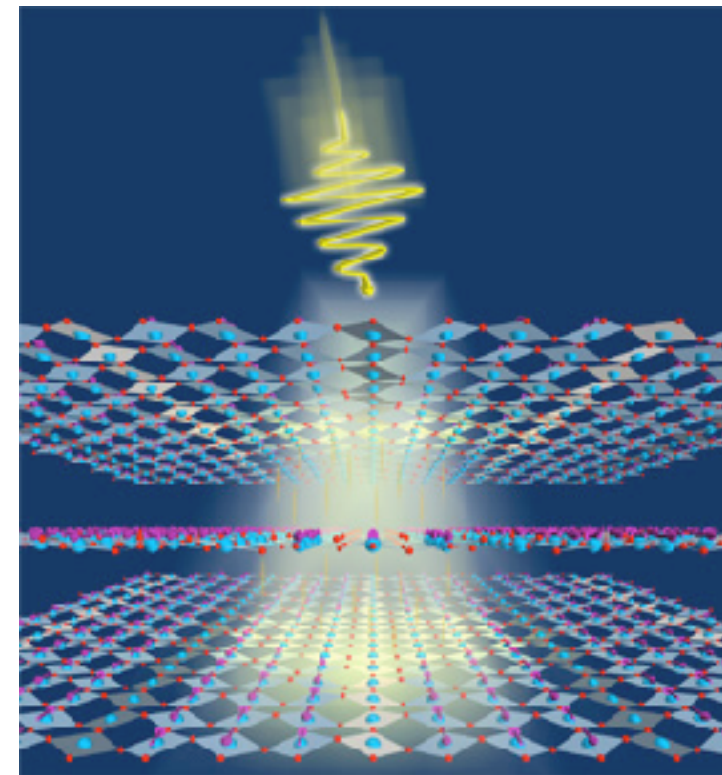
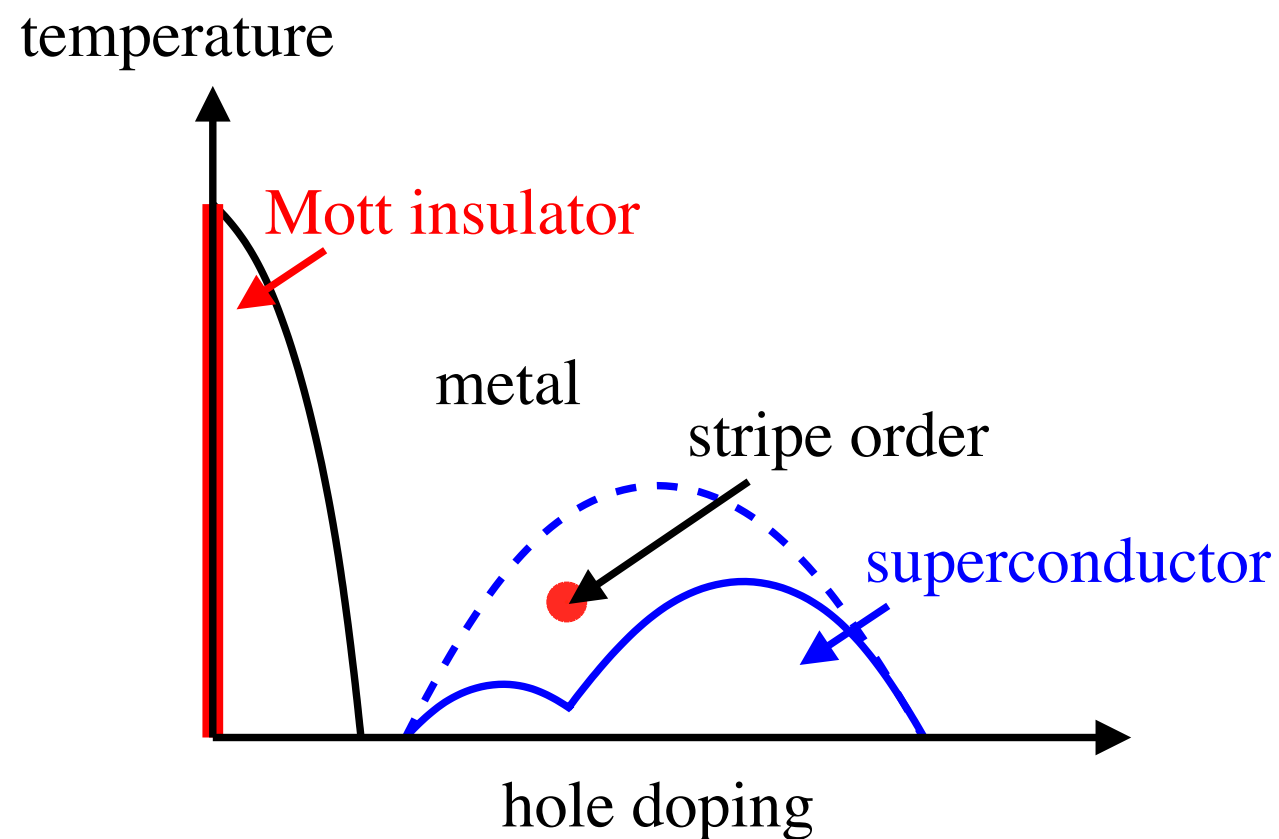


Motivation

“Tuning” of material properties by external driving

- Create long-lived transient states with novel properties
e. g. light-induced high-temperature superconductivity

Fausti et al. (2010), Kaiser et al. (2013)



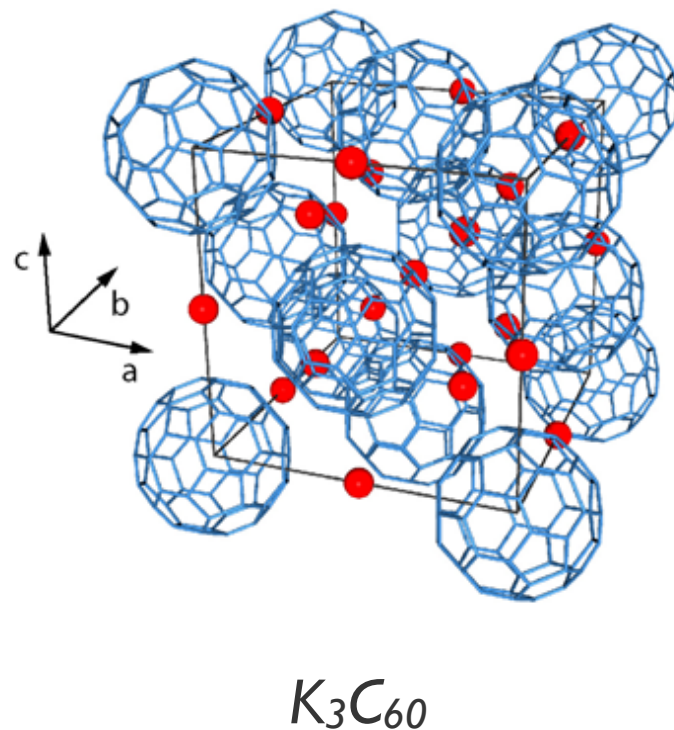
THz pulse couples to phonons

Motivation

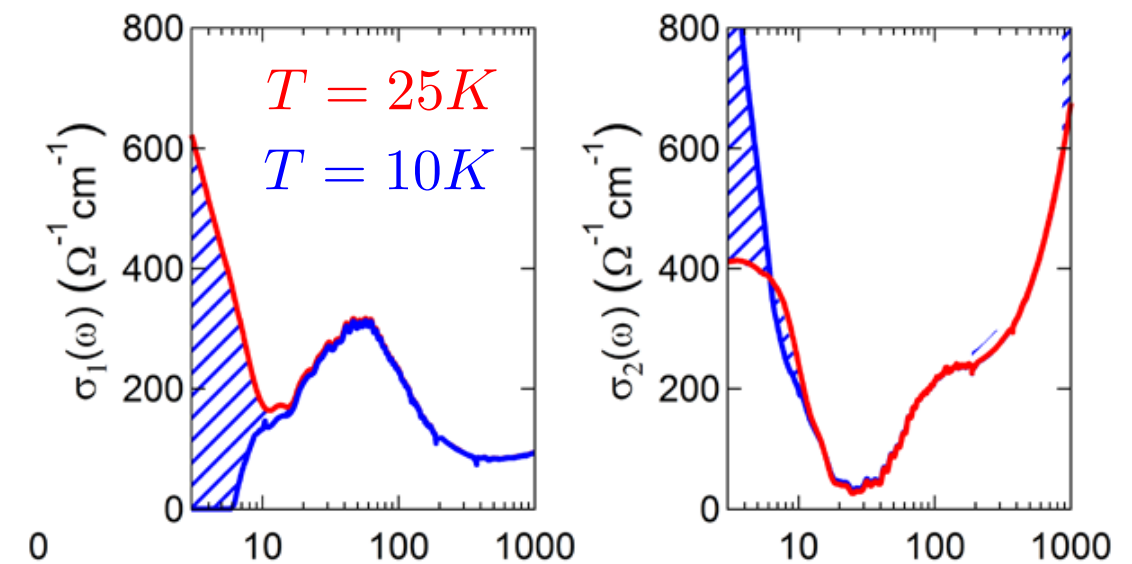
“Tuning” of material properties by external driving

- Create long-lived transient states with novel properties
e. g. light-induced high-temperature superconductivity

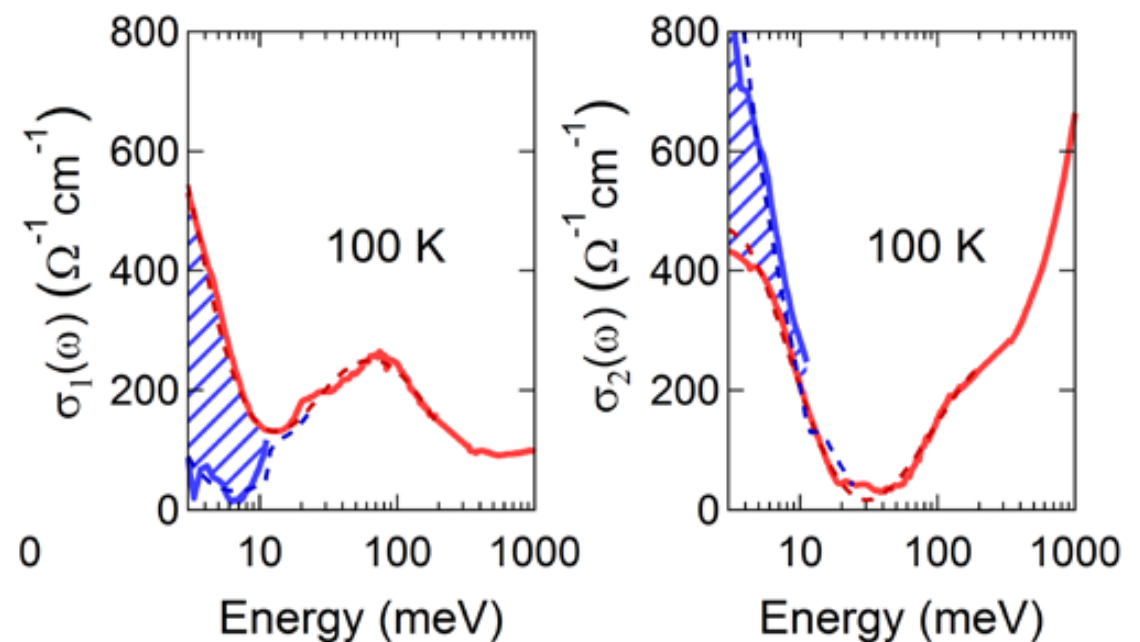
Mitrano et al. (2015)



equilibrium



driven phonons

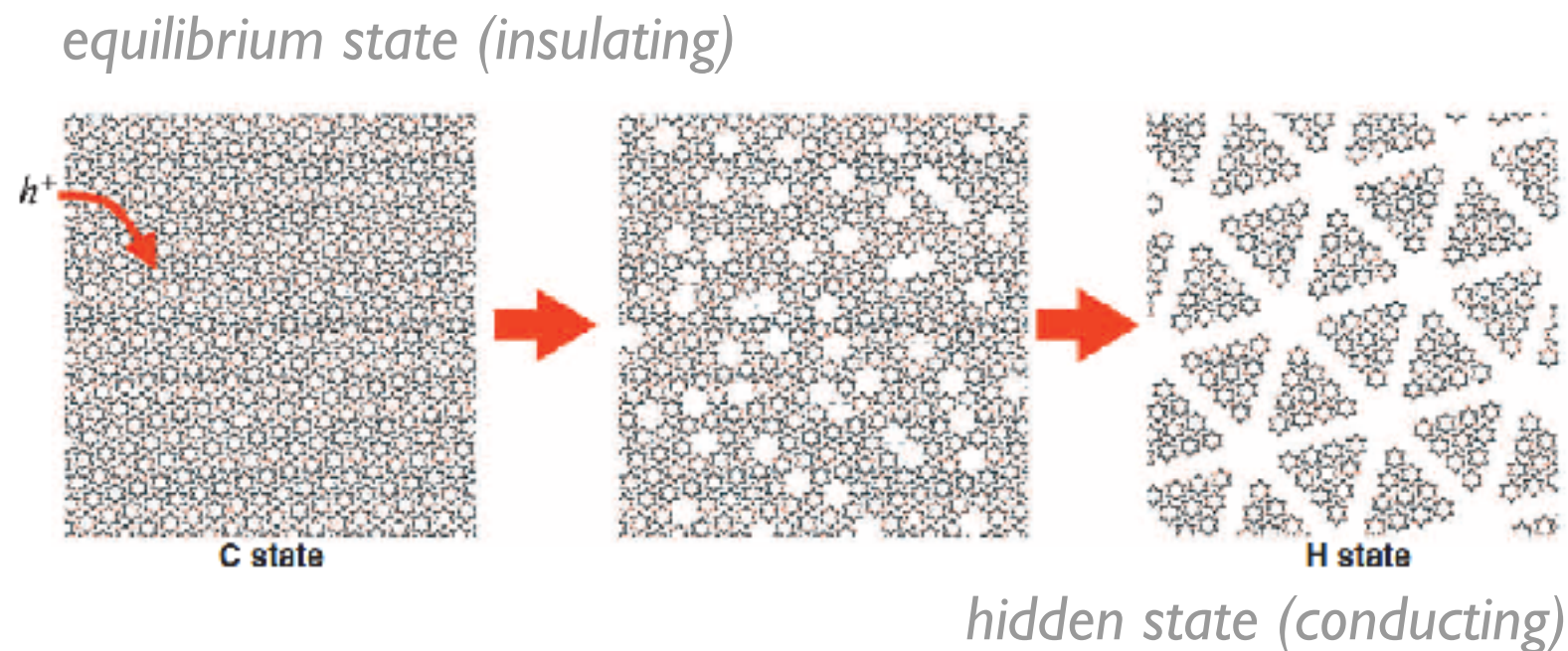


Motivation

“Tuning” of material properties by external driving

- Switching into metastable, but long-lived “hidden states”
e. g. Reversible switching of TaS_2 into / out of a metallic hidden state

Stojchevska et al. (2014)

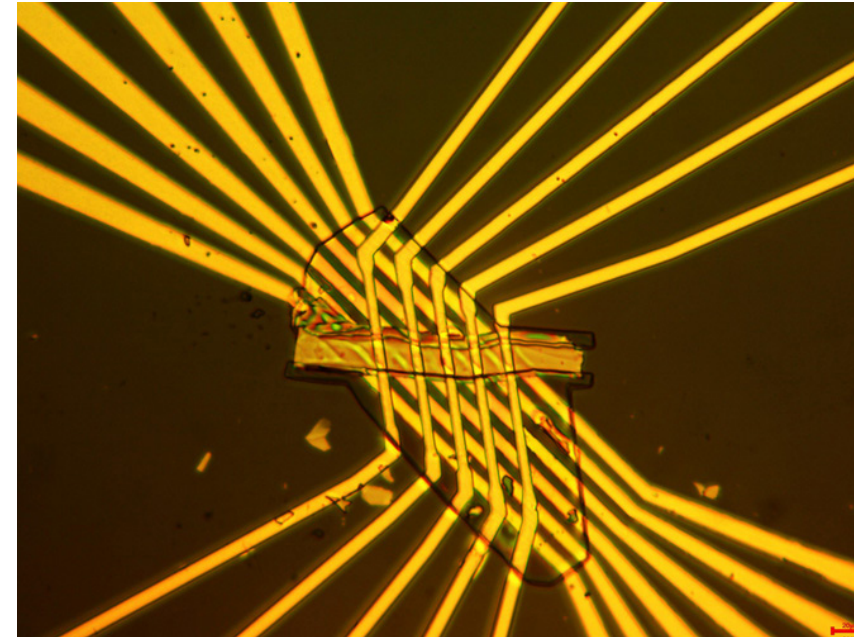
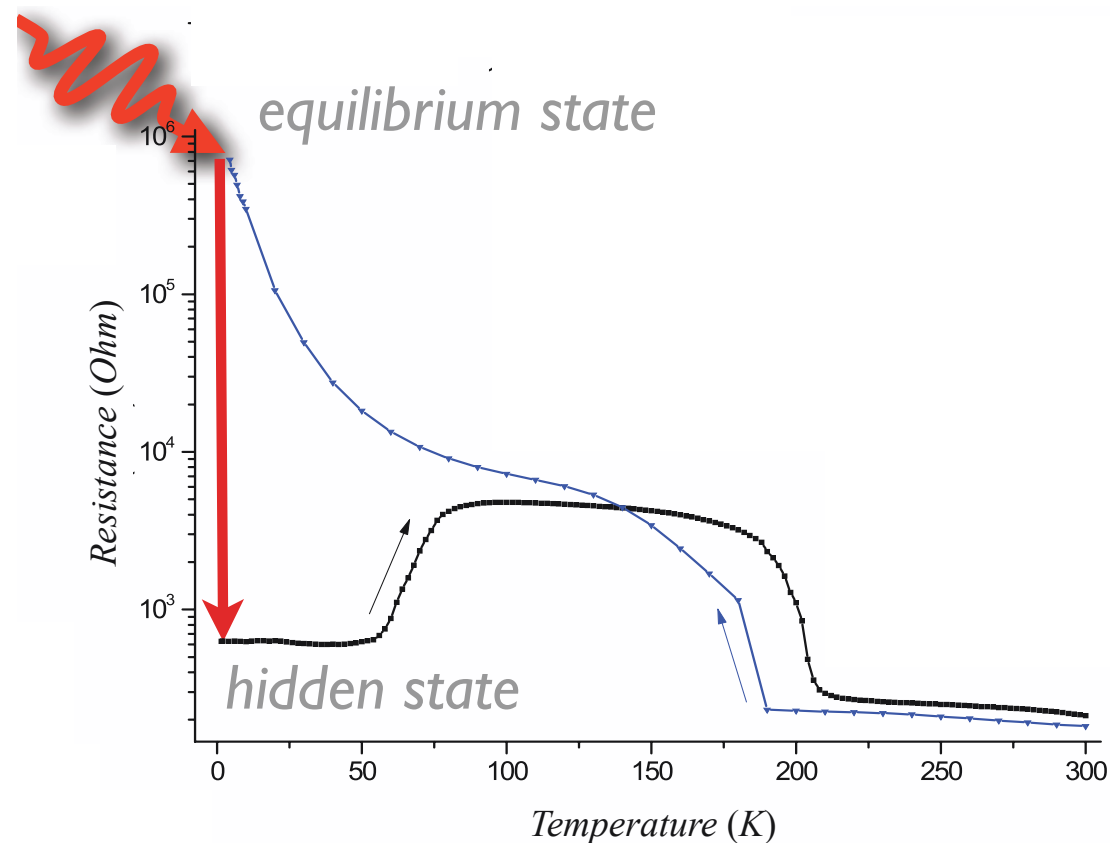


Motivation

“Tuning” of material properties by external driving

- Switching into metastable, but long-lived “hidden states”
e. g. Reversible switching of TaS_2 into / out of a metallic hidden state

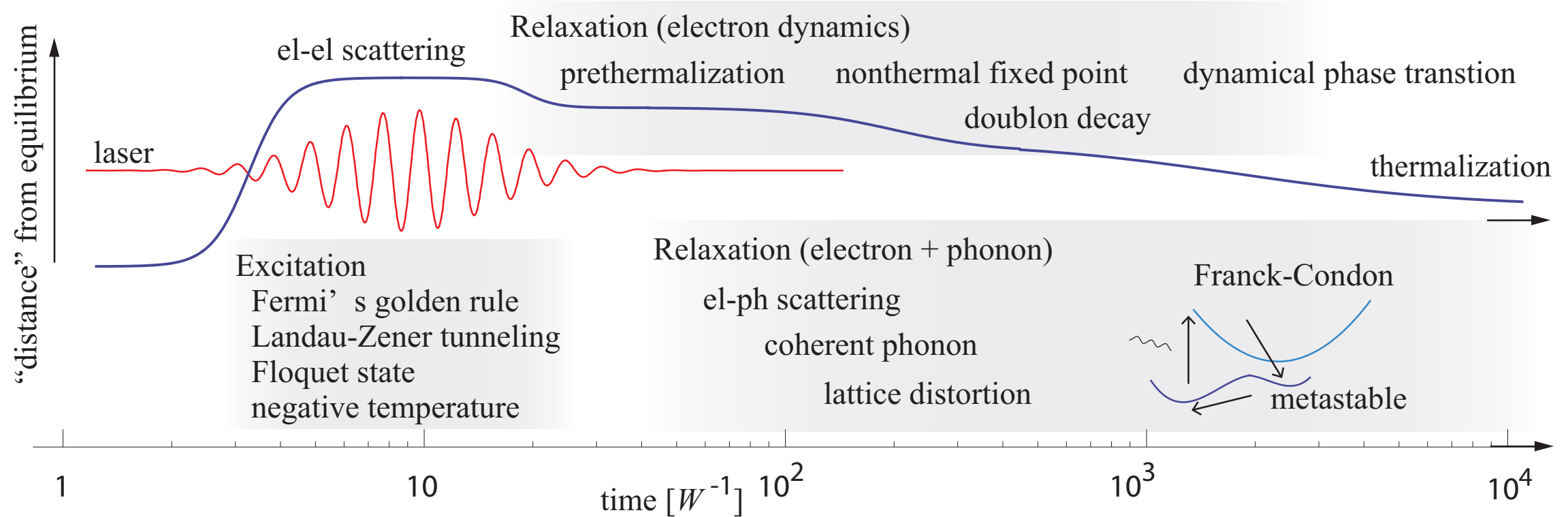
Stojchevska et al. (2014)



*memory device with unprecedented speed
and very low power consumption*

Motivation

- **Challenge for theory/numerics** *Aoki et al. (2014)*



- Strongly interacting many-particle systems
- Strong perturbations
- Different relevant time scales

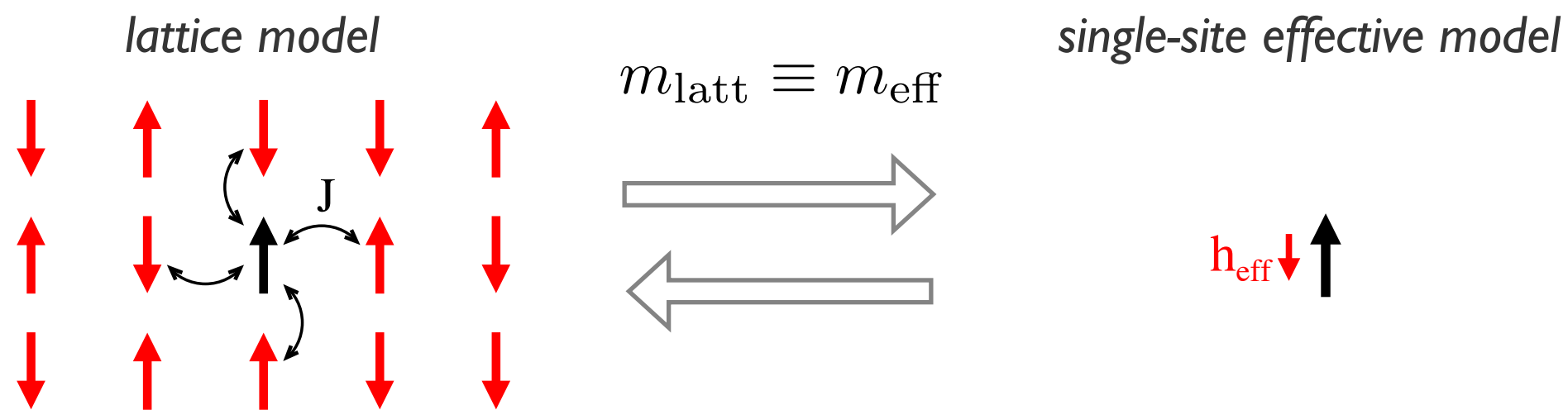
Overview

- *Dynamical mean field theory*
- *Cluster extension*
- *Nonequilibrium extension*
- *Nonequilibrium solvers and benchmarks*
- *Illustrations:*
 - *AC field quench - tuning of the interaction strength by external driving*
 - *Nonequilibrium phase transition - nonthermal fixed points*
 - *Cooling by photo-doping*

Model and method

- **Static mean field theory:** mapping to a single-site problem

Weiss (1903)

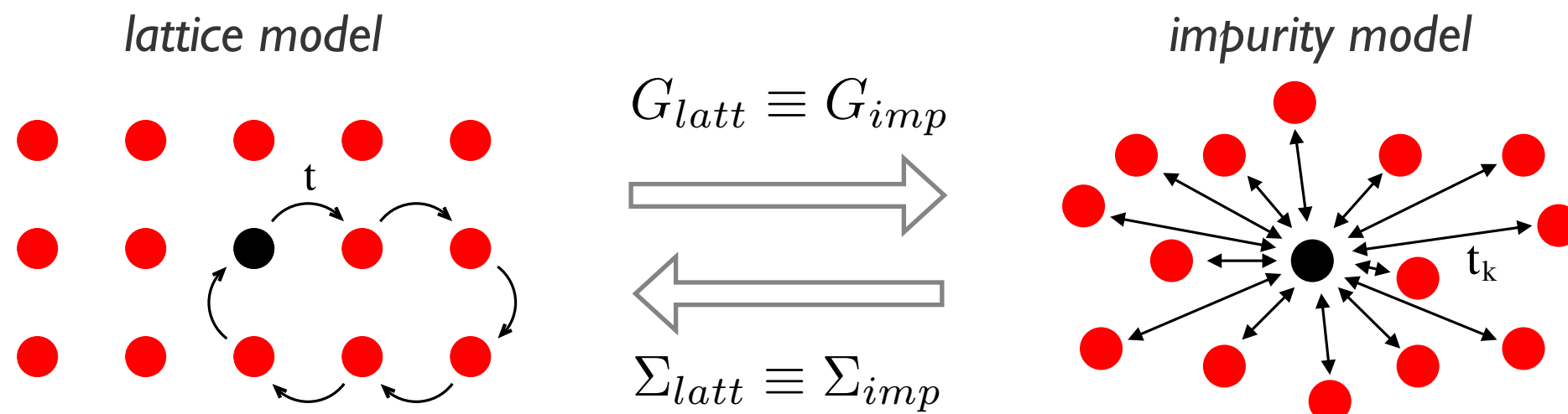


- **Effective model:** yields local observables (magnetization)
- **Parameter of the effective model (“mean field”):** optimized by requesting consistency between the lattice and single-site model

Model and method

- **Dynamical mean field theory DMFT:** mapping to an impurity problem

Georges & Kotliar (1992)

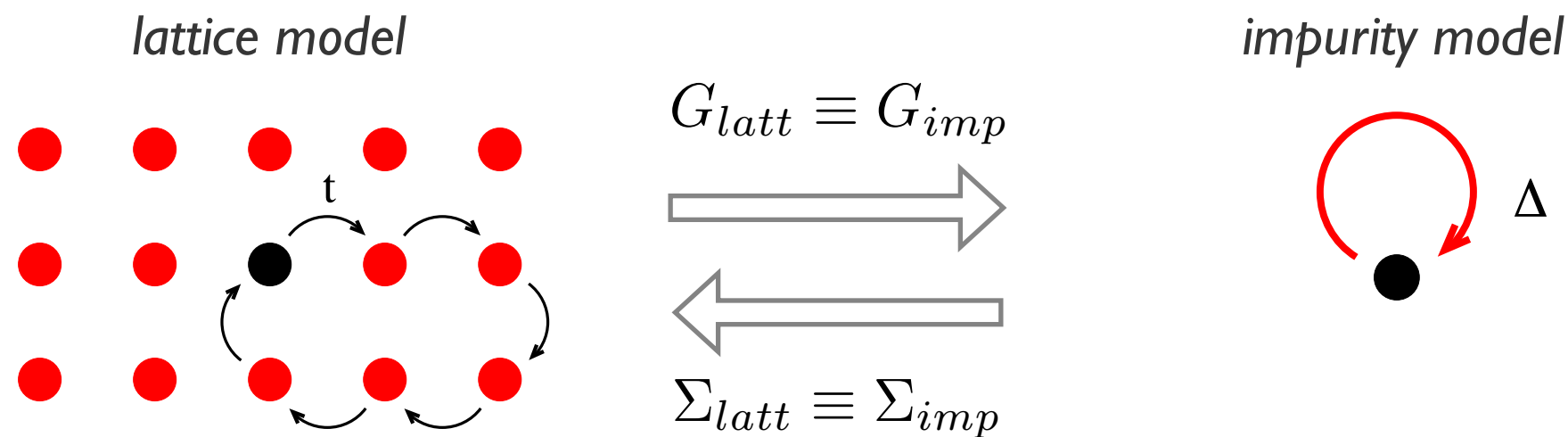


- **Impurity solver:** computes the Green's function of the correlated site
- **Bath parameters = "mean field":** optimized in such a way that the bath mimics the lattice environment

Model and method

- **Dynamical mean field theory DMFT:** mapping to an impurity problem

Georges & Kotliar (1992)



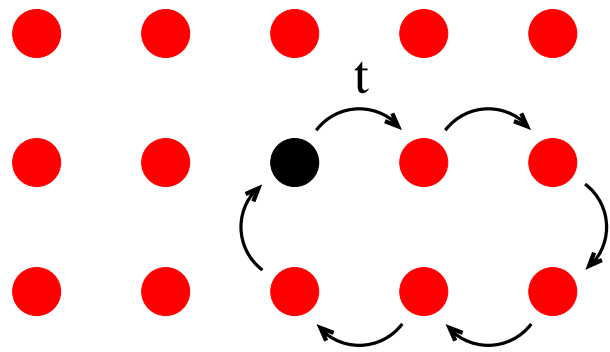
- **Impurity solver:** computes the Green's function of the correlated site
- **Bath parameters = "mean field":** optimized in such a way that the bath mimics the lattice environment

Model and method

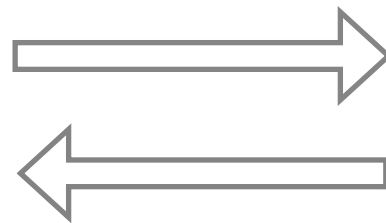
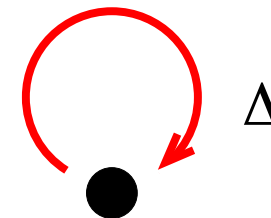
- **Dynamical mean field theory DMFT:** mapping to an impurity problem

Georges & Kotliar (1992)

lattice model



impurity model



DMFT self-consistency



$$G_{\text{loc}}^{\text{latt}} \equiv G_{\text{imp}}$$

$$S_{\text{imp}}[\Delta(i\omega_n)]$$



impurity solver

$$G_{\text{imp}}(i\omega_n), \Sigma_{\text{imp}}(i\omega_n)$$

momentum average



$$G_{\text{loc}}^{\text{latt}}(i\omega_n)$$

$$\Sigma_k^{\text{latt}} \equiv \Sigma_{\text{imp}}$$



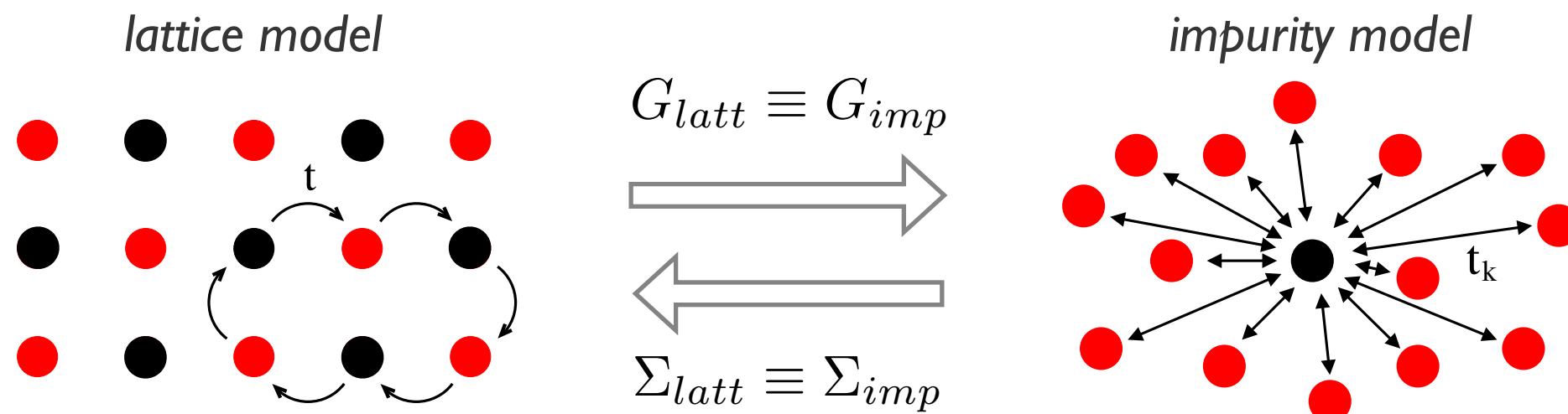
DMFT approximation

$$G_k^{\text{latt}} = \frac{1}{i\omega_n + \mu - \epsilon_k - \Sigma_k^{\text{latt}}}$$

Model and method

- **Dynamical mean field theory DMFT:** mapping to an impurity problem

Georges & Kotliar (1992)



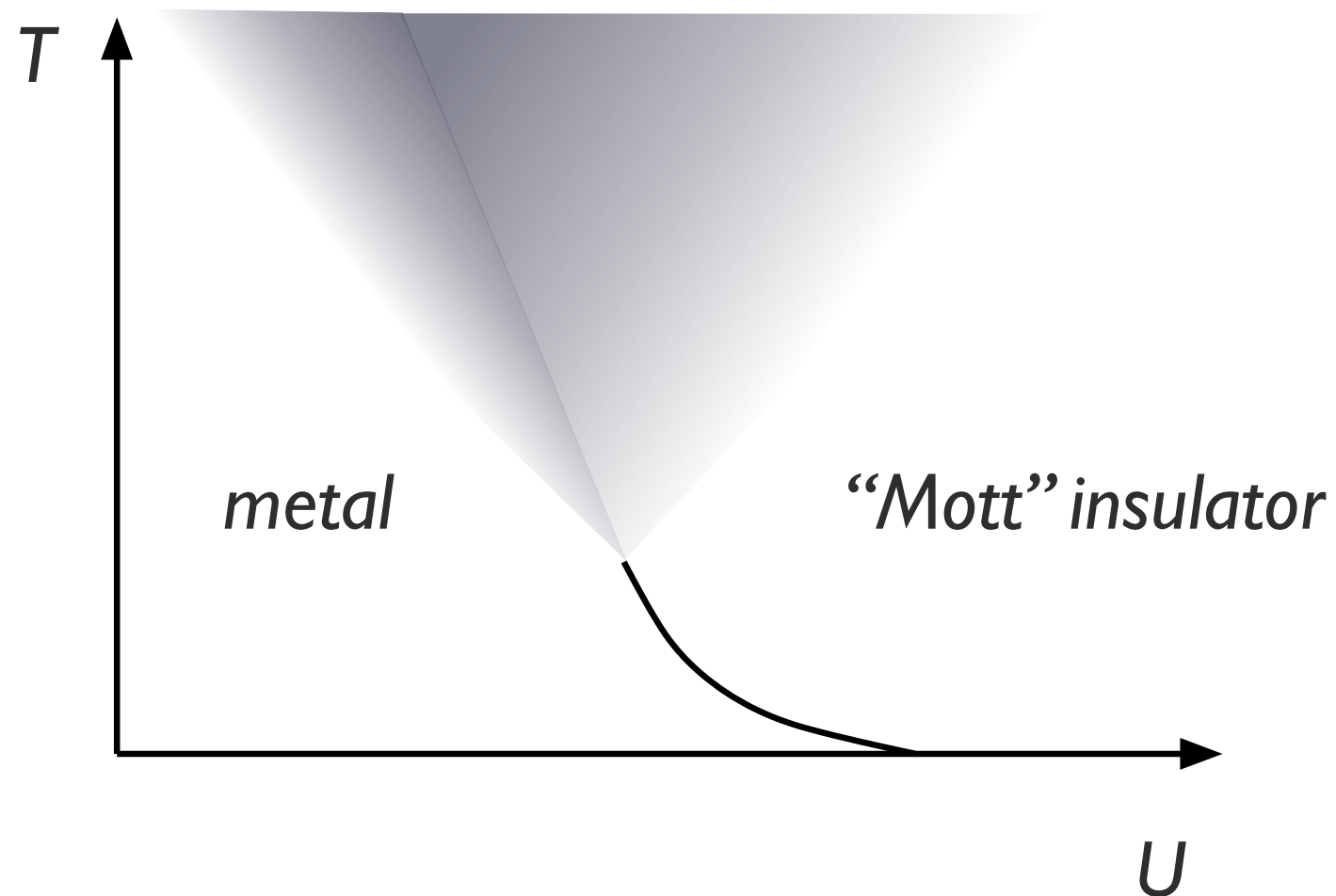
- Single-site DMFT can treat two-sublattice order (e. g. AFM)

$$\text{Bath}_{B,\sigma}[G_{A,\sigma}], \quad \text{Bath}_{A,\sigma}[G_{B,\sigma}]$$

- Pure Neel order: $\text{Bath}_{B,\sigma} = \text{Bath}_{A,\bar{\sigma}} \rightarrow \text{Bath}_{A,\bar{\sigma}}[G_{A,\sigma}]$

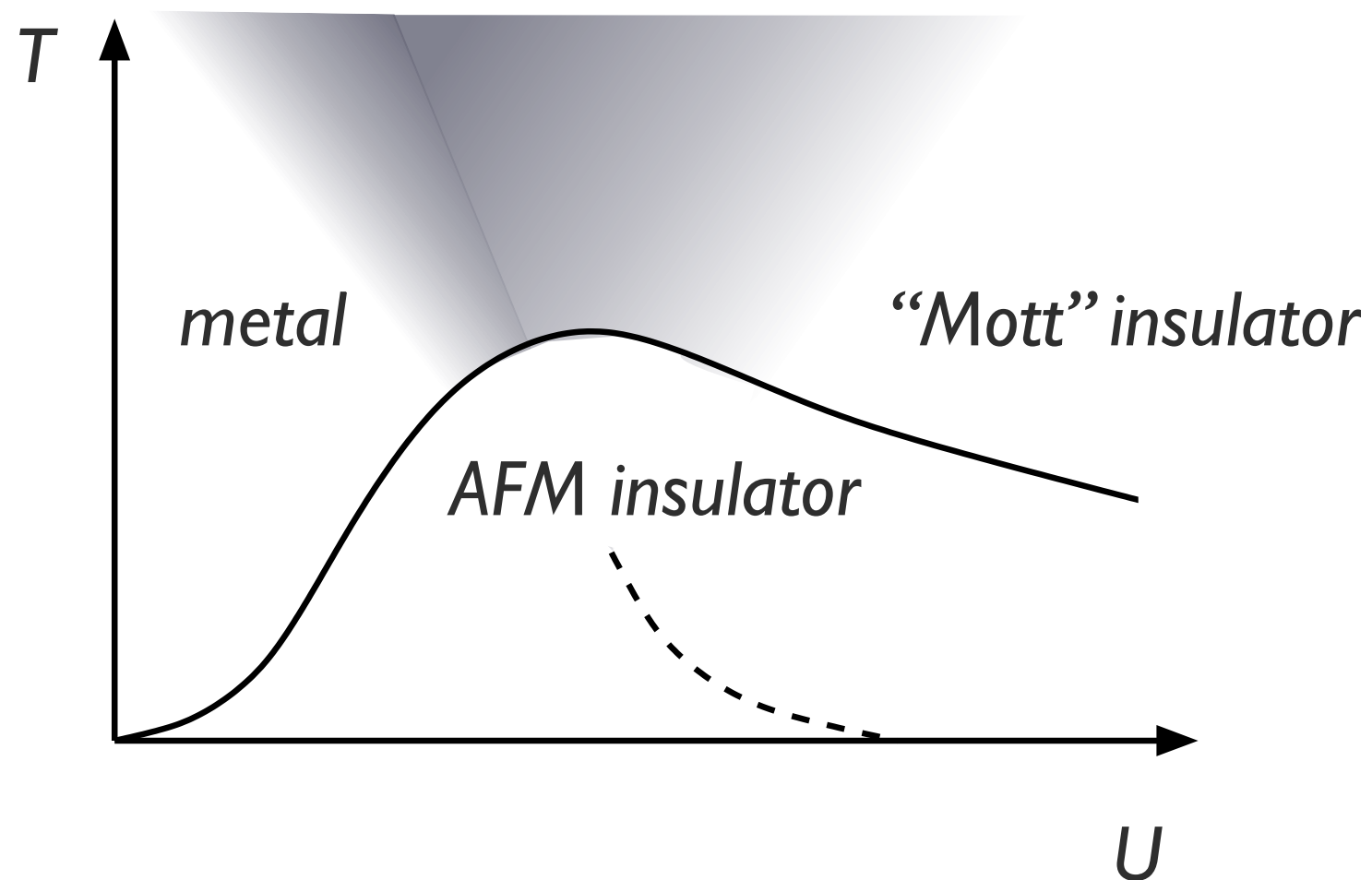
Model and method

- Equilibrium DMFT phase diagram (half-filling)
- Paramagnetic calculation: Metal - Mott insulator transition at low T
- Smooth crossover at high T



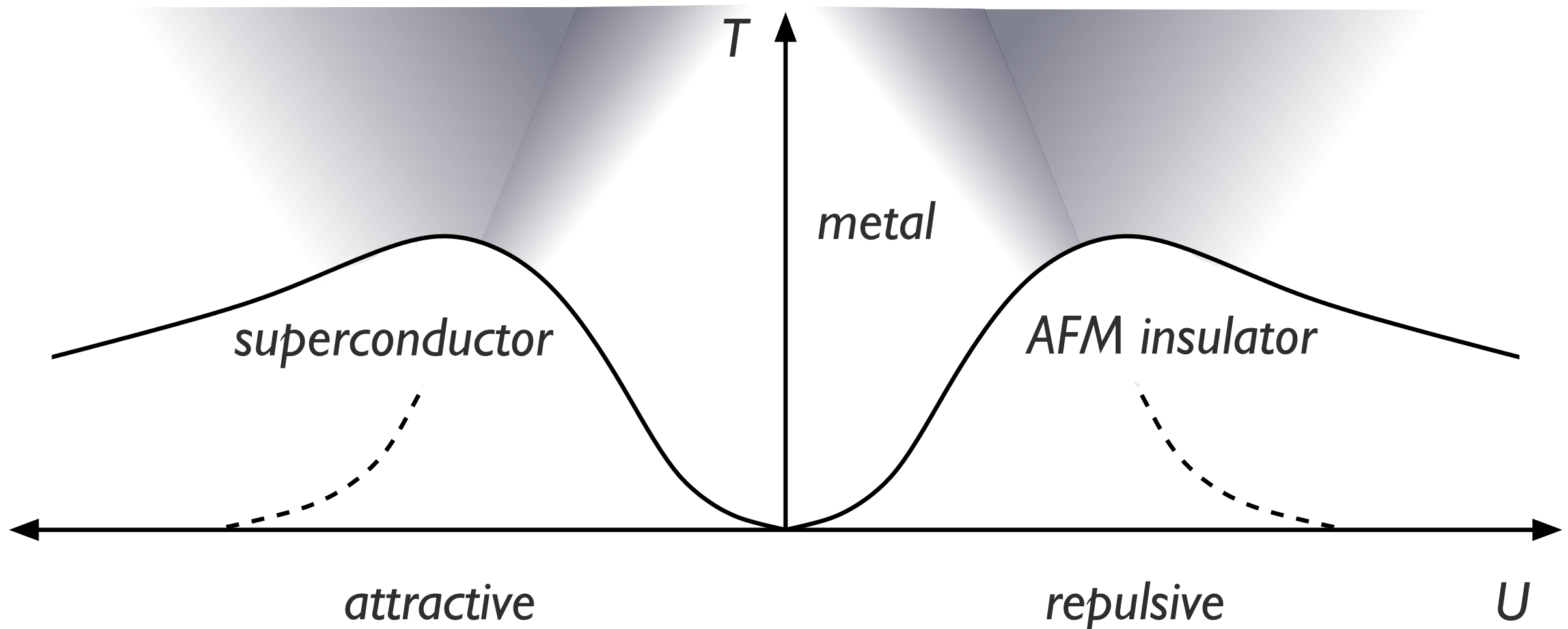
Model and method

- Equilibrium DMFT phase diagram (half-filling)
- With 2-sublattice order: Antiferromagnetic insulator at low T
- Smooth crossover at high T



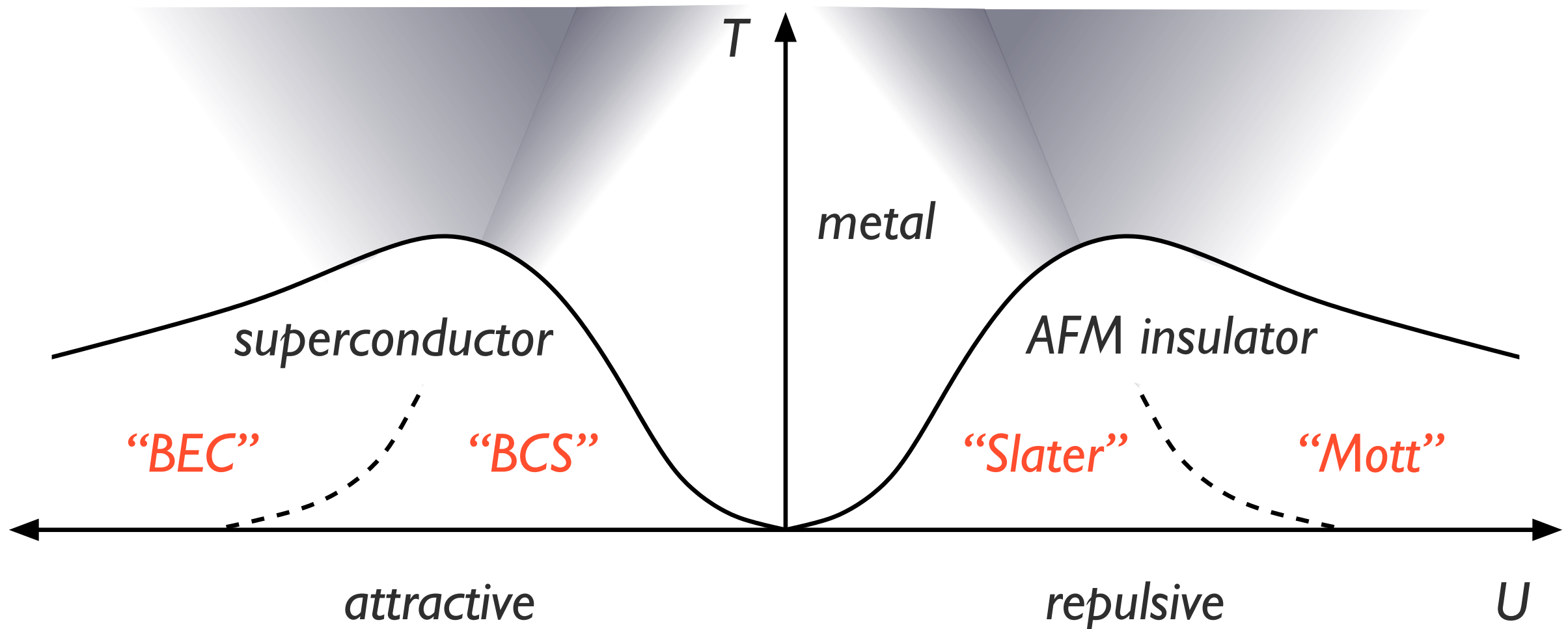
Model and method

- **Equilibrium DMFT phase diagram (half-filling)**
- Transformation $c_{i\uparrow} \rightarrow c_{i\uparrow}^\dagger$ ($i \in A$), $c_{i\uparrow} \rightarrow -c_{i\uparrow}^\dagger$ ($i \in B$)
maps repulsive model onto attractive model



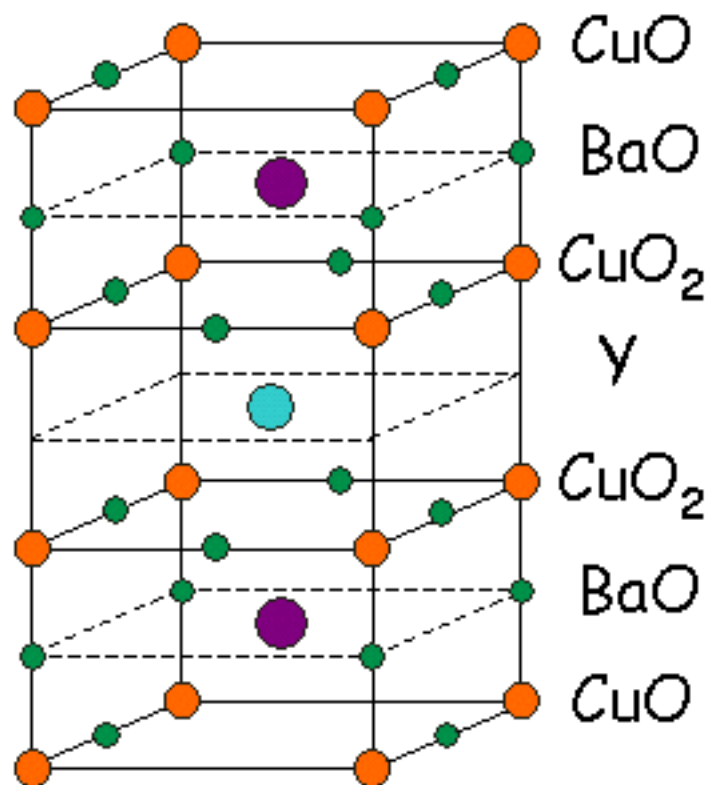
Model and method

- Equilibrium DMFT phase diagram
- Half-filling: transformation $c_{i\uparrow} \rightarrow c_{i\uparrow}^\dagger$ ($i \in A$), $c_{i\uparrow} \rightarrow -c_{i\uparrow}^\dagger$ ($i \in B$)
maps repulsive model onto attractive model

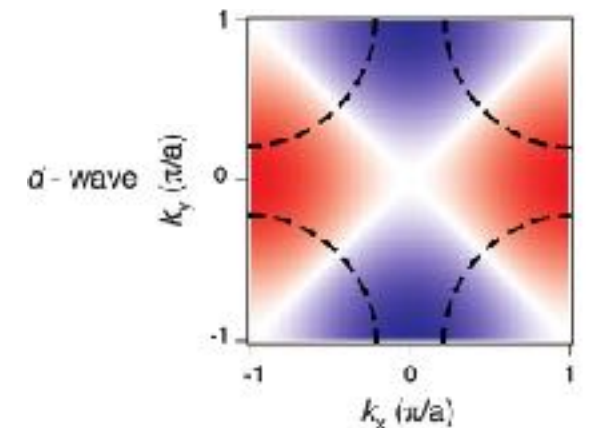
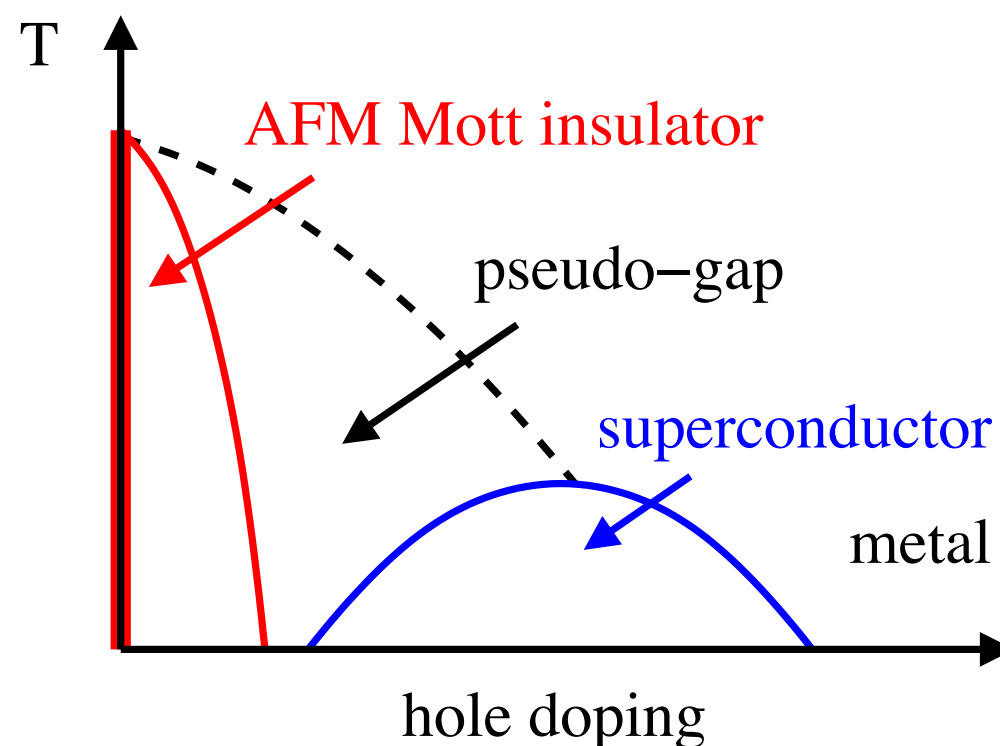


Cluster extension

- **Low-dimensional systems**
- DMFT is exact in $d = \infty$ Metzner & Vollhardt (1989)
- Neglect of spatial fluctuations problematic in $d < 3$
- $d = 2$ Hubbard model is believed to describe the physics of high- T_c (cuprate) superconductors



to describe the physics of the cuprates, we need a cluster extension of DMFT, with at least 4 sites

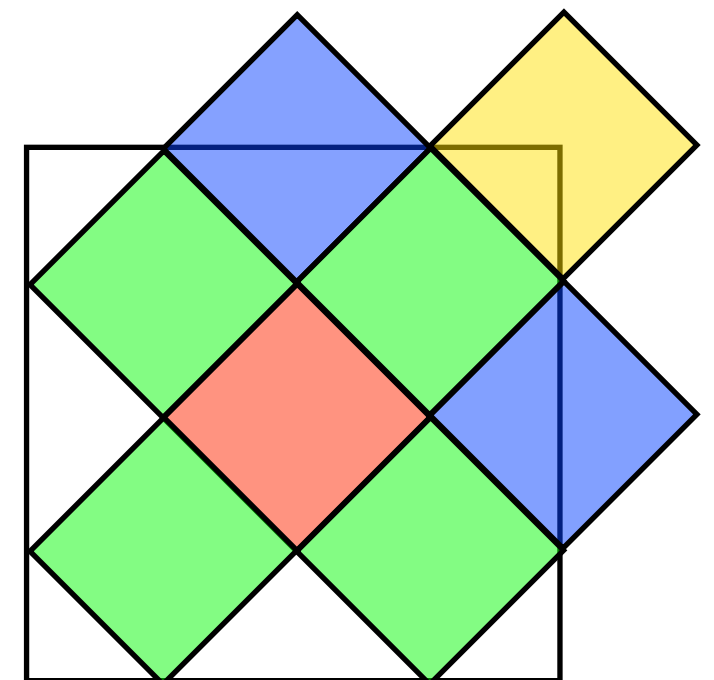
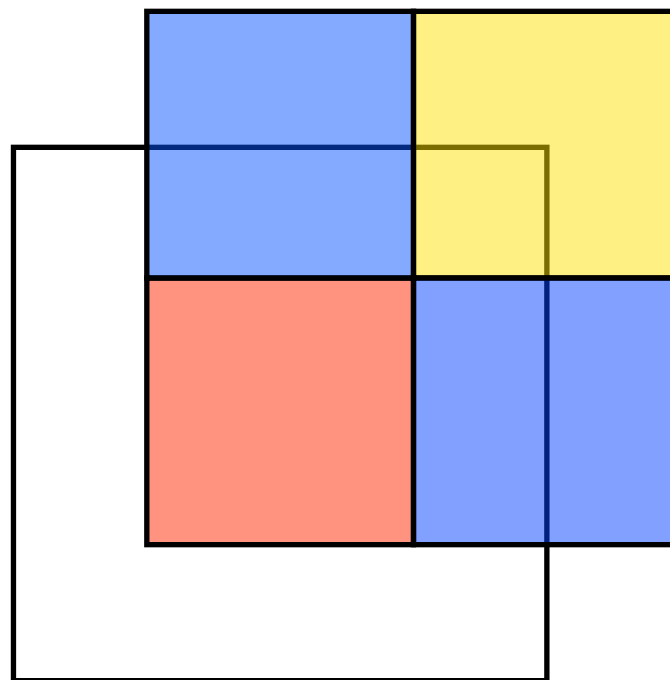
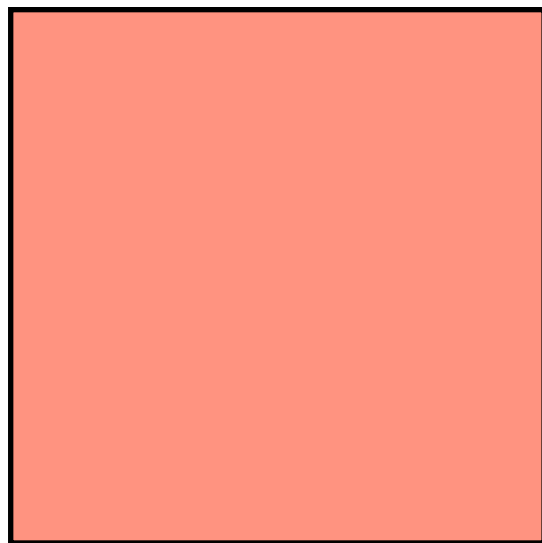


Cluster extension

- **Low-dimensional systems**
- Cluster DMFT self-consistently embeds a cluster of N_c sites into a fermionic bath *Hettler, Prushke, Krishnamurthy & Jarrell (1998)*
- If cluster is periodized: coarse-graining of the momentum-dependence

$$\Sigma(k, \omega) = \sum_a \phi_a(k) \Sigma_a(\omega)$$

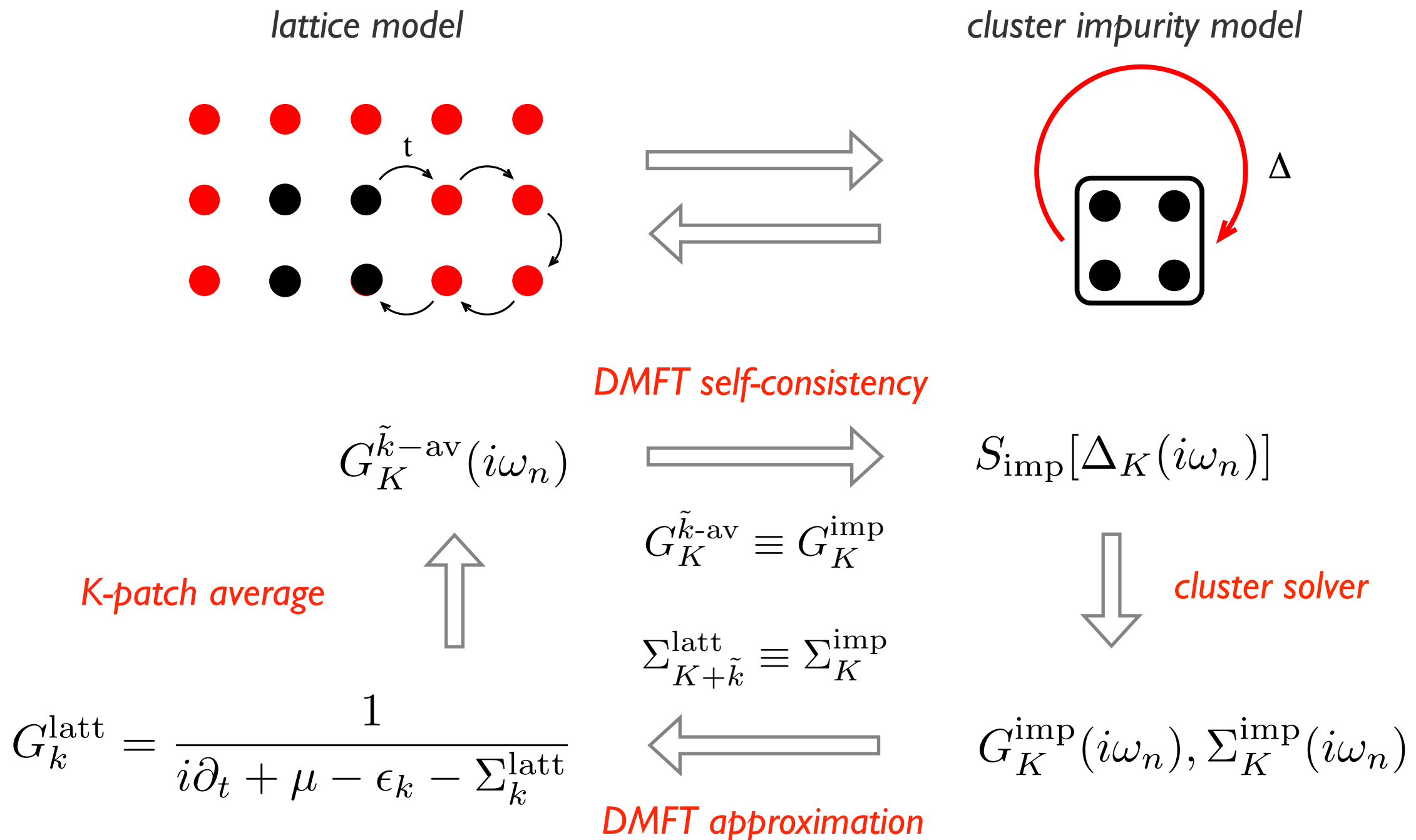
- “Tiling” of the Brillouin zone



Cluster extension

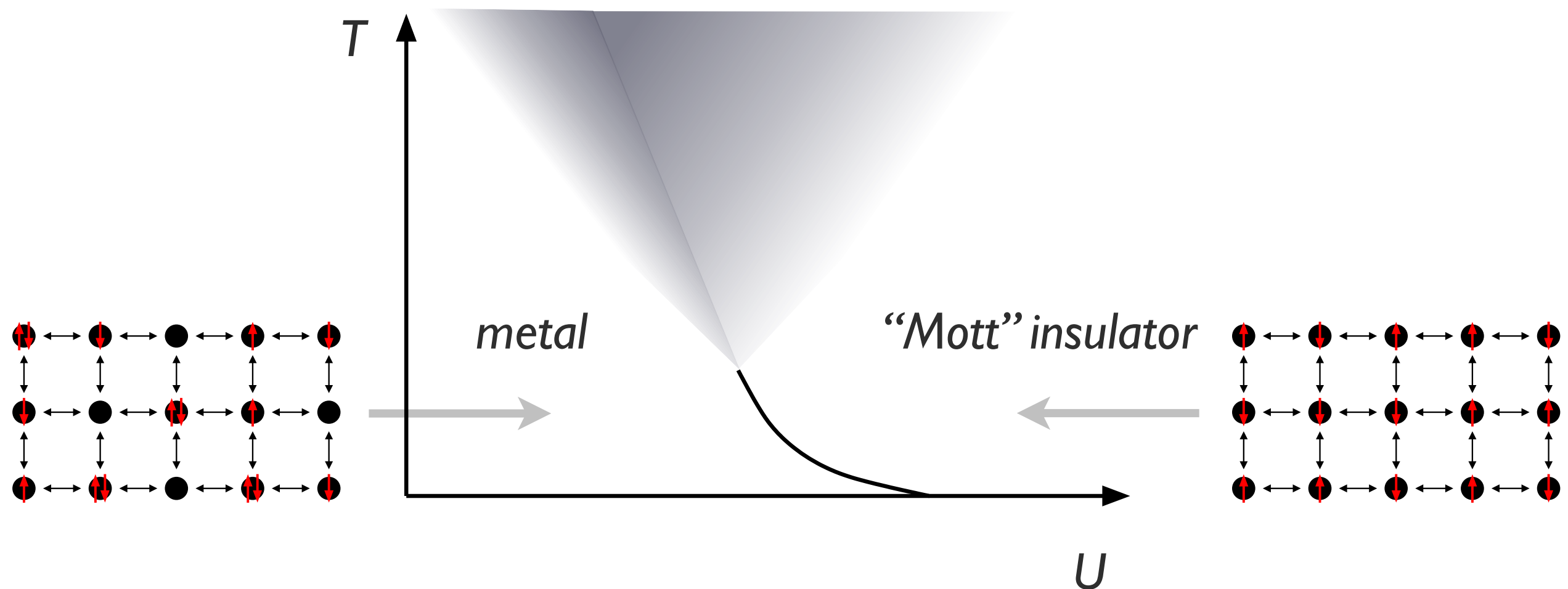
- **Dynamical cluster approach:** mapping to an impurity cluster

Hettler et al. (1998)



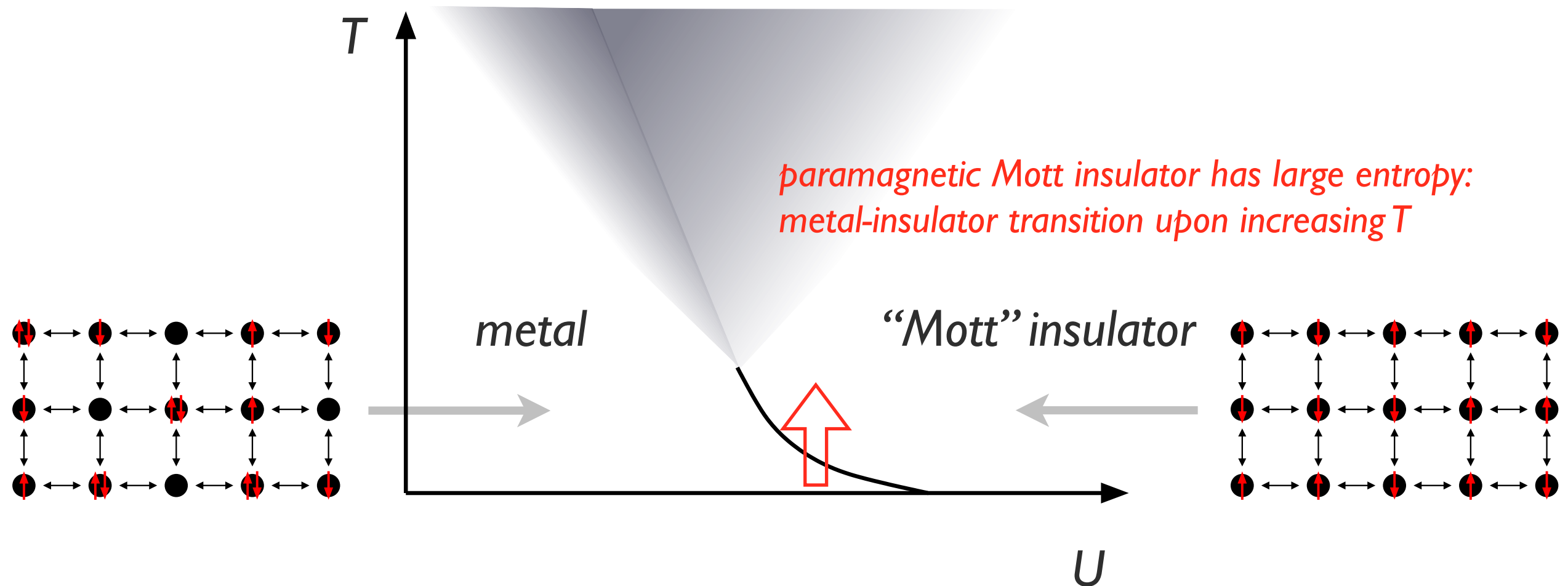
Cluster extension

- Equilibrium DMFT phase diagram (half-filling)
- Paramagnetic calculation: Metal - Mott insulator transition at low T
- Smooth crossover at high T



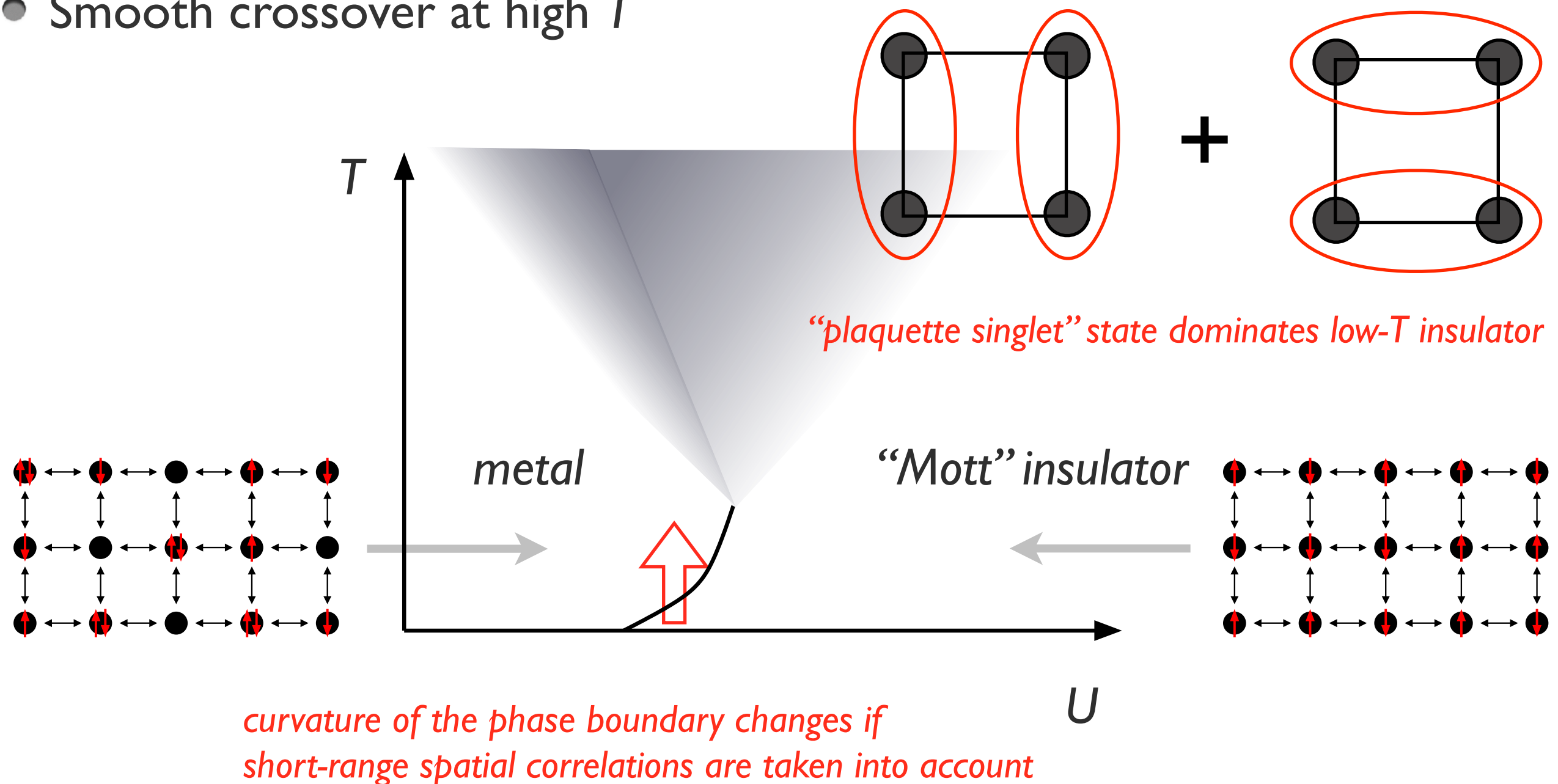
Cluster extension

- Equilibrium DMFT phase diagram (half-filling)
- Paramagnetic calculation: Metal - Mott insulator transition at low T
- Smooth crossover at high T



Cluster extension

- Equilibrium cluster DMFT phase diagram (half-filling)
- Paramagnetic calculation: Metal - Mott insulator transition at low T
- Smooth crossover at high T



Nonequilibrium extension

- **Kadanoff-Baym contour**

- Initial state described by the density matrix $\rho(0) = \frac{1}{Z} e^{-\beta H(0)}$

- State at time t described by $\rho(t) = U(t, 0) \rho(0) U(0, t)$

$$U(t, t') = \begin{cases} \mathcal{T} \exp \left(-i \int_{t'}^t d\bar{t} H(\bar{t}) \right) & t > t' \\ \tilde{\mathcal{T}} \exp \left(-i \int_{t'}^t d\bar{t} H(\bar{t}) \right) & t < t' \end{cases}$$

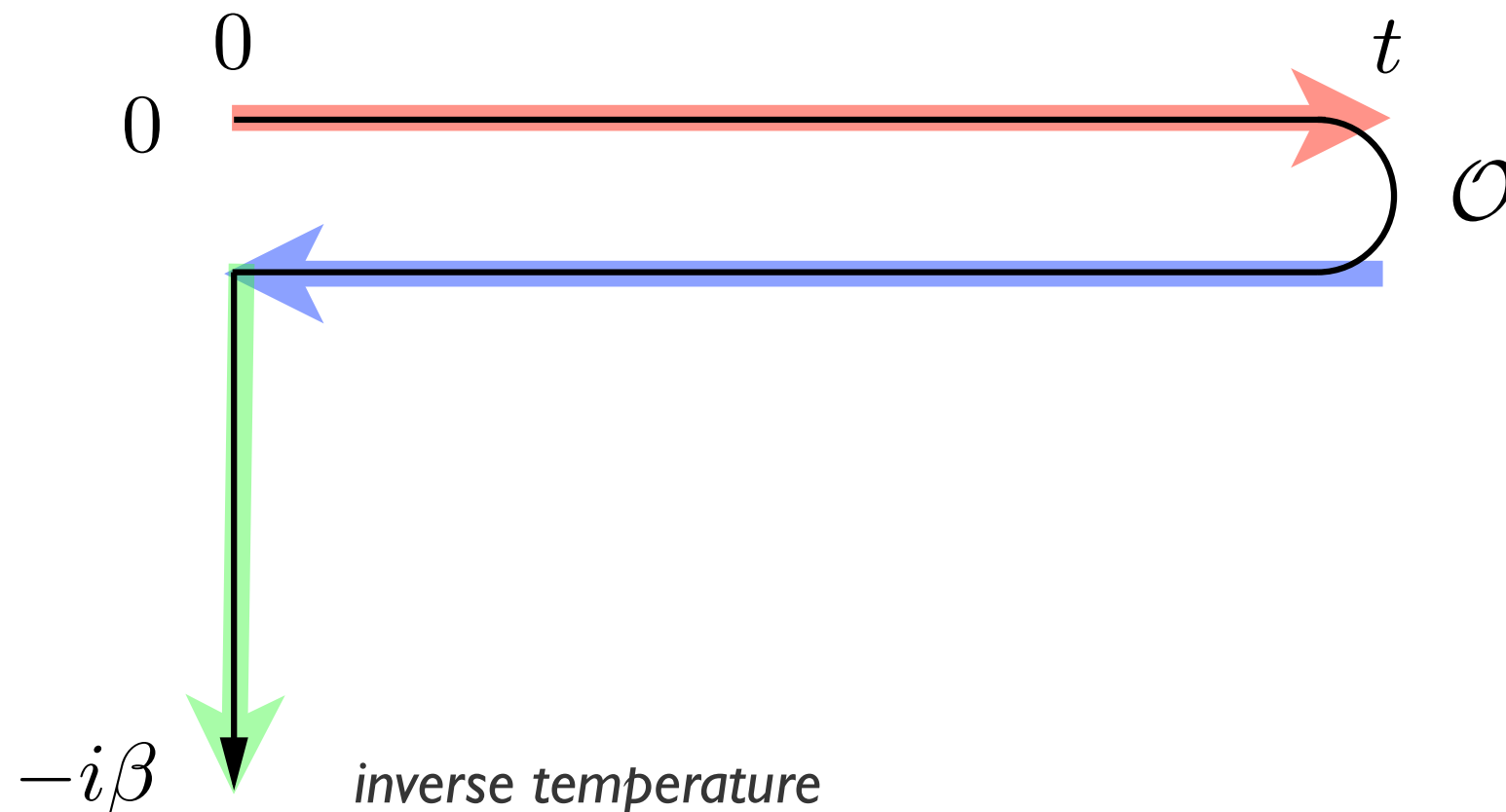
- Time dependent expectation value of observable \mathcal{O}

$$\langle \mathcal{O}(t) \rangle = \text{Tr} [\rho(t) \mathcal{O}] = \text{Tr} [U(t, 0) \rho(0) U(0, t) \mathcal{O}]$$

Nonequilibrium extension

- **Kadanoff-Baym contour**
- Express $\rho(0)$ as time-propagation along an imaginary time branch

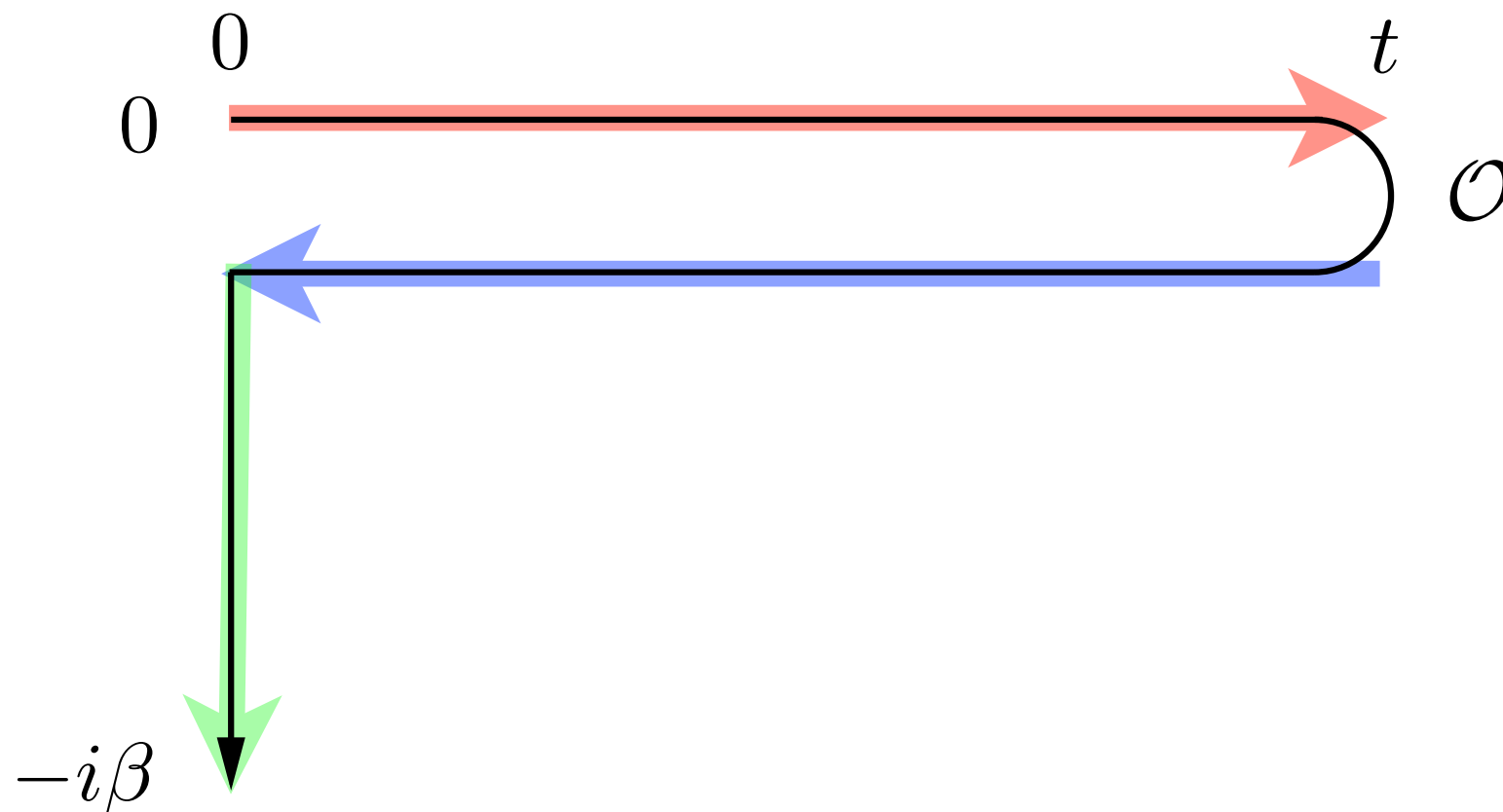
$$\begin{aligned}\langle \mathcal{O} \rangle(t) &= \text{Tr} \left[\frac{1}{Z} e^{-\beta H(0)} U(0, t) \mathcal{O} U(t, 0) \right] \\ &= \text{Tr} \left[\frac{1}{Z} \left(\mathcal{T}_\tau e^{-\int_0^\beta d\tau H(\tau)} \right) \left(\tilde{\mathcal{T}} e^{i \int_0^t ds H(s)} \right) \mathcal{O} \left(\mathcal{T} e^{-i \int_0^t ds H(s)} \right) \right]\end{aligned}$$



Nonequilibrium extension

- **Kadanoff-Baym contour**
- Define contour ordering $\mathcal{T}_{\mathcal{C}}$ on the contour $\mathcal{C} : 0 \rightarrow t \rightarrow 0 \rightarrow -i\beta$

$$\langle \mathcal{O}(t) \rangle = \frac{1}{Z} \text{Tr} \left[\mathcal{T}_{\mathcal{C}} e^{-i \int_{\mathcal{C}} ds H(s)} \mathcal{O}(t) \right]$$



Nonequilibrium extension

- **Kadanoff-Baym contour**
- Define contour ordering \mathcal{T}_C on the contour $C : 0 \rightarrow t \rightarrow 0 \rightarrow -i\beta$

$$\langle \mathcal{O}(t) \rangle = \frac{1}{Z} \text{Tr} \left[\mathcal{T}_C e^{-i \int_C ds H(s)} \mathcal{O}(t) \right]$$

- Contour-ordered formalism can also be applied to 2-point functions

$$\langle \mathcal{T}_C \mathcal{A}(t) \mathcal{B}(t') \rangle \equiv \frac{1}{Z} \text{Tr} \left[\mathcal{T}_C e^{-i \int_C ds H(s)} \mathcal{A}(t) \mathcal{B}(t') \right]$$

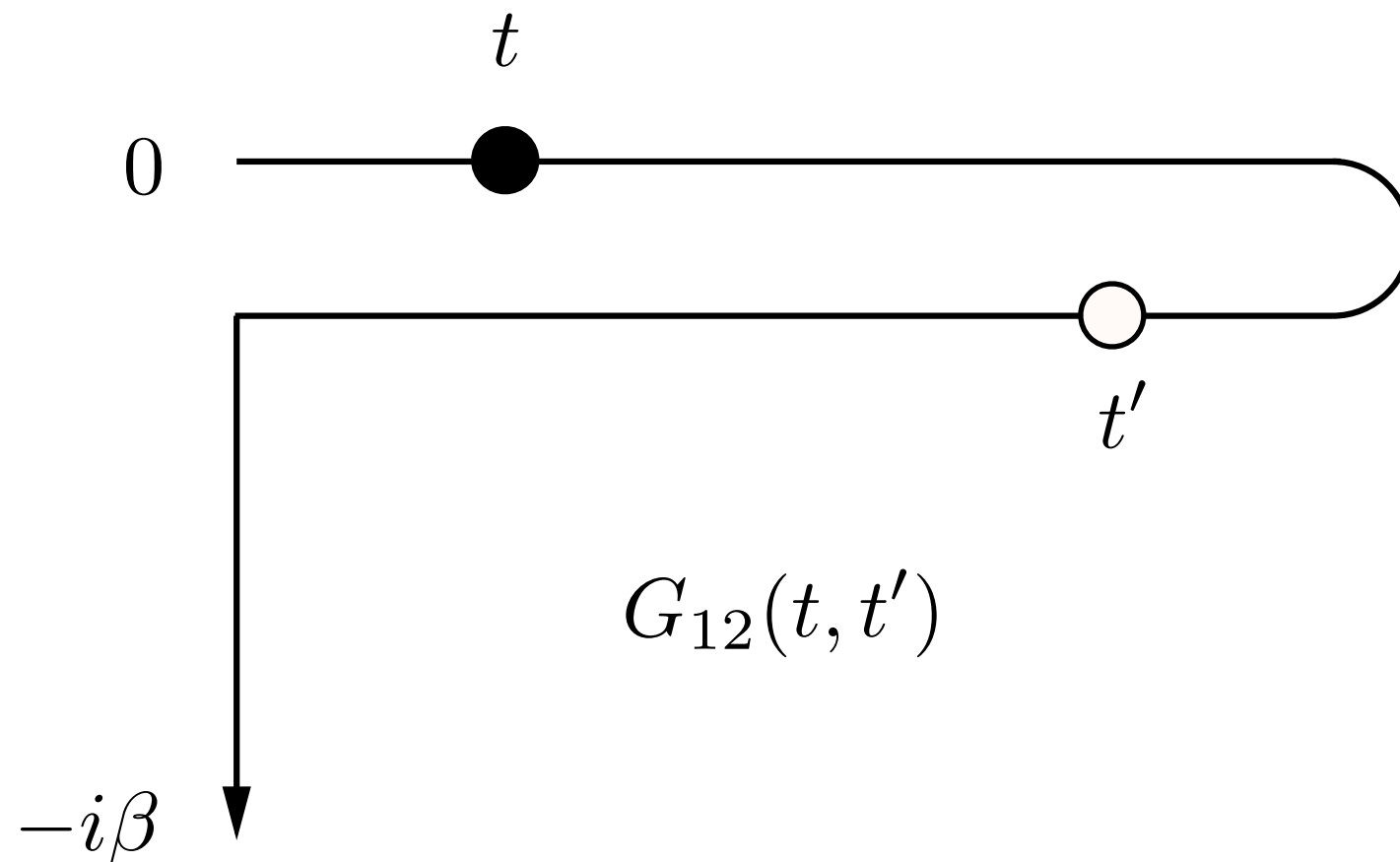
- Particularly relevant: Green's function

$$G(t, t') \equiv -i \langle \mathcal{T}_C d(t) d^\dagger(t') \rangle$$

Nonequilibrium extension

- **Kadanoff-Baym contour**
- Due to the 3 branches, the Green's function has 9 components

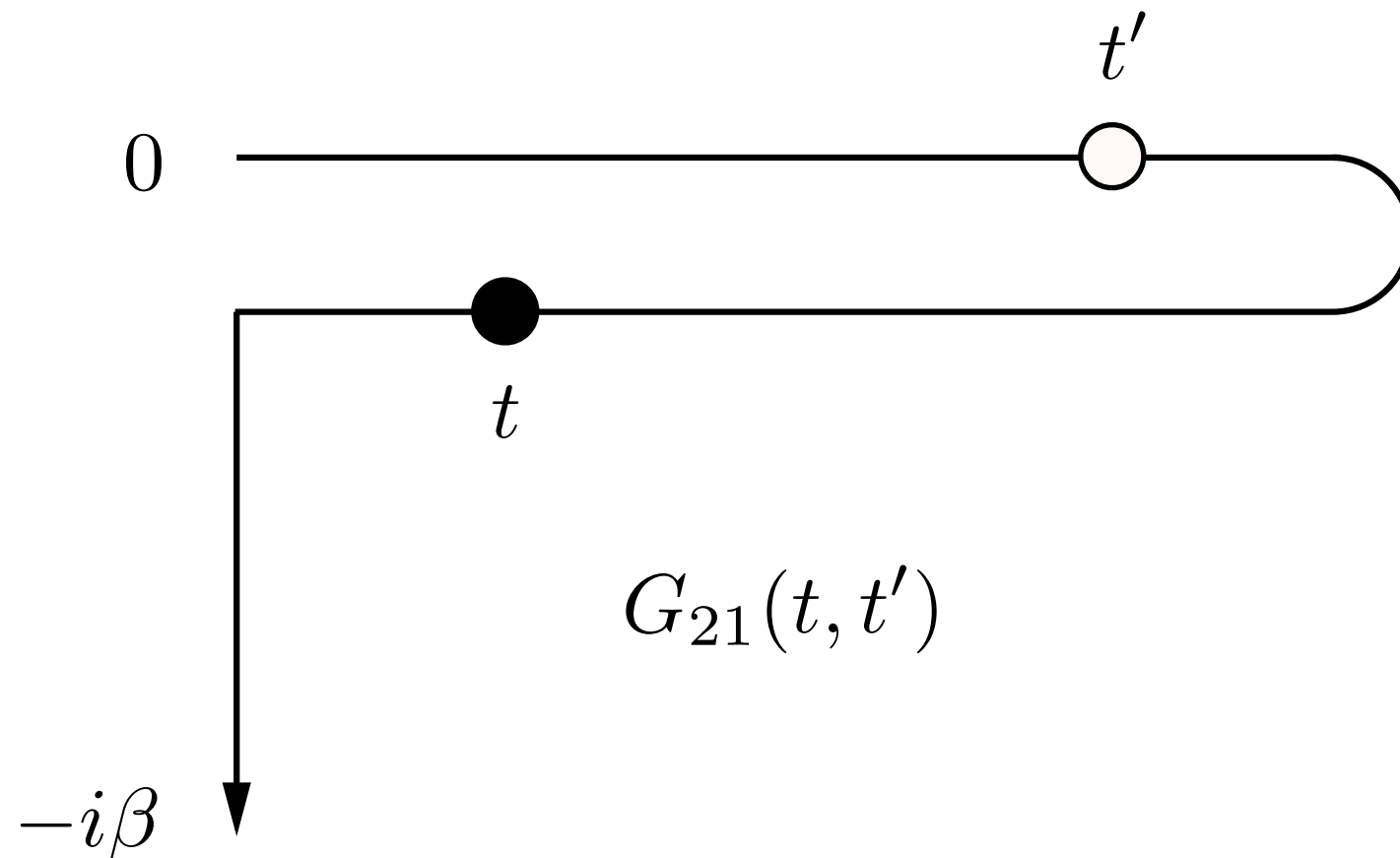
$$G(t, t') \equiv G_{ij}(t, t'), \quad t \in \mathcal{C}_i, t' \in \mathcal{C}_j, \quad i, j = 1, 2, 3$$



Nonequilibrium extension

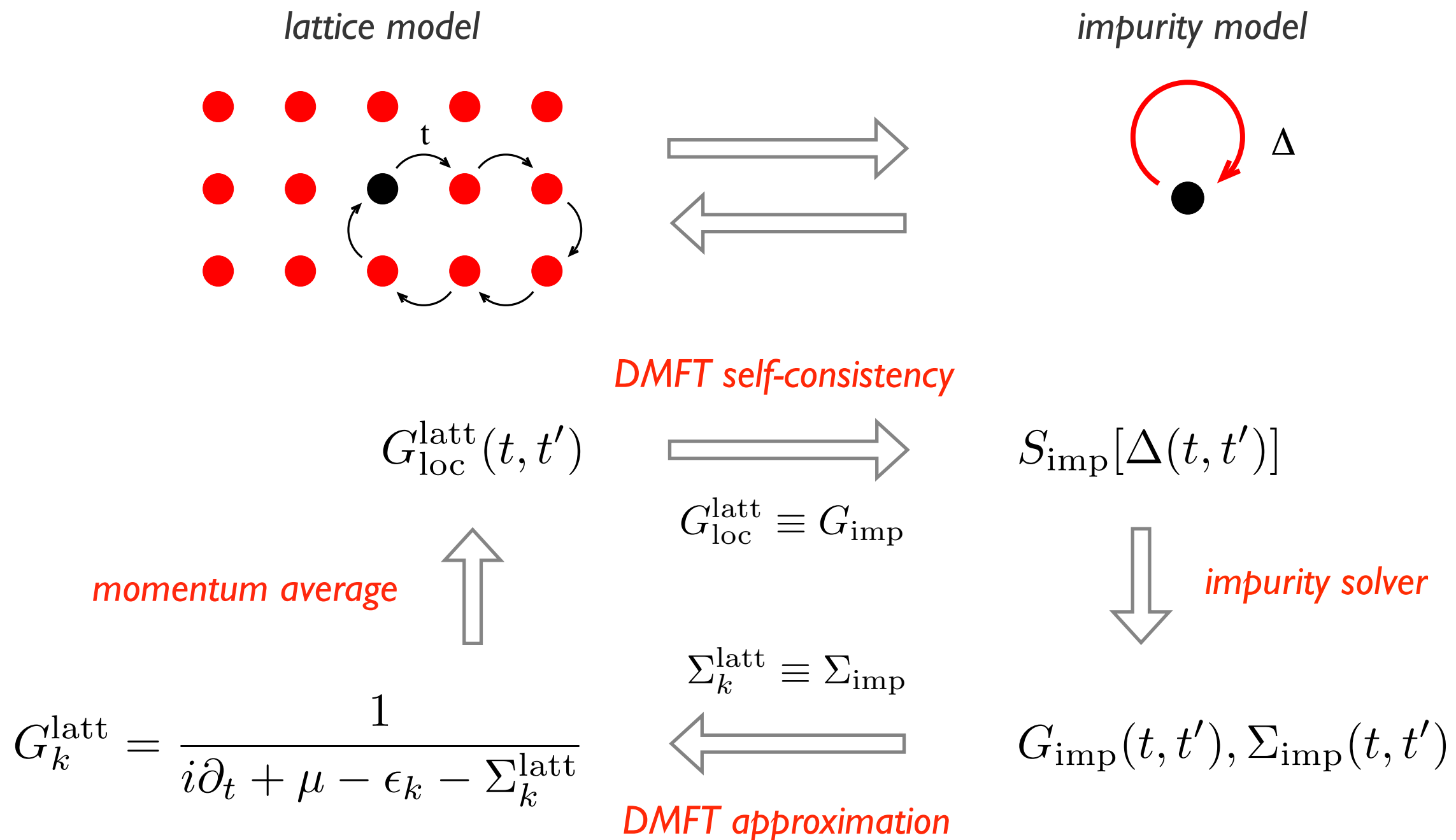
- **Kadanoff-Baym contour**
- Due to the 3 branches, the Green's function has 9 components

$$G(t, t') \equiv G_{ij}(t, t'), \quad t \in \mathcal{C}_i, t' \in \mathcal{C}_j, \quad i, j = 1, 2, 3$$



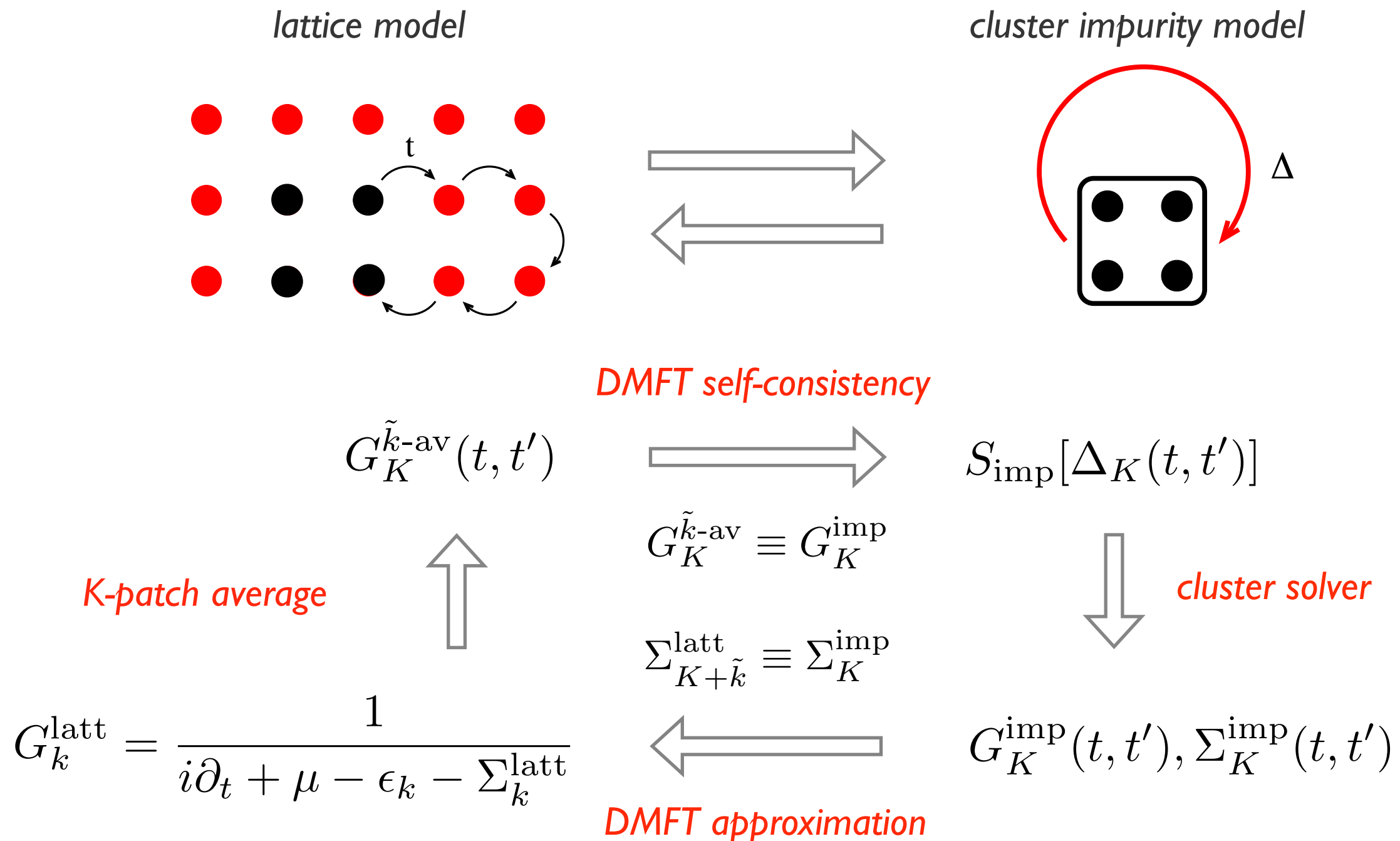
Nonequilibrium extension

- **Nonequilibrium DMFT:** Solve DMFT equations on the Kadanoff-Baym contour \mathcal{C} *Freericks et al. (2006)*



Nonequilibrium extension

- **Nonequilibrium DMFT:** Solve DMFT equations on the Kadanoff-Baym contour \mathcal{C} *Tsui et al. (2014)*



Nonequilibrium extension

- **Nonequilibrium DMFT:** Solve DMFT equations on the Kadanoff-Baym contour \mathcal{C}
- Nonequilibrium Anderson impurity model

$$S_{\text{imp}} = -i \int_{\mathcal{C}} dt H_{\text{loc}}(t) - i \sum_{\sigma} \int_{\mathcal{C}} dt dt' d_{\sigma}^{\dagger}(t) \Delta(t, t') d_{\sigma}(t')$$

\uparrow \uparrow

interaction and chemical potential terms *contour hybridization function*

- Hybridization function is equivalent to “Weiss” Green’s function

$$\mathcal{G}_0(t, t') = (i\partial_t + \mu(t))\delta_{\mathcal{C}}(t, t') - \Delta(t, t')$$

Nonequilibrium extension

- **Nonequilibrium DMFT:** Solve DMFT equations on the Kadanoff-Baym contour \mathcal{C}
- Nonequilibrium Anderson impurity model

$$S_{\text{imp}} = -i \int_{\mathcal{C}} dt H_{\text{loc}}(t) - i \sum_{\sigma} \int_{\mathcal{C}} dt dt' d_{\sigma}^{\dagger}(t) \Delta(t, t') d_{\sigma}(t')$$

\uparrow \uparrow

interaction and chemical potential terms *contour hybridization function*

- Impurity Green's function

$$G_{\text{imp}}(t, t') = -i \langle \mathcal{T}_{\mathcal{C}} d(t) d^{\dagger}(t') \rangle_{S_{\text{imp}}}$$

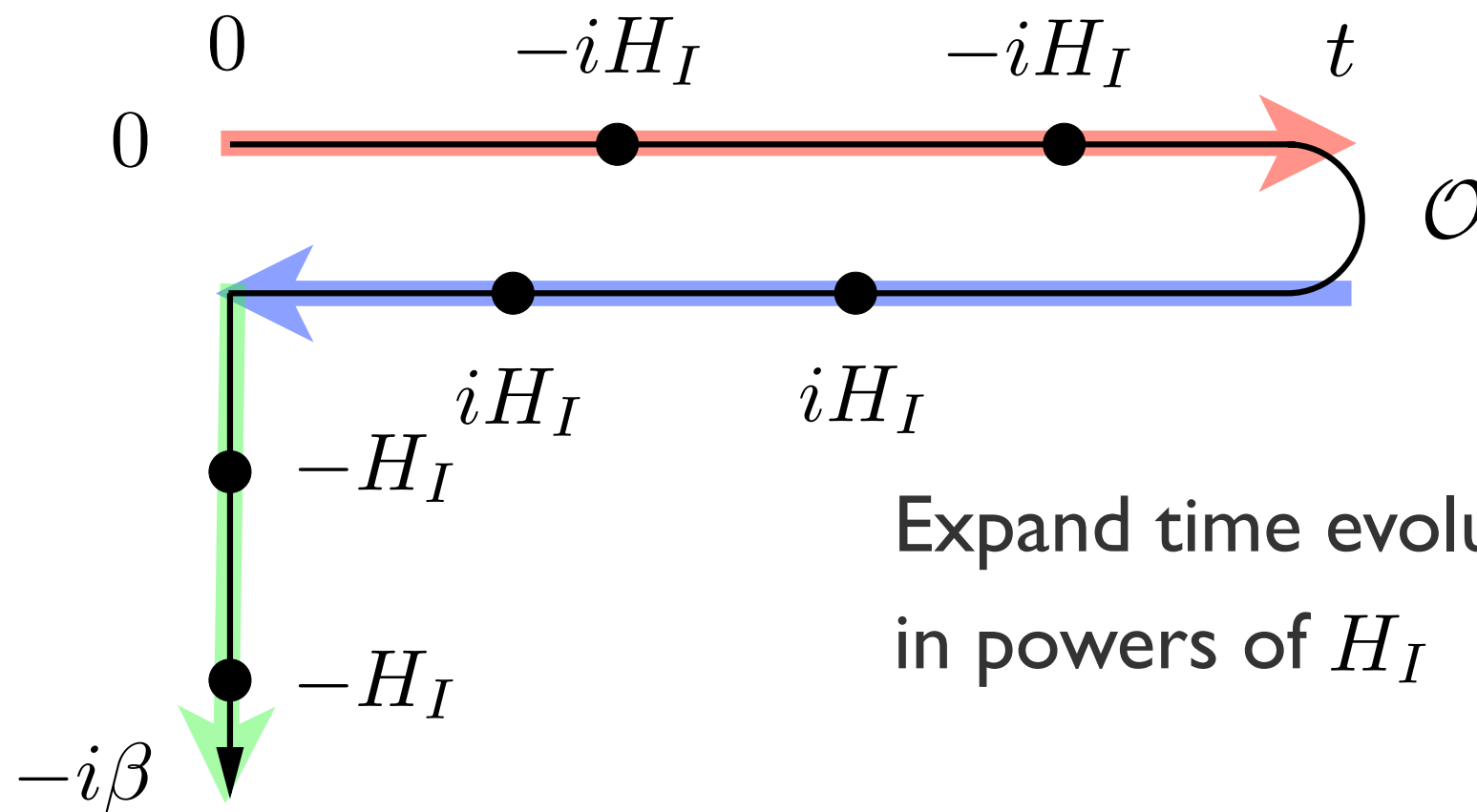
$$\langle \cdots \rangle_{S_{\text{imp}}} = \frac{\text{Tr}[\mathcal{T}_{\mathcal{C}} \exp(S_{\text{imp}}) \cdots]}{\text{Tr}[\mathcal{T}_{\mathcal{C}} \exp(S_{\text{imp}})]}$$

Nonequilibrium extension

- **Impurity solver:** weak-coupling continuous-time QMC Werner et al. (2009)

$$\langle \mathcal{O} \rangle(t) = \text{Tr} \left[\frac{1}{Z} e^{-\beta H} U(0, t) \mathcal{O} U(t, 0) \right]$$

$$= \text{Tr} \left[\frac{1}{Z} e^{-\beta H_0} \left(T_\tau e^{-\int_0^\beta d\tau H_I(\tau)} \right) \left(\tilde{T} e^{i \int_0^t ds H_I(s)} \right) \mathcal{O}(t) \left(T e^{-i \int_0^t ds H_I(s)} \right) \right]$$



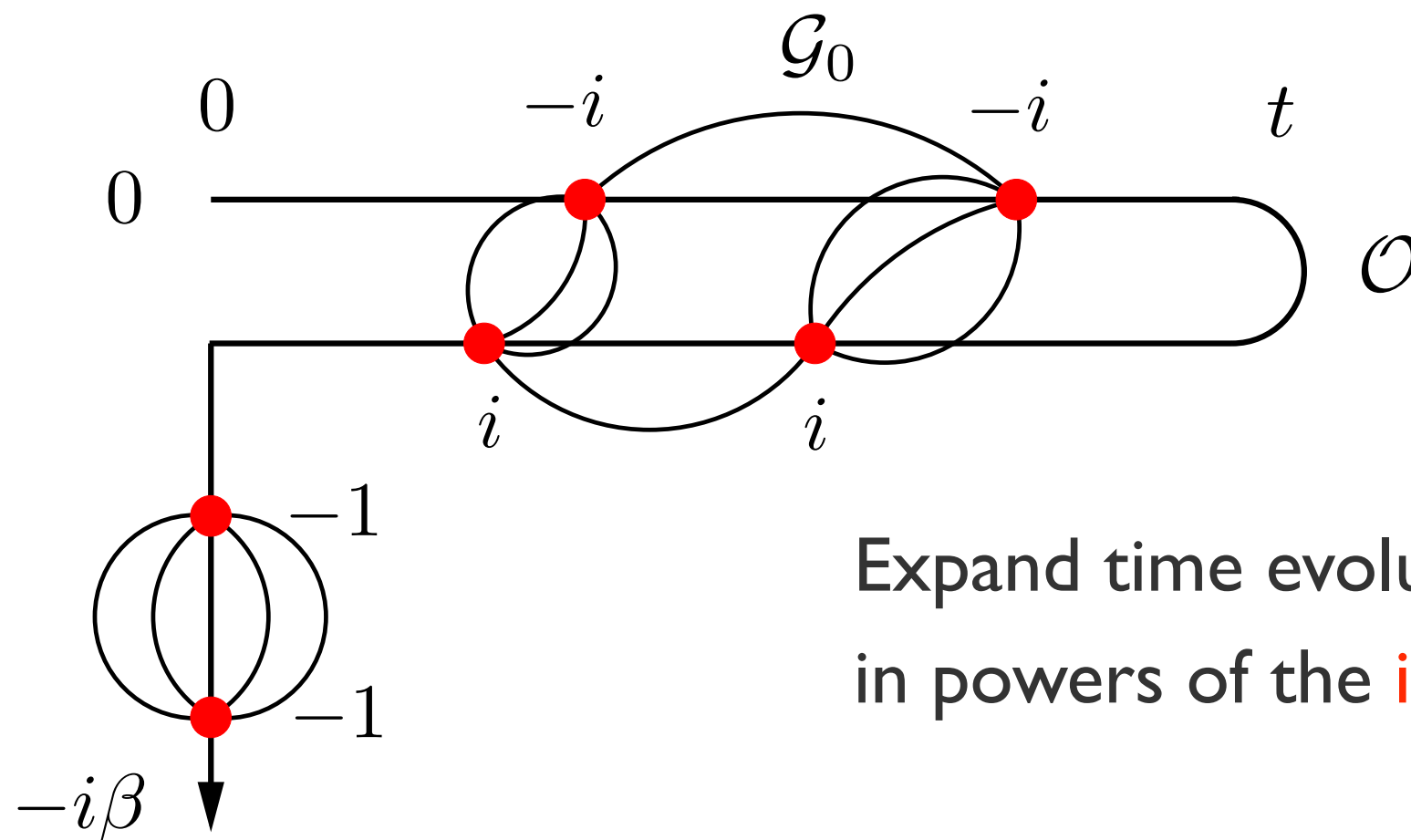
Expand time evolution operators
in powers of H_I

Nonequilibrium extension

- **Impurity solver:** weak-coupling continuous-time QMC Werner et al. (2009)

$$\langle \mathcal{O} \rangle(t) = \text{Tr} \left[\frac{1}{Z} e^{-\beta H} U(0, t) \mathcal{O} U(t, 0) \right]$$

$$= \text{Tr} \left[\frac{1}{Z} e^{-\beta H_0} \left(T_\tau e^{-\int_0^\beta d\tau H_I(\tau)} \right) \left(\tilde{T} e^{i \int_0^t ds H_I(s)} \right) \mathcal{O}(t) \left(T e^{-i \int_0^t ds H_I(s)} \right) \right]$$



Expand time evolution operators
in powers of the **interaction term**

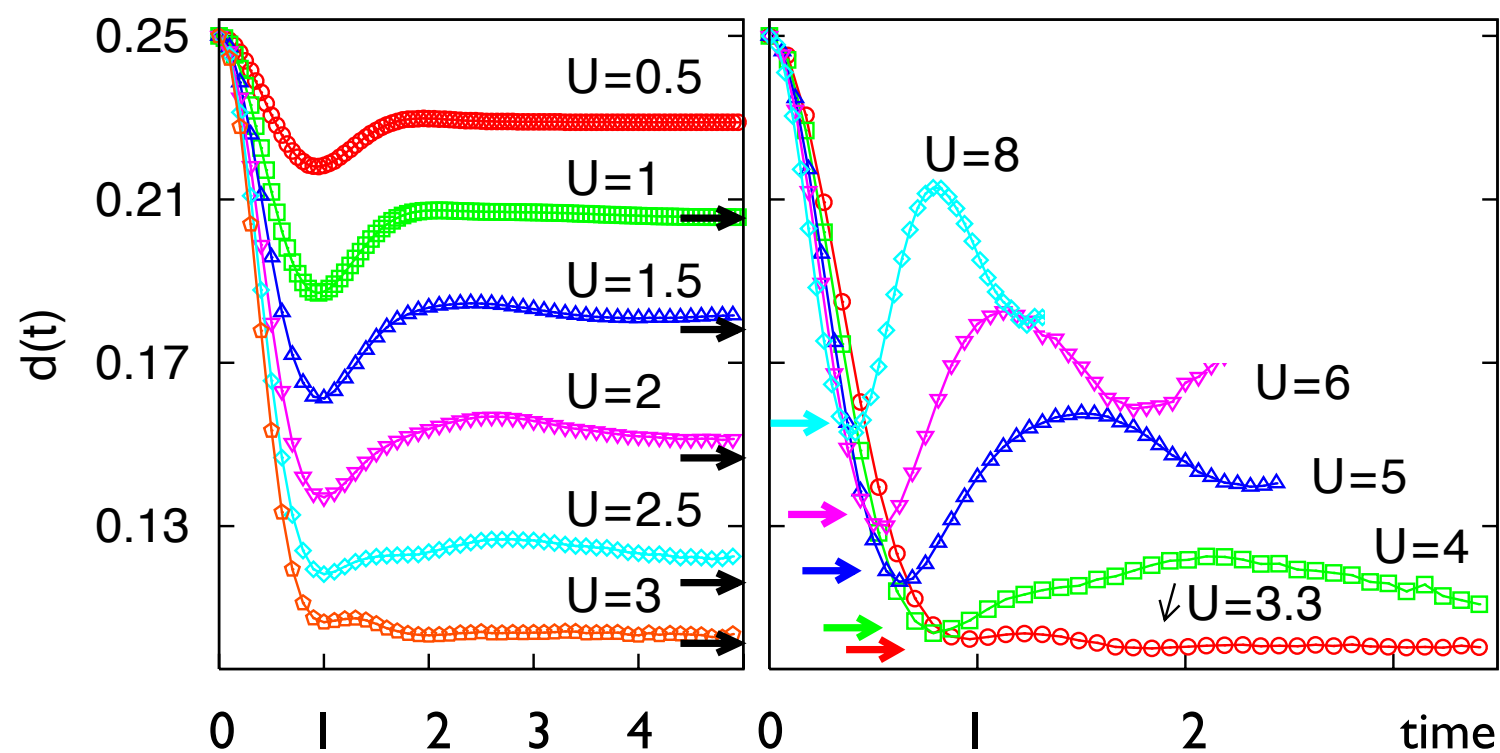
Nonequilibrium extension

- **Impurity solver:** weak-coupling continuous-time QMC *Werner et al. (2009)*

$$\langle \mathcal{O} \rangle(t) = \text{Tr} \left[\frac{1}{Z} e^{-\beta H} U(0, t) \mathcal{O} U(t, 0) \right]$$

$$= \text{Tr} \left[\frac{1}{Z} e^{-\beta H_0} \left(T_\tau e^{-\int_0^\beta d\tau H_I(\tau)} \right) \left(\tilde{T} e^{i \int_0^t ds H_I(s)} \right) \mathcal{O}(t) \left(T e^{-i \int_0^t ds H_I(s)} \right) \right]$$

- Time evolution of double occupation after a quench from $U=0$



intermediate/strong
correlation regime:
**can reach a few
inverse hopping times**

Eckstein et al. (2009)

Nonequilibrium extension

- **Impurity solver:** weak-coupling perturbation theory
- Generate a subset of all weak-coupling diagrams by **approximating the self-energy**
- Truncation at second order: *Iterated Perturbation Theory (IPT)*

$$\Sigma_{\text{imp}} = \text{[Diagram: A dashed box with two horizontal lines. The bottom line has arrows pointing right from t to t'. The top line has a loop with two arrows pointing right. The box is labeled U to its right.]}$$

$$G_{\text{imp}} = G_0 + G_0 \star \Sigma_{\text{imp}} \star G_{\text{imp}}$$

$$G_{\text{imp}} = \text{[Diagram: A single horizontal line with an arrow pointing right, labeled G_0 above it.]}$$

$$+ \text{[Diagram: A horizontal line with an arrow pointing right, with a dashed box containing a loop (like the Σ_{imp} diagram) inserted above it.]}$$

$$+ \text{[Diagram: A horizontal line with an arrow pointing right, with two dashed boxes containing loops inserted above it.]}$$

$$+ \dots$$

Nonequilibrium extension

- **Impurity solver:** weak-coupling perturbation theory
- Generate a subset of all weak-coupling diagrams by **approximating the self-energy**
- Boldfied expansion: conserving, but not accurate

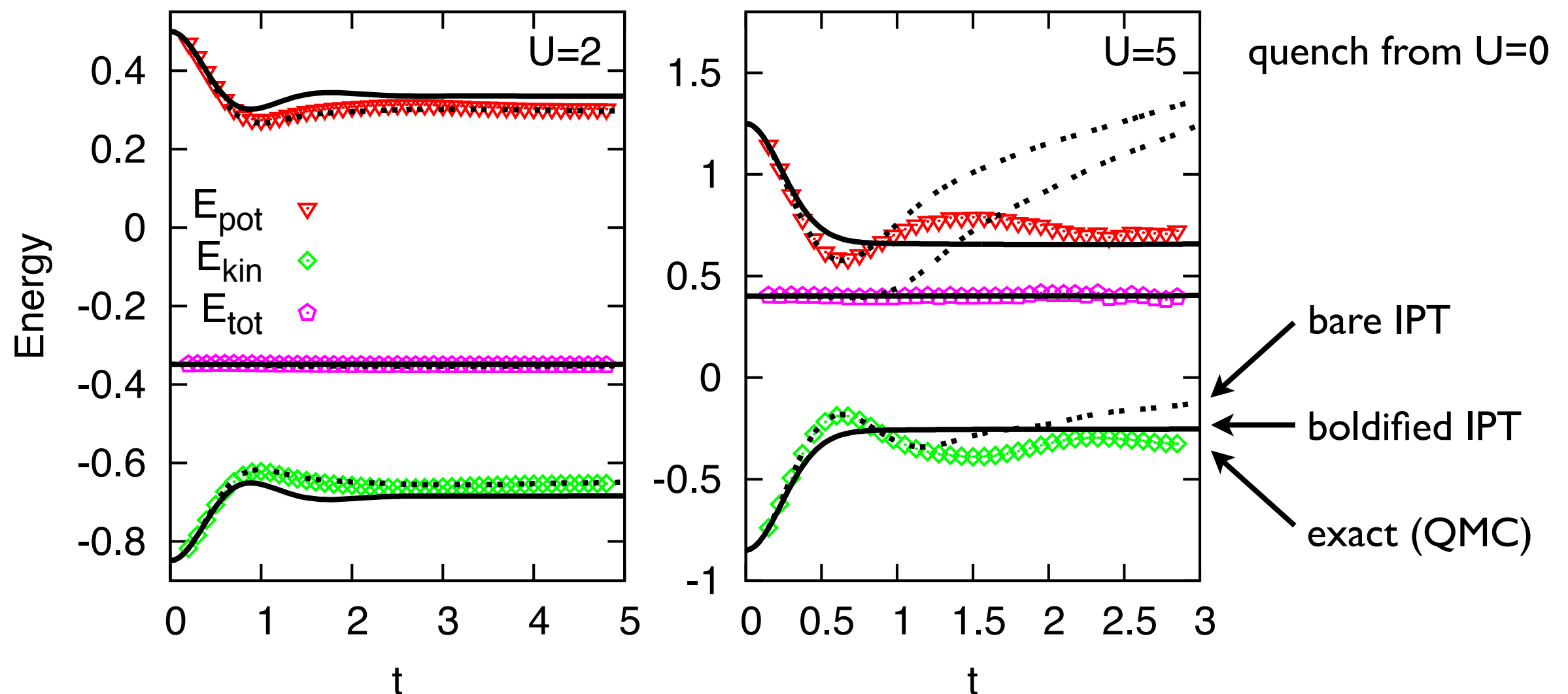
$$\Sigma_{\text{imp}} = \text{[Diagram: A dashed box with a horizontal arrow from } t \text{ to } t' \text{ and a circular loop above it, labeled } U \text{ to the right.]} U$$

$$G_{\text{imp}} = \mathcal{G}_0 + \mathcal{G}_0 \star \Sigma_{\text{imp}} \star G_{\text{imp}}$$

$$G_{\text{imp}} = \text{[Diagram: A horizontal arrow labeled } \mathcal{G}_0 \text{ with a red L-shaped arrow pointing to the } \Sigma_{\text{imp}} \text{ diagram above.]} + \text{[Diagram: A horizontal arrow with a dashed box and loop above it.]} + \text{[Diagram: A horizontal arrow with two dashed boxes and loops above it.]} + \dots$$

Nonequilibrium extension

- **Impurity solver:** weak-coupling perturbation theory
- Generate a subset of all weak-coupling diagrams by **approximating the self-energy**
- **Boldfied expansion:** conserving, but not accurate *Eckstein et al. (2009)*

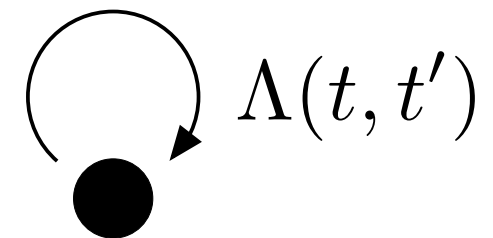


Nonequilibrium extension

- **Impurity solver:** Strong-coupling perturbation theory
- Introduce pseudo-particle propagators G_α for local states $\{0, \uparrow, \downarrow, \uparrow\downarrow\}$
- Approximate pseudo-particle self-energy

$$\Sigma_\alpha = \text{---} \overset{\Lambda}{\curvearrowright} \text{---}$$

$t \quad G_\beta \quad t'$



$$G_\alpha = \text{---} \overset{G_{0,\alpha}}{\longrightarrow} \text{---}$$

$$+ \text{---} \overset{\Lambda}{\curvearrowright} \text{---}$$

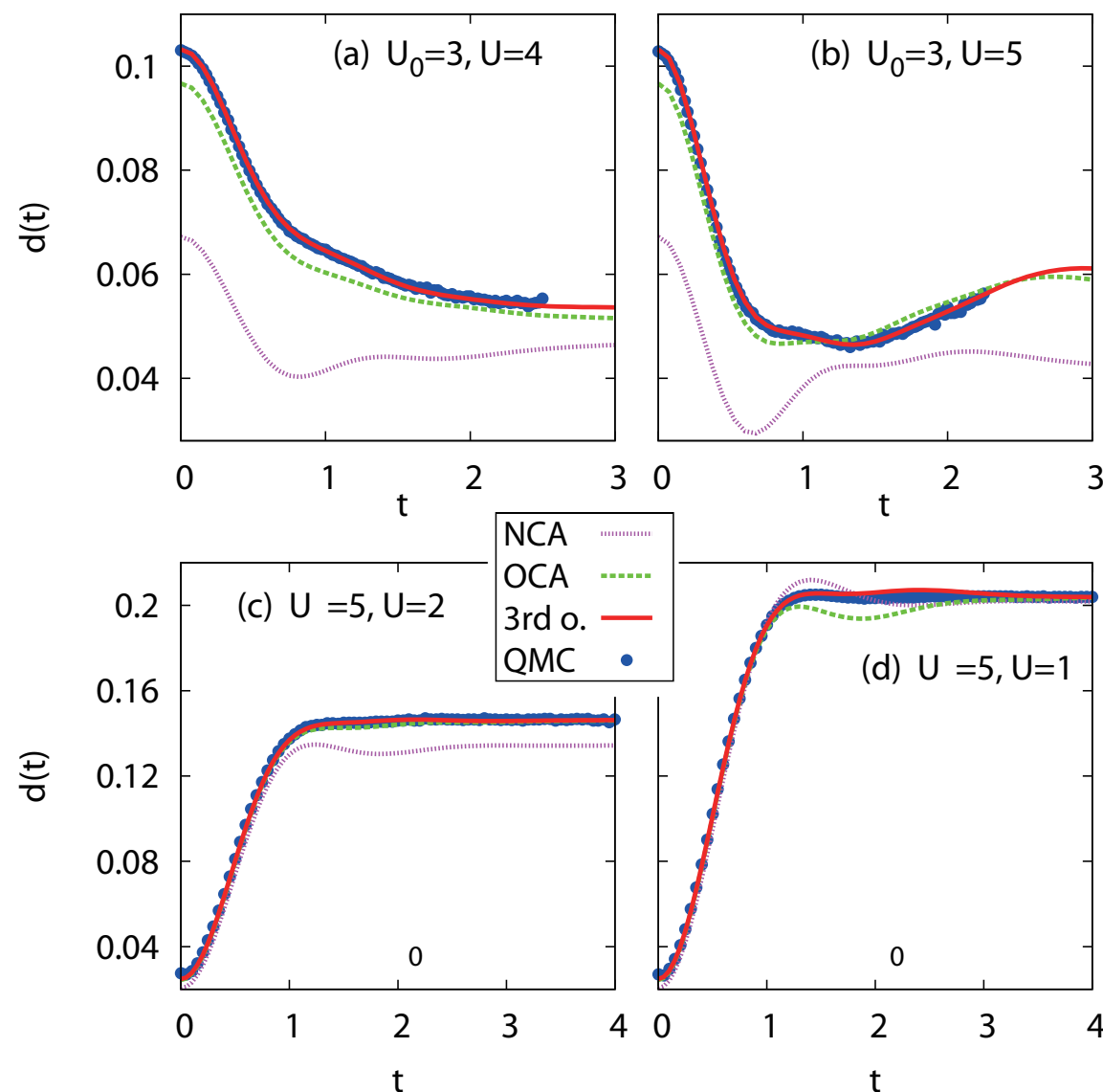
$$+ \text{---} \overset{\Lambda}{\curvearrowright} \text{---} \overset{\Lambda}{\curvearrowright} \text{---} + \dots$$

Non-crossing approximation (NCA)

Keiter & Kimball (2009)

Nonequilibrium extension

- **Impurity solver:** Strong-coupling perturbation theory
- Introduce pseudo-particle propagators G_α for local states $\{0, \uparrow, \downarrow, \uparrow\downarrow\}$
- Approximate pseudo-particle self-energy



conserving approximation

systematically converging
to the exact result

accurate in the strong-
coupling regime

Eckstein & Werner (2010)

Nonequilibrium extension

- **Calculation of the lattice Green's function**
- Noninteracting lattice:

$$H_0(t) = \sum_k [\epsilon_k(t) - \mu(t)] d_k^\dagger d_k$$

$$G_{0,k}(t, t') = -i \langle \mathcal{T}_C d_k(t) d_k^\dagger(t') \rangle_0$$

- Green's function satisfies:

$$[i\partial_t + \mu(t) - \epsilon_k(t)] G_{0,k}(t, t') = \delta_C(t, t')$$

$$G_{0,k}(t, t') [-i\overleftarrow{\partial}_{t'} + \mu(t') - \epsilon_k(t')] = \delta_C(t, t')$$

- **Inverse lattice Green's function:**

$$G_{0,k}^{-1}(t, t') = \delta_C(t, t') [i\partial_t + \mu(t) - \epsilon_k(t)]$$

$$G_{0,k}^{-1} \star G_{0,k} = G_{0,k} \star G_{0,k}^{-1} = \delta_C$$

Nonequilibrium extension

- **Calculation of the lattice Green's function**
- Interacting lattice Green's function satisfies Dyson equation:

$$\begin{aligned}
 G_k &= G_{0,k} + G_{0,k} \star \Sigma \star G_k \\
 &= G_{0,k} + G_k \star \Sigma \star G_{0,k}
 \end{aligned}$$

integral form



impurity self-energy (DMFT)

$$[G_{0,k}^{-1} - \Sigma] \star G_k = G_k \star [G_{0,k}^{-1} - \Sigma] = \delta_C$$

differential form

- **Imaginary-time branch: boundary-value problem** → solve by FT

$$G_k(i\omega_n) = \frac{1}{G_{0,k}^{-1}(i\omega_n) - \Sigma(i\omega_n)} = \frac{1}{i\omega_n + \mu(0) - \epsilon_k(0) - \Sigma(i\omega_n)}$$

- Usual equilibrium DMFT calculation for the initial equilibrium state

Nonequilibrium extension

- **Calculation of the lattice Green's function**
- Interacting lattice Green's function satisfies Dyson equation:

$$\begin{aligned} G_k &= G_{0,k} + G_{0,k} \star \Sigma \star G_k \\ &= G_{0,k} + G_k \star \Sigma \star G_{0,k} \end{aligned} \quad \text{integral form}$$



impurity self-energy (DMFT)

$$[G_{0,k}^{-1} - \Sigma] \star G_k = G_k \star [G_{0,k}^{-1} - \Sigma] = \delta_C \quad \text{differential form}$$

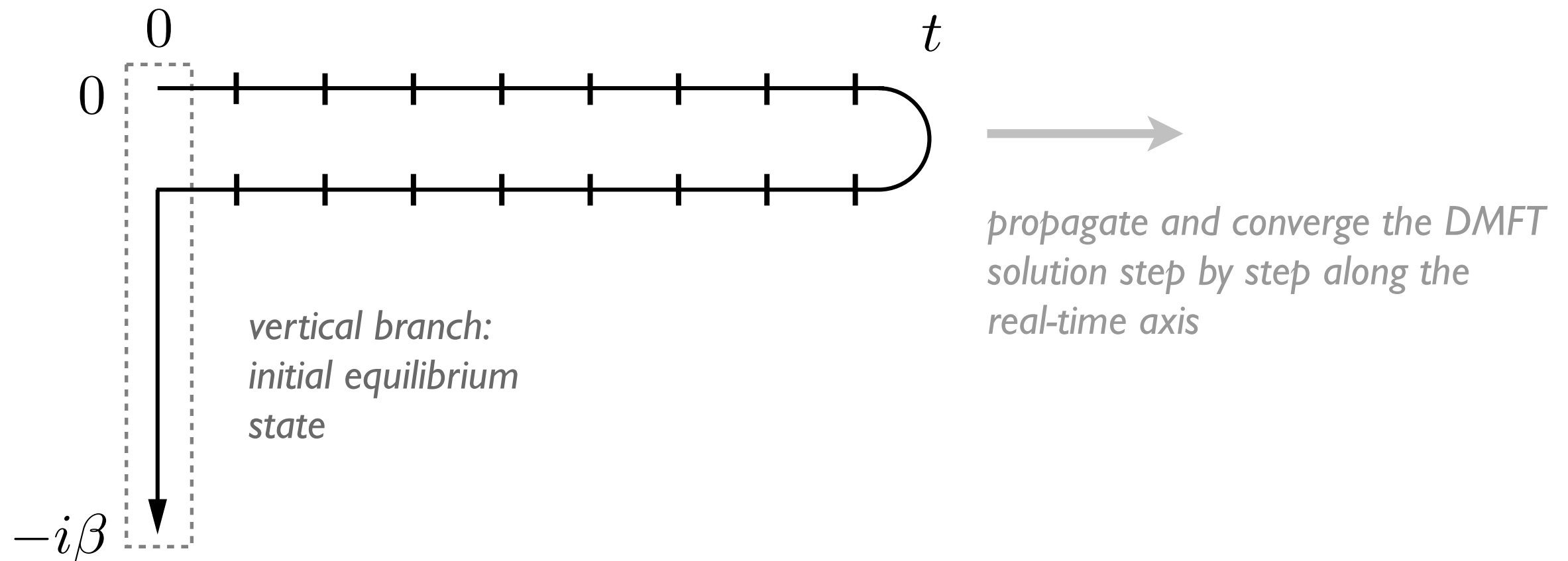
- **Real-time branches: initial-value problem**

$$[i\partial_t + \mu(t) - \epsilon_k(t)]G_k(t, t') - \int_C d\bar{t} \Sigma(t, \bar{t})G_k(\bar{t}, t') = \delta_C(t, t')$$

- Defines time-propagation scheme for G in which the self-energy plays the role of a memory-kernel

Nonequilibrium extension

- Calculation of the lattice Green's function



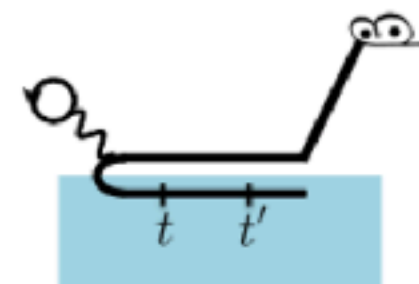
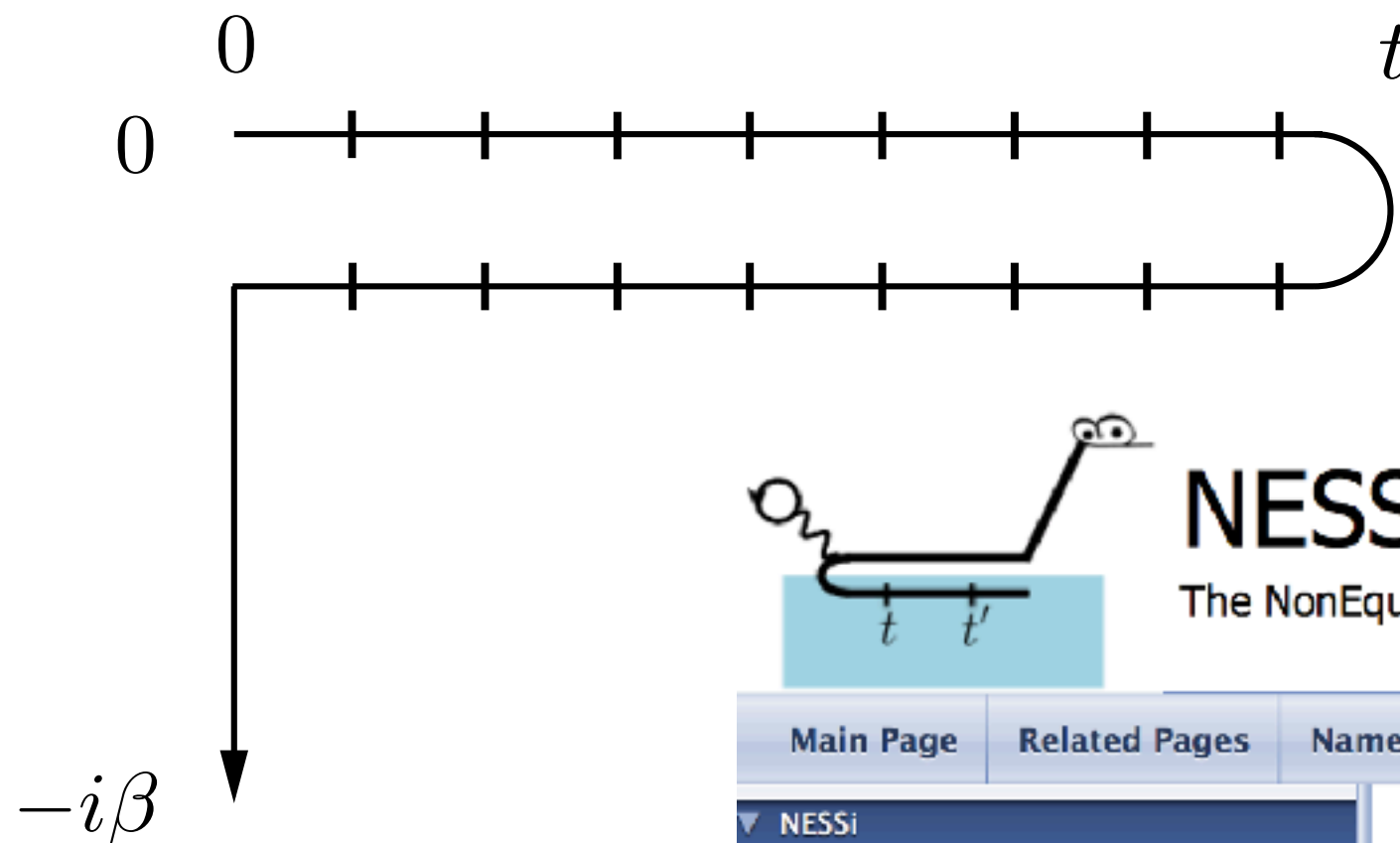
- Real-time branches: initial-value problem

$$[i\partial_t + \mu(t) - \epsilon_k(t)]G_k(t, t') - \int_{\mathcal{C}} d\bar{t} \Sigma(t, \bar{t})G_k(\bar{t}, t') = \delta_{\mathcal{C}}(t, t')$$

- Defines time-propagation scheme for G in which the self-energy plays the role of a memory-kernel

Nonequilibrium extension

- Calculation of the lattice Green's function



NESSi v1.0.1

The NonEquilibrium Systems Simulation Library

Main Page

Related Pages

Namespaces ▾

Classes ▾

Files ▾

NESSi

▶ Welcome to the Non-Equilibrium Syst

▶ Getting started with NESSi

▶ Physics background

▶ Manual

▶ Example programs

Bibliography

▶ Namespaces

▶ Classes

▶ Files

Core functionalities

The `libentx` library provides highly accurate methods for calculating Green's functions. A summary of the core functionalities is presented below. All routines work for fermions and bosons.

Summary

Green's function for a constant or time-dependent Hamiltonian

Constructs the free Green's functions

Dyson equation

Solves the Dyson equation along the given self-energy $\Sigma(t, t')$. In particular,

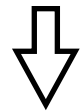
- Open source library:
nessi.tuxfamily.org

Nonequilibrium extension

- **Electric fields**

- Vector potential $A(r, t)$, scalar potential $\Phi(r, t)$: $E = -\nabla\Phi - \partial_t A$

$$v_{ij}(t) = v_{ij} \exp\left(-ie \int_{R_i}^{R_j} dr A(r, t)\right)$$



$$H(t) = - \sum_{\langle ij \rangle \sigma} v_{ij}(t) (d_{i\sigma}^\dagger d_{j\sigma} + d_{j\sigma}^\dagger d_{i\sigma})$$

$$+ U(t) \sum_i n_{i\uparrow} n_{i\downarrow} - \sum_{i\sigma} \mu(t) n_{i\sigma}$$



$$\mu(t) = \mu + e\Phi(R_i, t)$$

- Convenient choice: gauge with pure vector potential:

$$\Phi \equiv 0, E = -\partial_t A$$

Nonequilibrium extension

- **Electric fields**
- Neglecting the r -dependence of A (assumption: field varies slowly on the atomic scale):

$$v_{ij}(t) = v_{ij} \exp\left(-ie \int_{R_i}^{R_j} dr A(t)\right) \quad A(t) = - \int_0^t ds E(s)$$

↓ *Fourier transformation*

$$\epsilon_k(t) = \epsilon_{k-eA(t)}$$

- Electric field enters in the lattice Dyson equation in the form of a time-dependent dispersion:

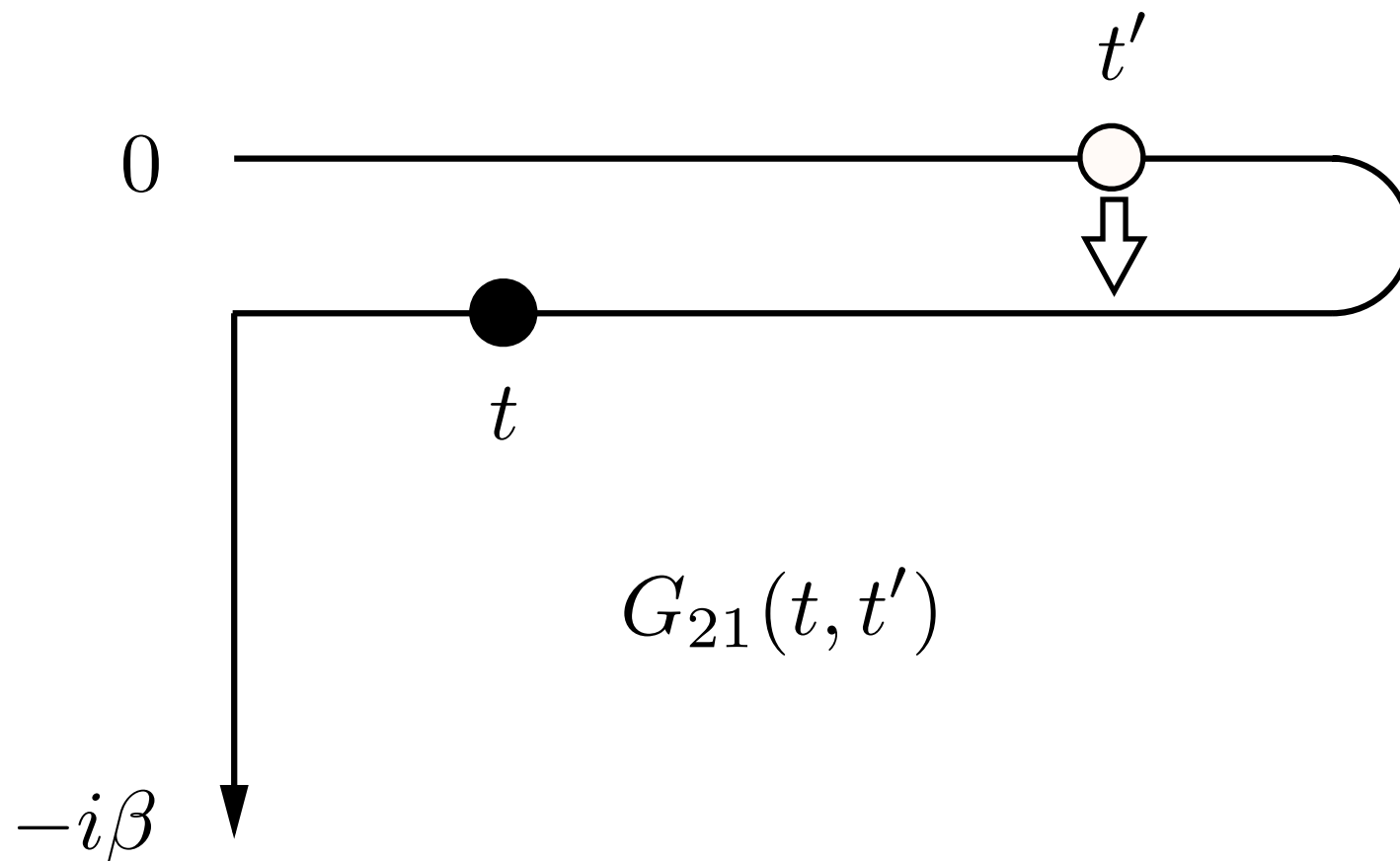
$$[i\partial_t + \mu(t) - \epsilon_k(t)]G_k(t, t') - \int_{\mathcal{C}} d\bar{t} \Sigma(t, \bar{t})G_k(\bar{t}, t') = \delta_{\mathcal{C}}(t, t')$$

Spectroscopy

- “Physical” Green’s functions
- The 9 elements of the 3x3 Green’s function matrix

$$\hat{G} = \begin{pmatrix} G_{11} & G_{12} & G_{13} \\ G_{21} & G_{22} & G_{23} \\ G_{31} & G_{32} & G_{33} \end{pmatrix}$$

are not independent:

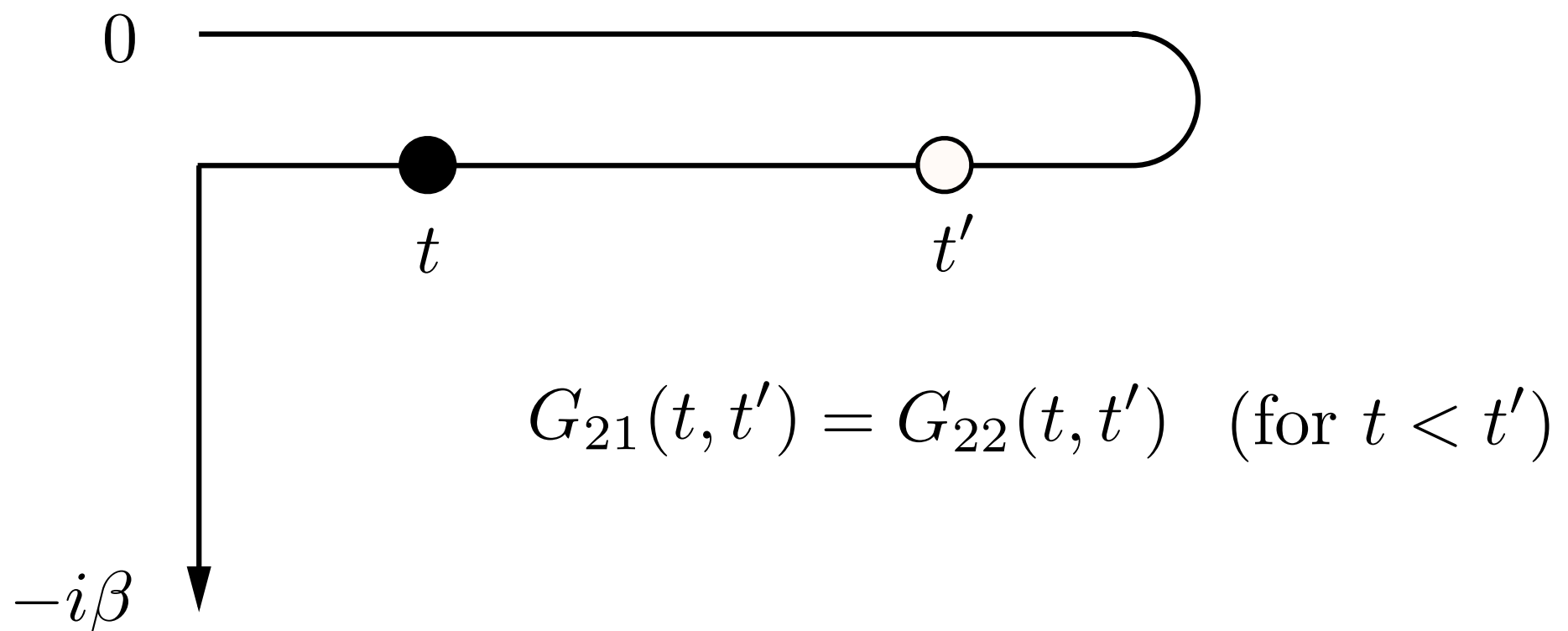


Spectroscopy

- “Physical” Green’s functions
- The 9 elements of the 3x3 Green’s function matrix

$$\hat{G} = \begin{pmatrix} G_{11} & G_{12} & G_{13} \\ G_{21} & G_{22} & G_{23} \\ G_{31} & G_{32} & G_{33} \end{pmatrix}$$

are not independent:



Spectroscopy

- “Physical” Green’s functions
- We have the following redundancies

$$G_{11}(t, t') = G_{12}(t, t') \quad (\text{for } t \leq t')$$

$$G_{11}(t, t') = G_{21}(t, t') \quad (\text{for } t > t')$$

$$G_{22}(t, t') = G_{21}(t, t') \quad (\text{for } t < t')$$

$$G_{22}(t, t') = G_{12}(t, t') \quad (\text{for } t \geq t')$$

$$G_{13}(t, \tau') = G_{23}(t, \tau')$$

$$G_{31}(\tau, t') = G_{32}(\tau, t')$$

which allow to eliminate 3 of the 9 components

→ define 6 “physical” Green’s functions

$$G^R, G^A, G^K, \dots$$

Spectroscopy

- “Physical” Green’s functions
- Relevant for the following discussion: Retarded Green’s function

$$G^R(t, t') = \frac{1}{2}(G_{11} - G_{12} + G_{21} - G_{22}) = -i\theta(t - t')\langle\{d(t), d^\dagger(t')\}\rangle$$

and lesser Green’s functions

$$G^<(t, t') = G_{12} = i\langle d^\dagger(t')d(t)\rangle$$

- In equilibrium:
 - Spectral function: $A(\omega) = -\frac{1}{\pi}\text{Im } G^R(\omega)$
 - Occupation: $N(\omega) = \frac{1}{2\pi}\text{Im } G^<(\omega)$
 - Distribution function: $N(\omega)/A(\omega) = f(\omega)$ *Fermi function*

Spectroscopy

- “Physical” Green’s functions
- Relevant for the following discussion: Retarded Green’s function

$$G^R(t, t') = \frac{1}{2}(G_{11} - G_{12} + G_{21} - G_{22}) = -i\theta(t - t')\langle\{d(t), d^\dagger(t')\}\rangle$$

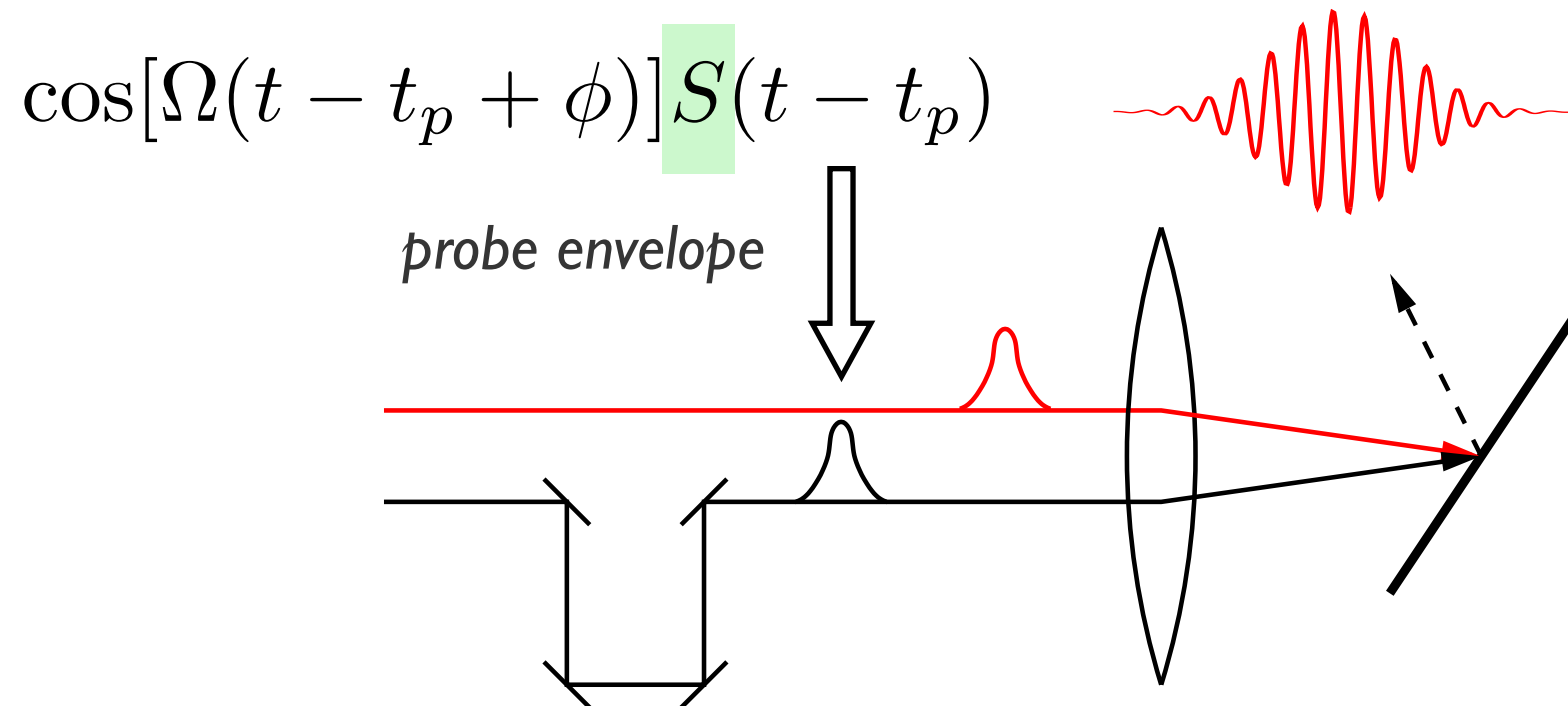
and lesser Green’s functions

$$G^<(t, t') = G_{12} = i\langle d^\dagger(t')d(t)\rangle$$

- **Out of equilibrium:** $t_{\text{av}} = (t + t')/2, t_{\text{rel}} = t - t'$
 - Spectral function: $A(\omega, t_{\text{av}}) = -\frac{1}{\pi}\text{Im} \int dt_{\text{rel}} e^{i\omega t_{\text{rel}}} G^R(t, t')$
 - Occupation: $N(\omega, t_{\text{av}}) = \frac{1}{2\pi}\text{Im} \int dt_{\text{rel}} e^{i\omega t_{\text{rel}}} G^<(t, t')$
 - “Distribution function”: $N(\omega, t_{\text{av}})/A(\omega, t_{\text{av}})$

Spectroscopy

- **Time-resolved photoemission spectrum** *Freericks et al. (2009)*



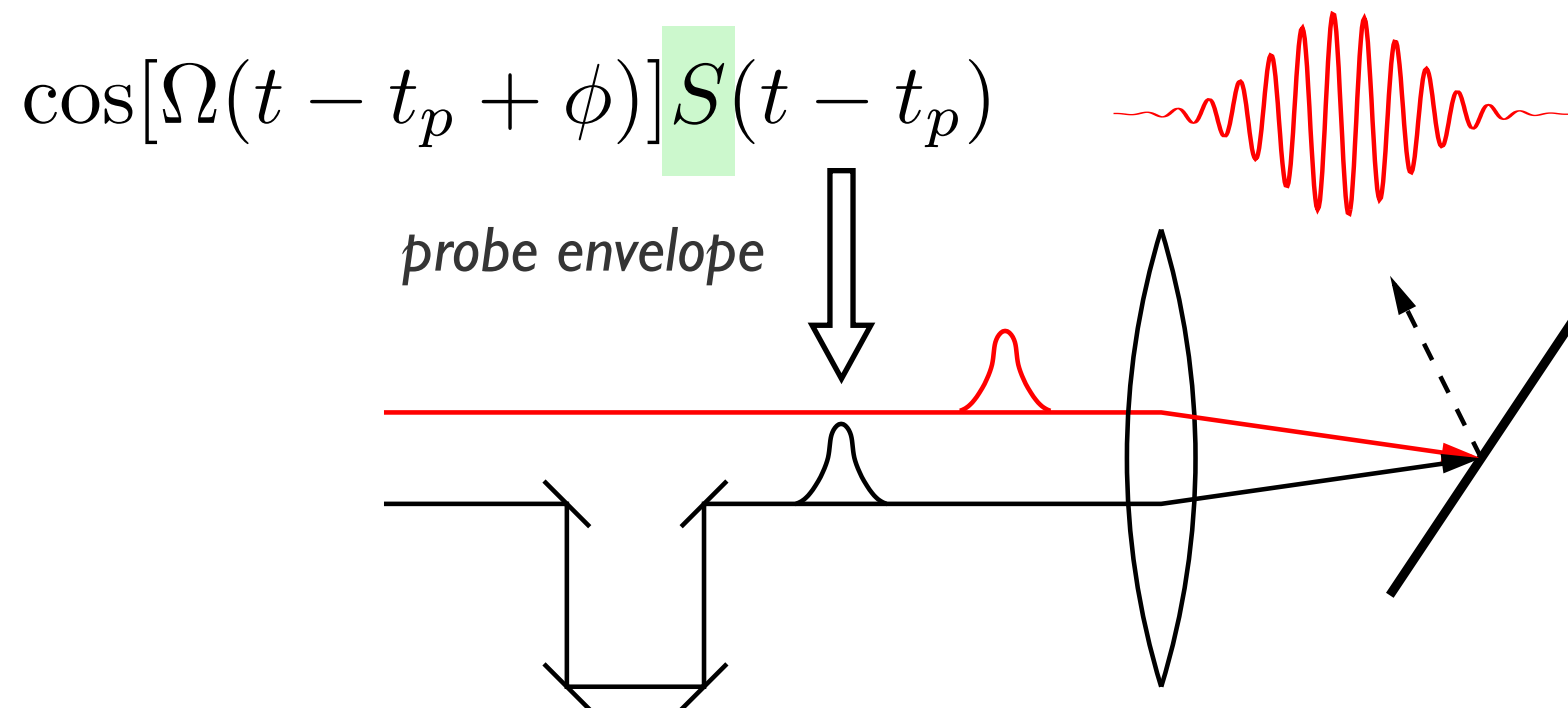
$$I(k_f, E; t_p) \propto \sum_k \delta_{k_{\parallel} + q_{\parallel}, k_{f\parallel}} I_k(E - \hbar\Omega_q - W; t_p),$$

$$I_k(\omega; t_p) = -i \int dt dt' S(t) S(t') e^{i\omega(t' - t)} G_k^<(t + t_p, t' + t_p)$$


 probe time

Spectroscopy

- **Time-resolved photoemission spectrum** *Freericks et al. (2009)*



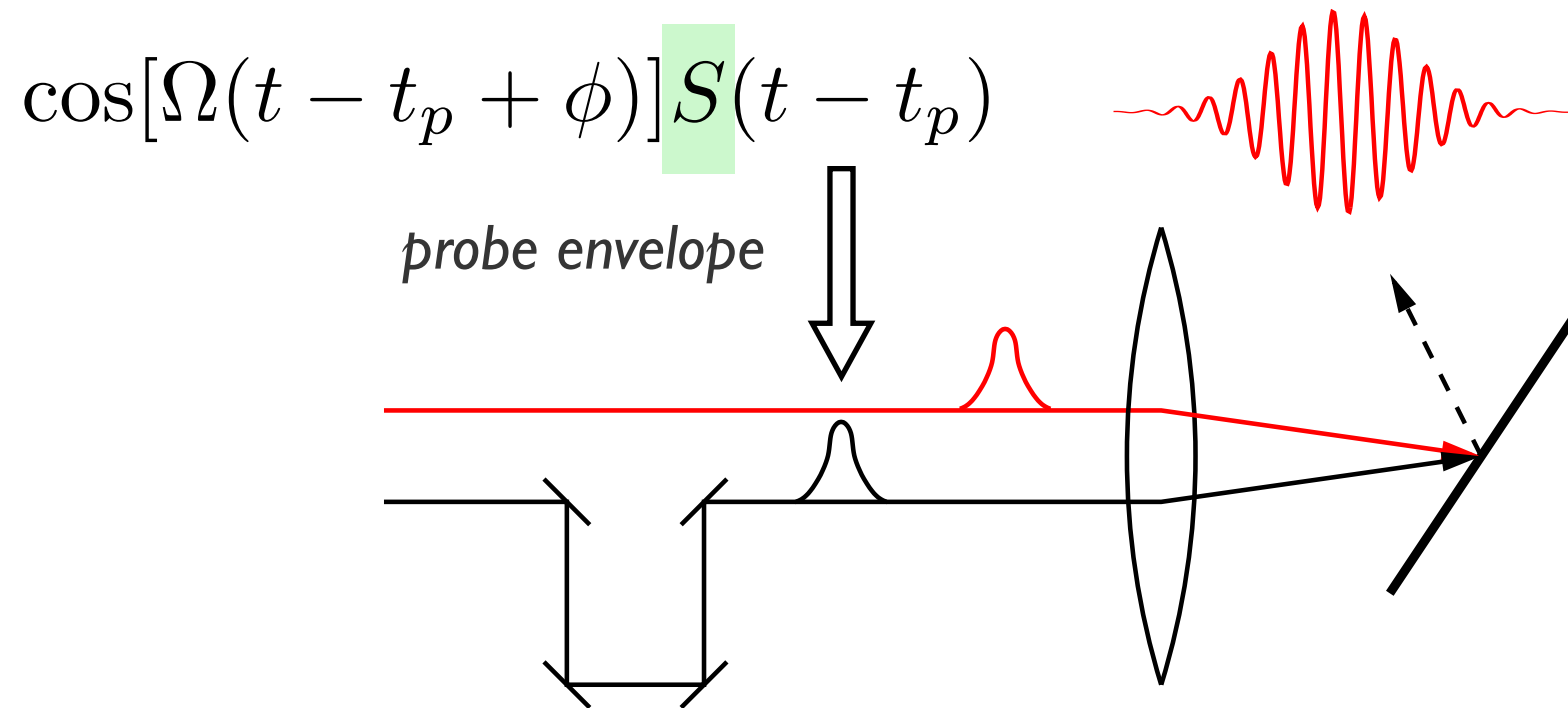
$$I(k_f, E; t_p) \propto \sum_k \delta_{k_{\parallel} + q_{\parallel}, k_{f\parallel}} I_k(E - \hbar\Omega_q - W; t_p),$$

$$I_k(\omega; t_p) = -i \int dt dt' S(t) S(t') e^{i\omega(t' - t)} G_k^<(t + t_p, t' + t_p)$$

- **Formula contains time-energy uncertainty**

Spectroscopy

- **Time-resolved photoemission spectrum** *Freericks et al. (2009)*



$S(t) \sim \delta(t - t_p)$: measure occupation $n_k(t_p)$

$S(t) \sim \text{const}$: measure spectral function $A_k(\omega, t_p)$

$$I_k(\omega; t_p) = -i \int dt dt' S(t) S(t') e^{i\omega(t' - t)} G_k^<(t + t_p, t' + t_p)$$

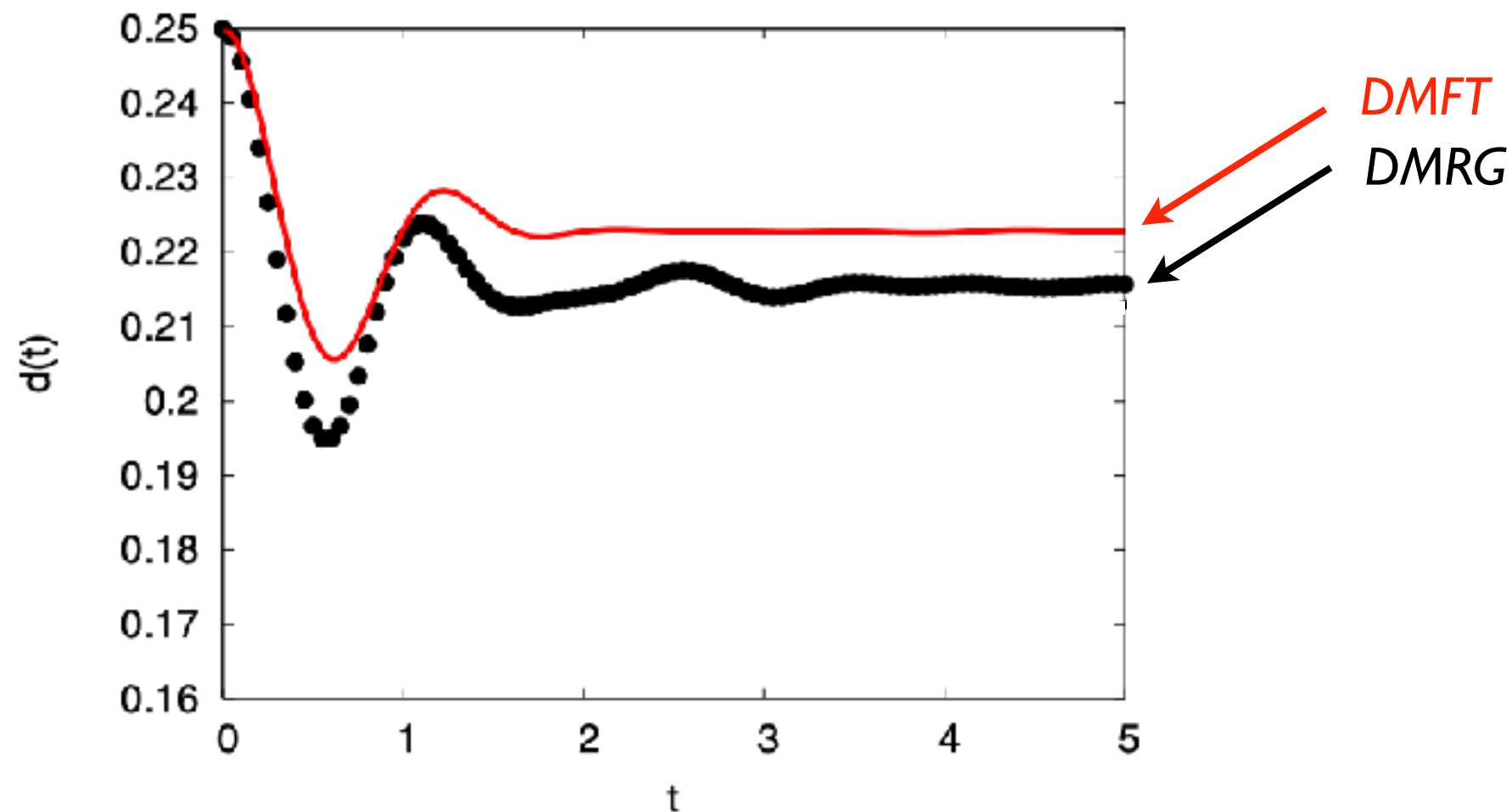
- **Formula contains time-energy uncertainty**

Accuracy of nonequilibrium DMFT

- Benchmark against DMRG for 1D Hubbard model

- Quench from $U=0$ to $U=1$

Tsuji, Barmettler, Aoki & Werner (2014)

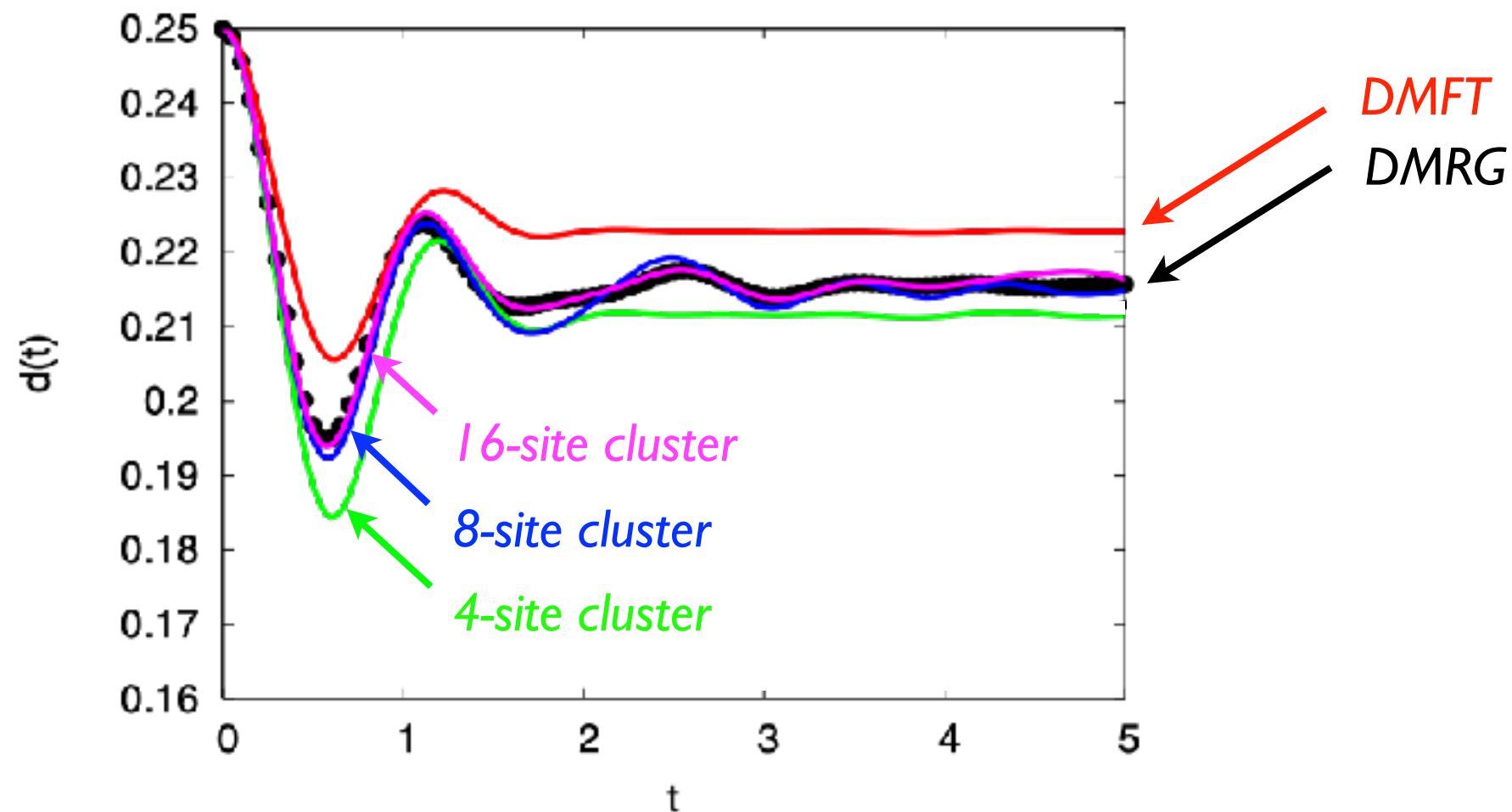


Accuracy of nonequilibrium DMFT

- **Benchmark against DMRG for 1D Hubbard model**

- Quench from $U=0$ to $U=1$

Tsuji, Barmettler, Aoki & Werner (2014)

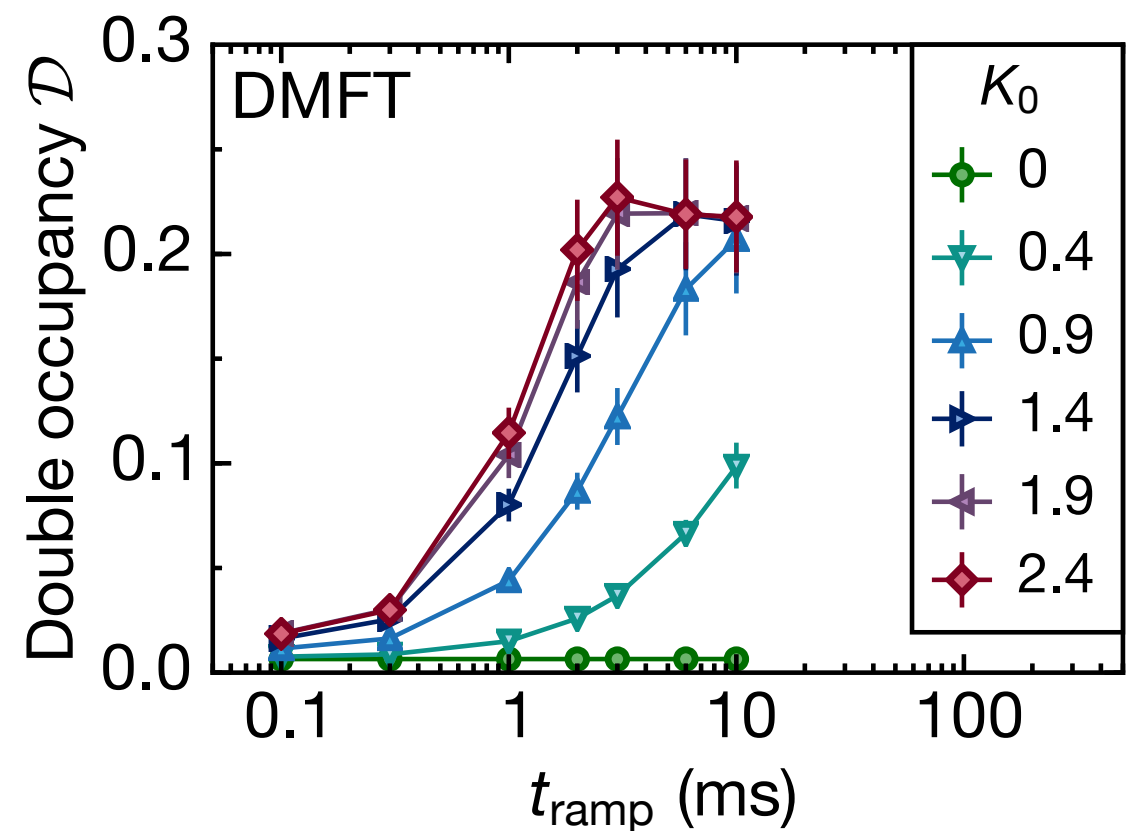
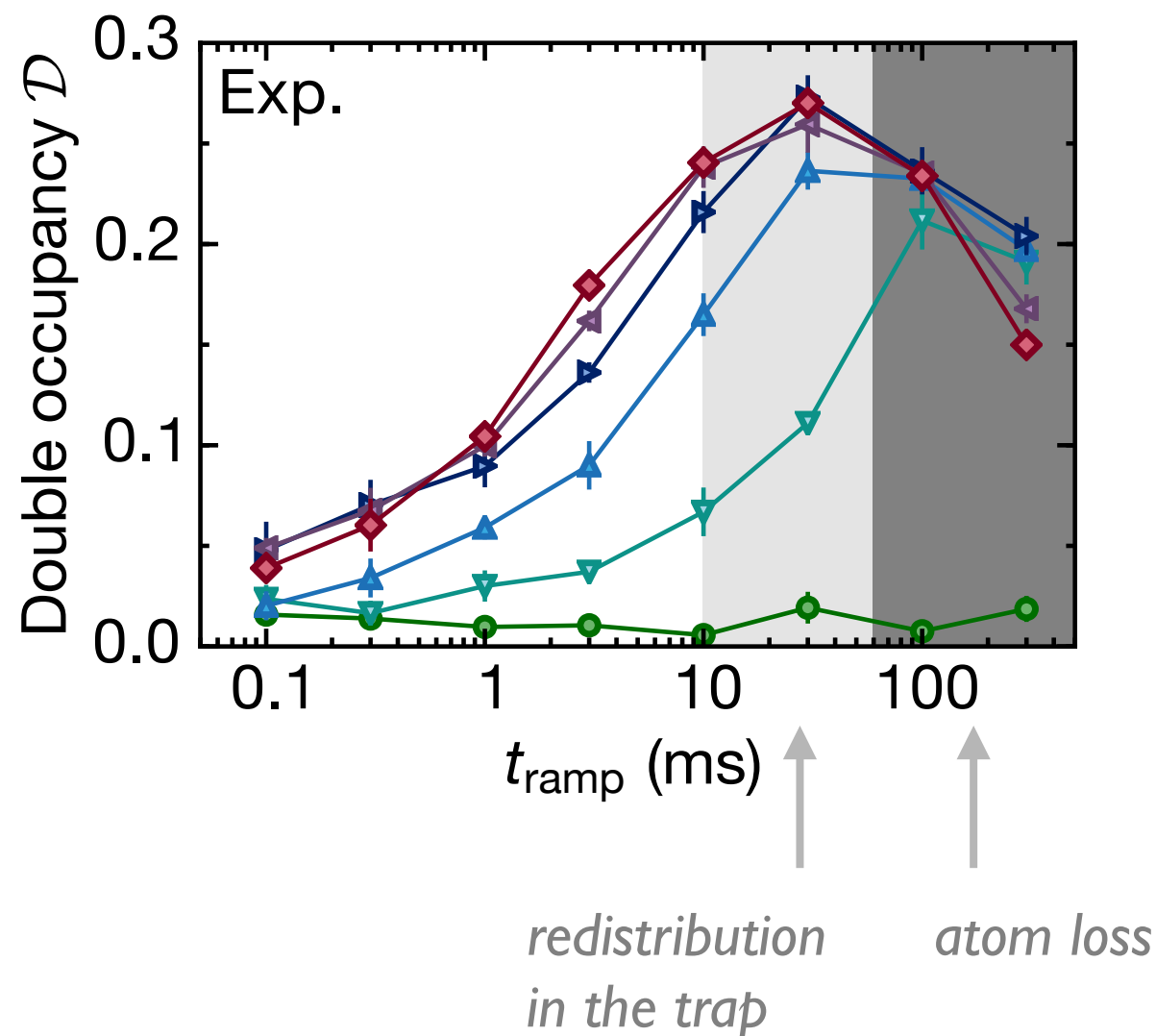


- **Cluster extensions of DMFT** capture short-range correlations

Tsuji et al. (2014); Eckstein & Werner (2016); Bittner et al. (2019)

Accuracy of nonequilibrium DMFT

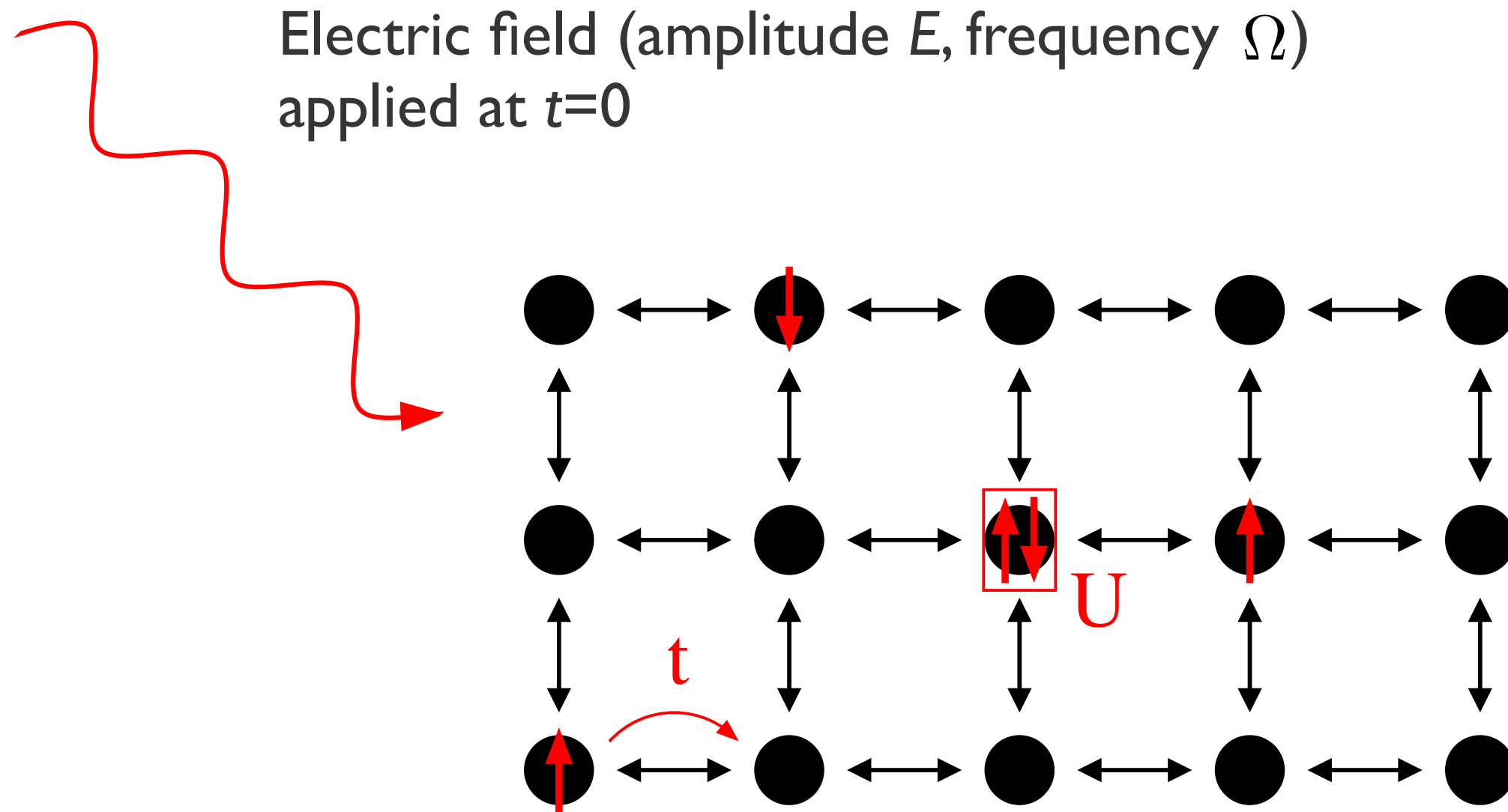
- **Benchmark against cold atom simulator** *Sandholzer et al. (2019)*
 - Resonant excitation ($\Omega = U$) of Mott insulating Hubbard model
 - linear ramp of pulse amplitude K_0



I. Periodic electric fields

- AC-field quench in the Hubbard model (metal phase)

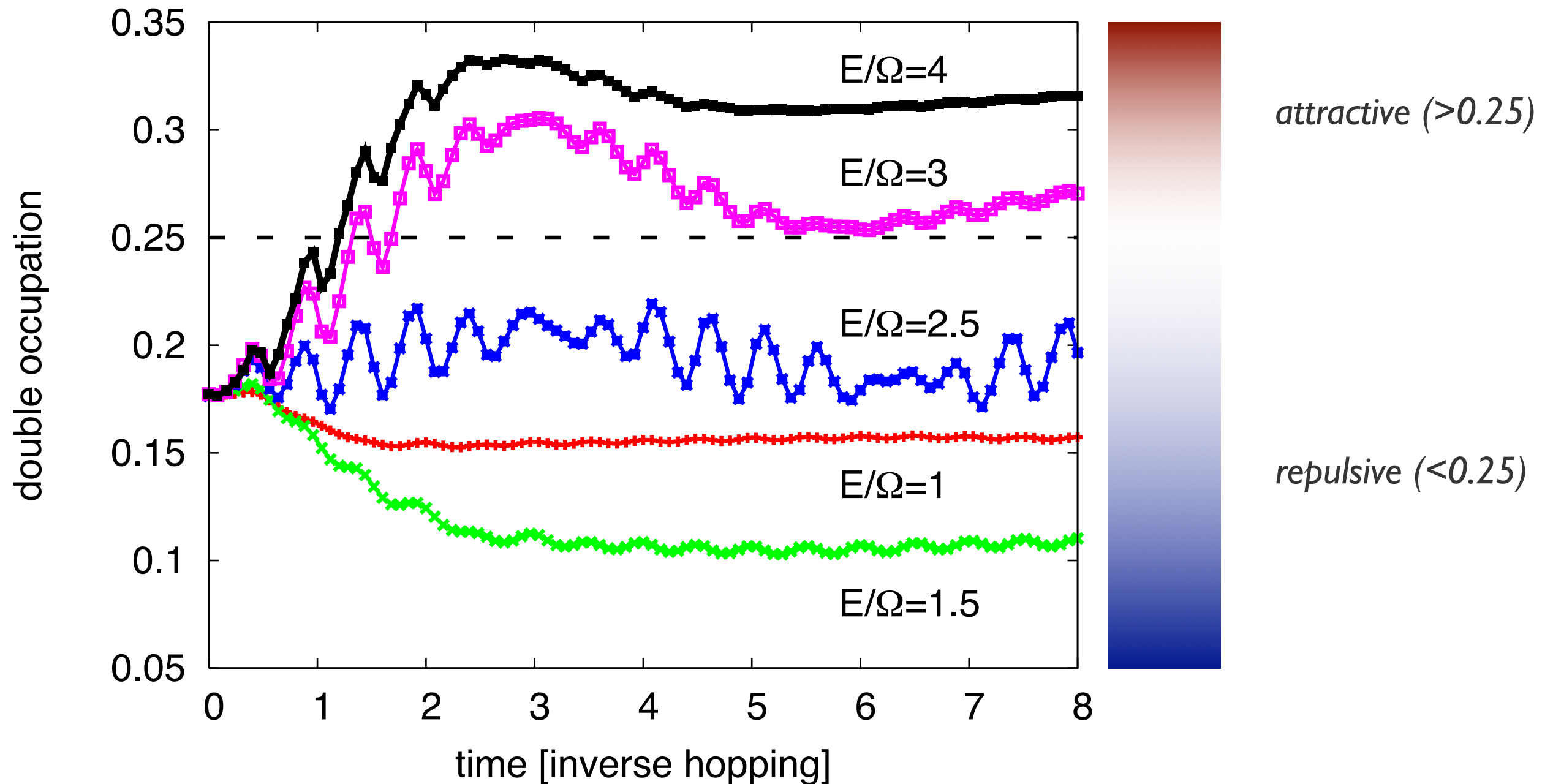
Tsuji, Oka, Werner and Aoki (2011)



I. Periodic electric fields

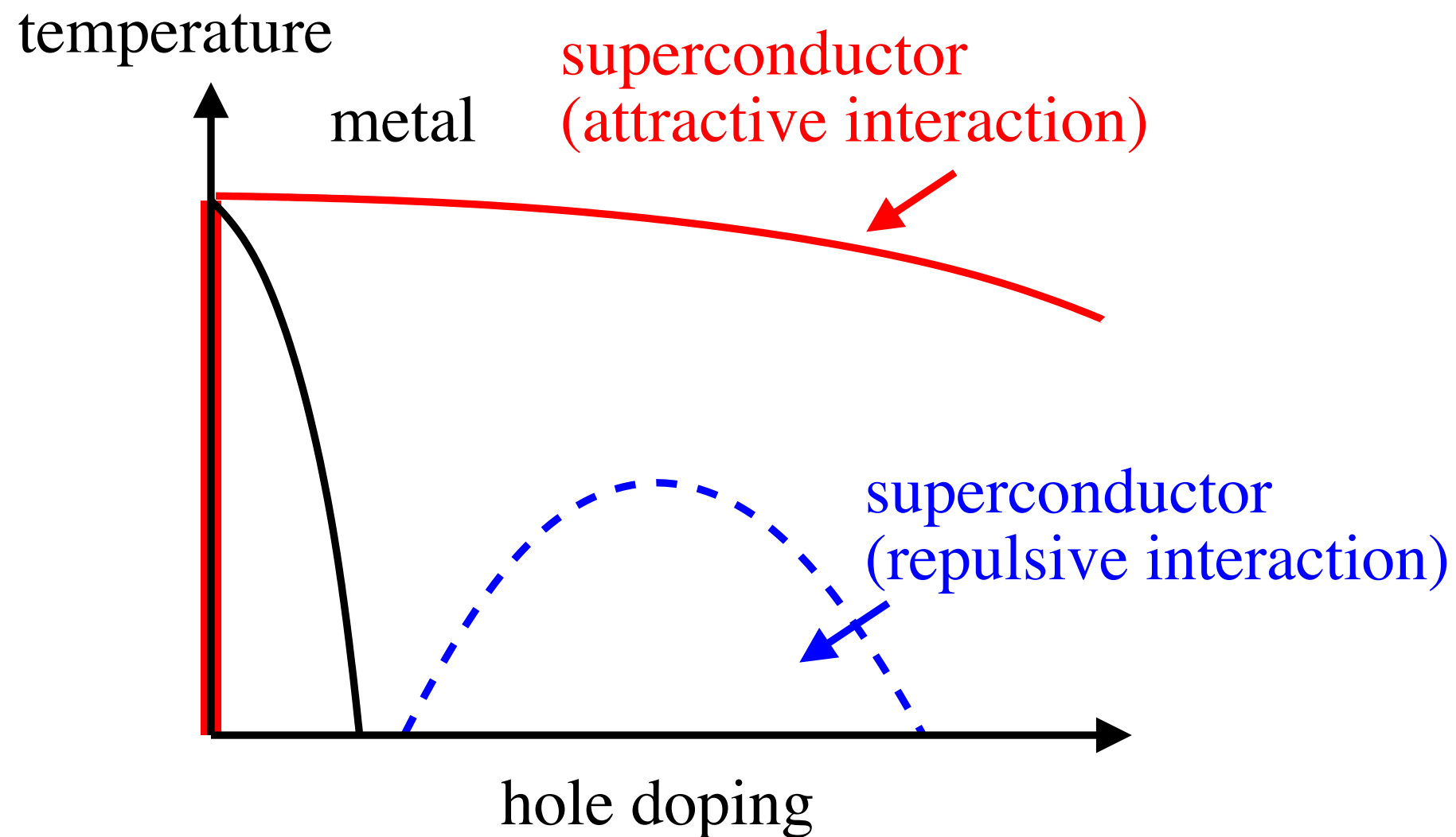
- AC-field quench in the Hubbard model (metal phase)

Tsuji, Oka, Werner and Aoki (2011)



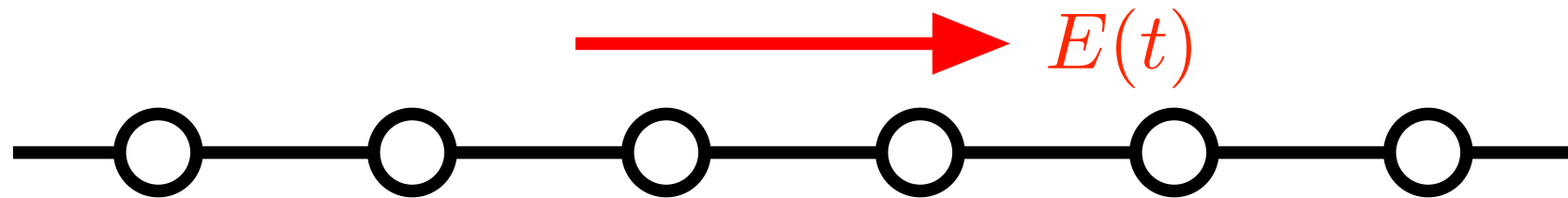
I. Periodic electric fields

- **AC-field quench in the Hubbard model (metal phase)**
 - Sign inversion of the interaction: **repulsive \leftrightarrow attractive**
 - *Dynamically generated high-T_c superconductivity?*



I. Origin of the attractive interaction

- Periodic E-field leads to a population inversion



- Gauge with pure vector potential

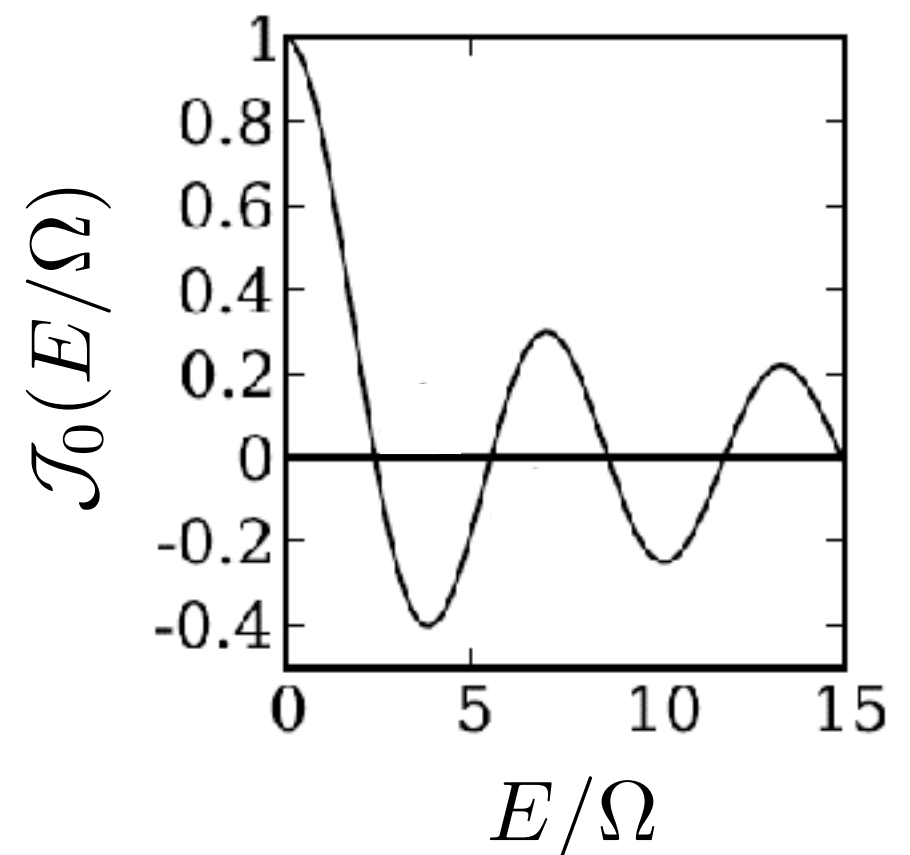
$$E(t) = E \cos(\Omega t) = -\partial_t A(t)$$

$$\Rightarrow A(t) = -\left(\frac{E}{\Omega}\right) \sin(\Omega t)$$

- Peierls substitution $\epsilon_k \rightarrow \epsilon_{k-A(t)}$

- Renormalized dispersion

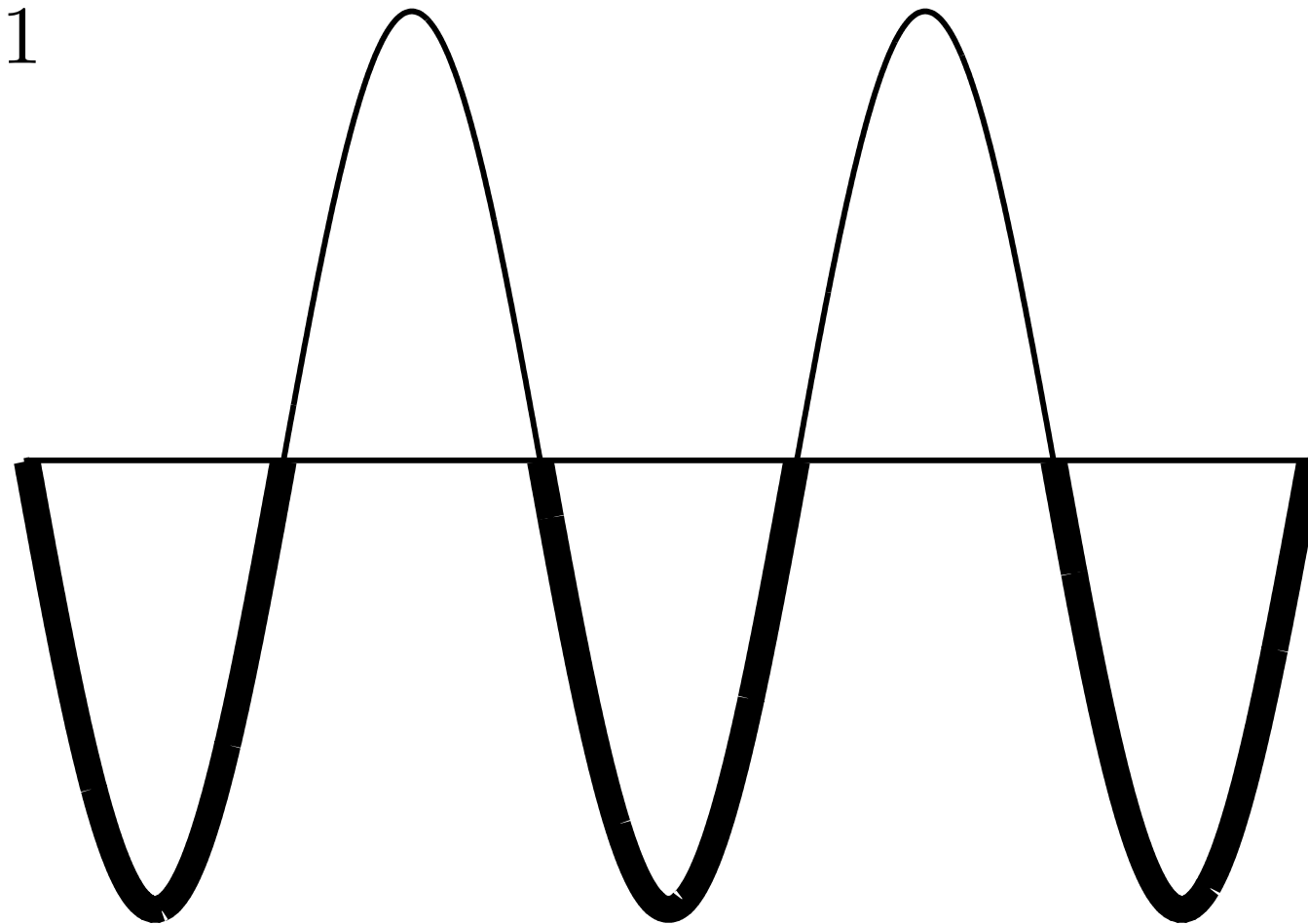
$$\overline{\epsilon}_k = \frac{\Omega}{2\pi} \int_0^{2\pi/\Omega} dt \epsilon_{k-A(t)} = \mathcal{J}_0(E/\Omega) \epsilon_k$$



I. Origin of the attractive interaction

- Periodic E-field leads to a population inversion

$$\mathcal{J}_0(E/\Omega) = 1$$



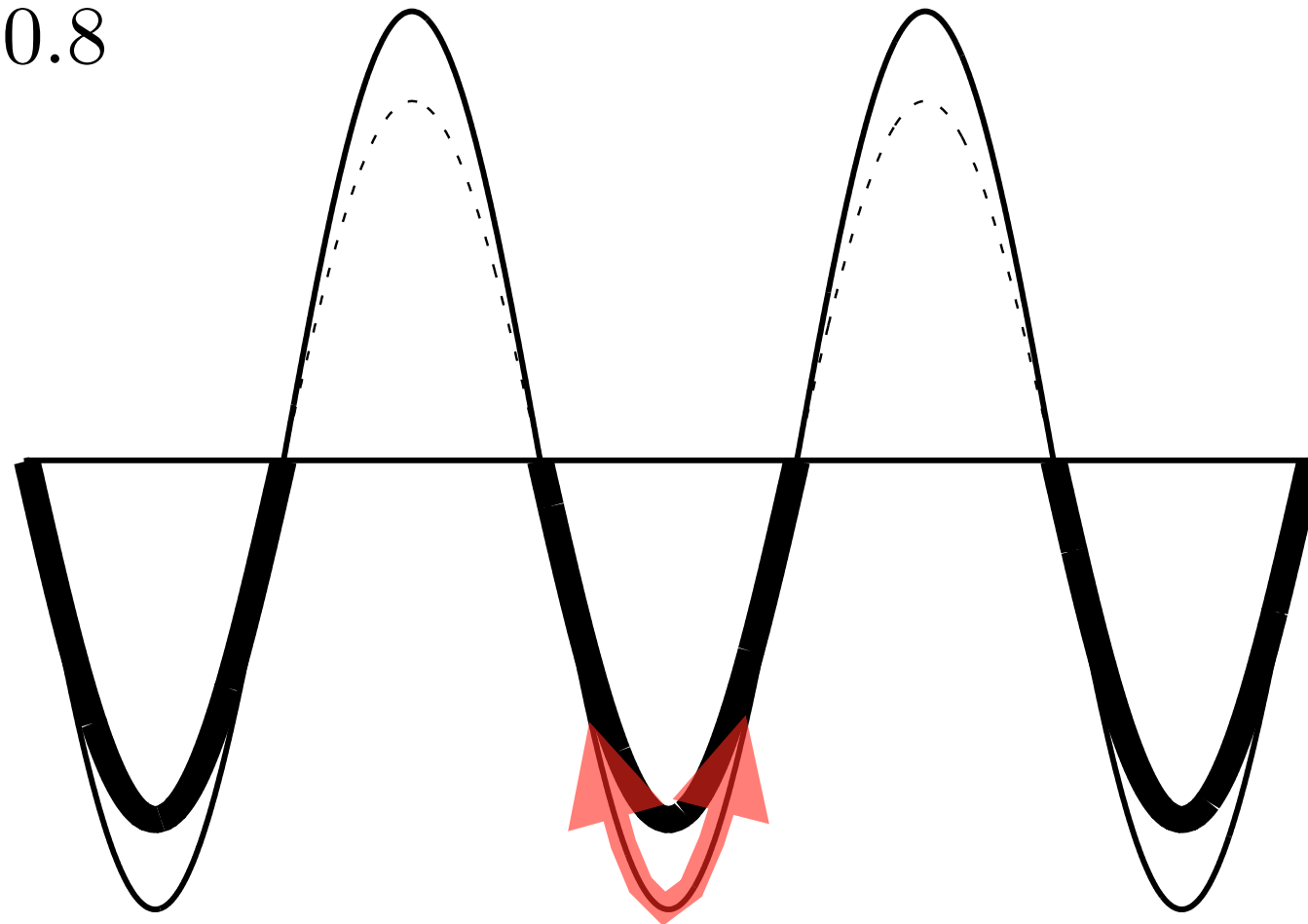
- Renormalized dispersion

$$\overline{\epsilon}_k = \frac{\Omega}{2\pi} \int_0^{2\pi/\Omega} dt \epsilon_{k-A(t)} = \mathcal{J}_0(E/\Omega) \epsilon_k$$

I. Origin of the attractive interaction

- Periodic E-field leads to a population inversion

$$\mathcal{J}_0(E/\Omega) = 0.8$$



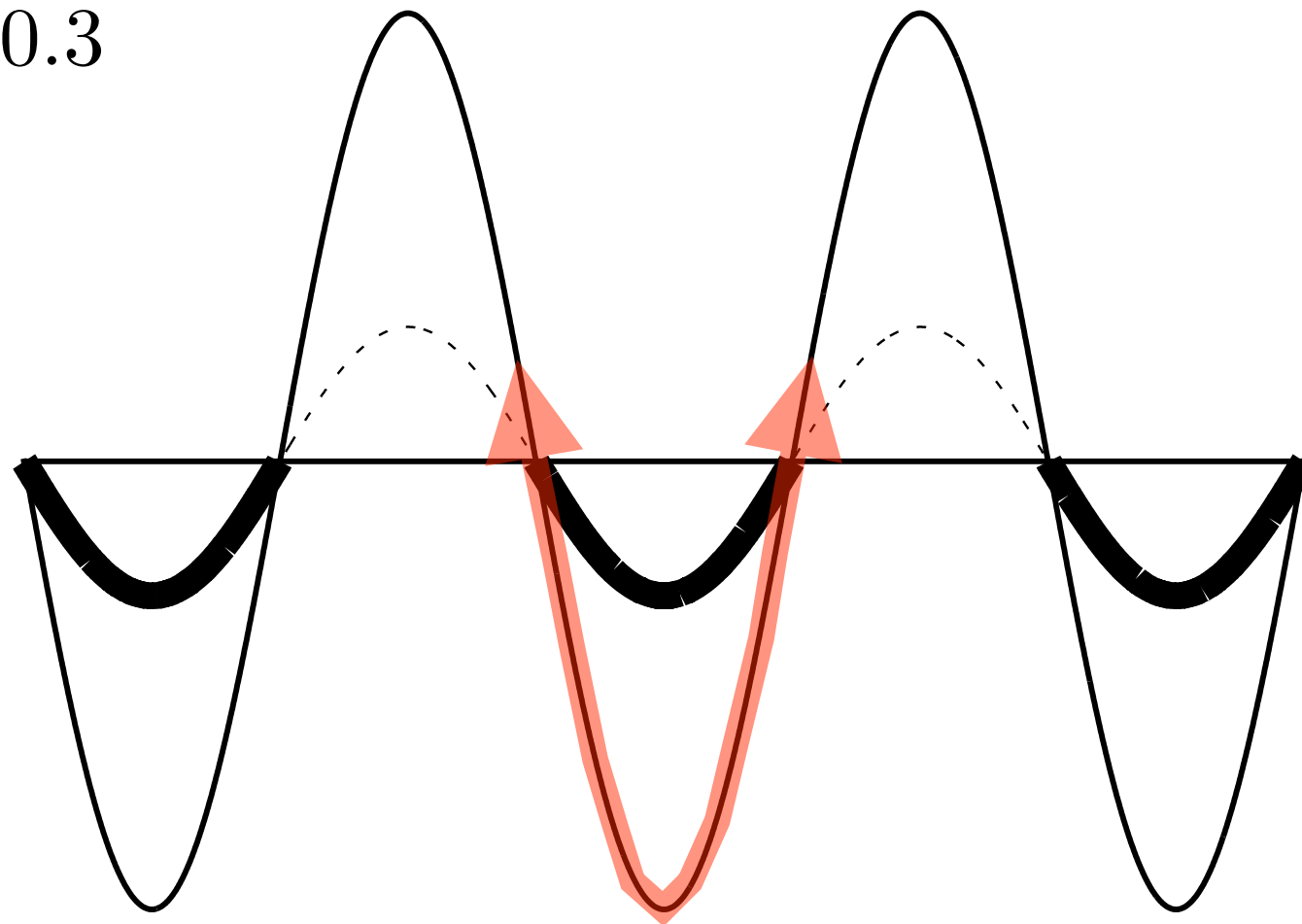
- Renormalized dispersion

$$\overline{\epsilon}_k = \frac{\Omega}{2\pi} \int_0^{2\pi/\Omega} dt \epsilon_{k-A(t)} = \mathcal{J}_0(E/\Omega) \epsilon_k$$

I. Origin of the attractive interaction

- **Periodic E-field leads to a population inversion**

$$\mathcal{J}_0(E/\Omega) = 0.3$$



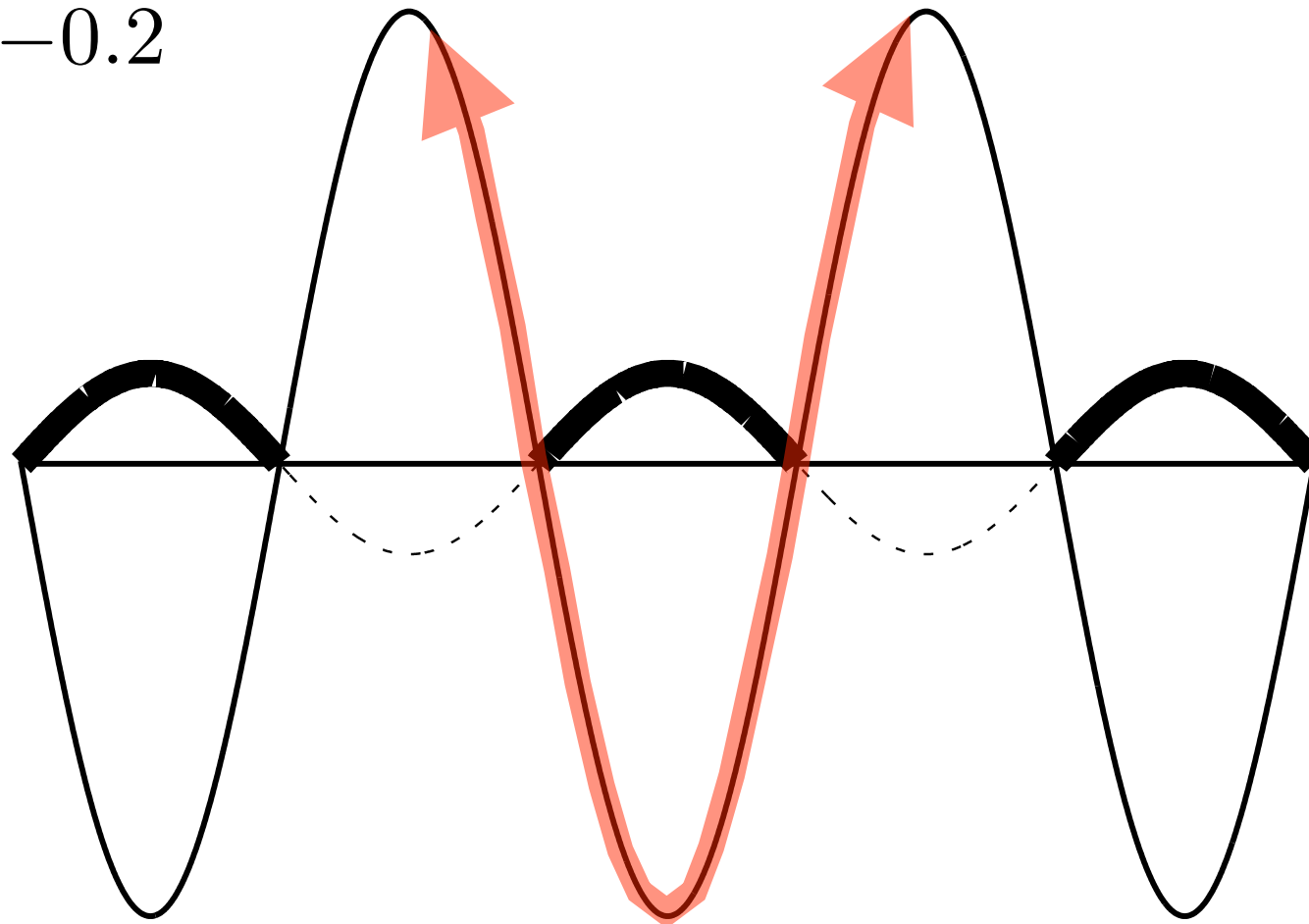
- Renormalized dispersion

$$\overline{\epsilon}_k = \frac{\Omega}{2\pi} \int_0^{2\pi/\Omega} dt \epsilon_{k-A(t)} = \mathcal{J}_0(E/\Omega) \epsilon_k$$

I. Origin of the attractive interaction

- **Periodic E-field leads to a population inversion**

$$\mathcal{J}_0(E/\Omega) = -0.2$$



- Renormalized dispersion

$$\overline{\epsilon}_k = \frac{\Omega}{2\pi} \int_0^{2\pi/\Omega} dt \epsilon_{k-A(t)} = \mathcal{J}_0(E/\Omega) \epsilon_k$$

I. Origin of the attractive interaction

- Inverted population = negative temperature
- State with $U > 0, T < 0$ is equivalent to state with $U < 0, T > 0$

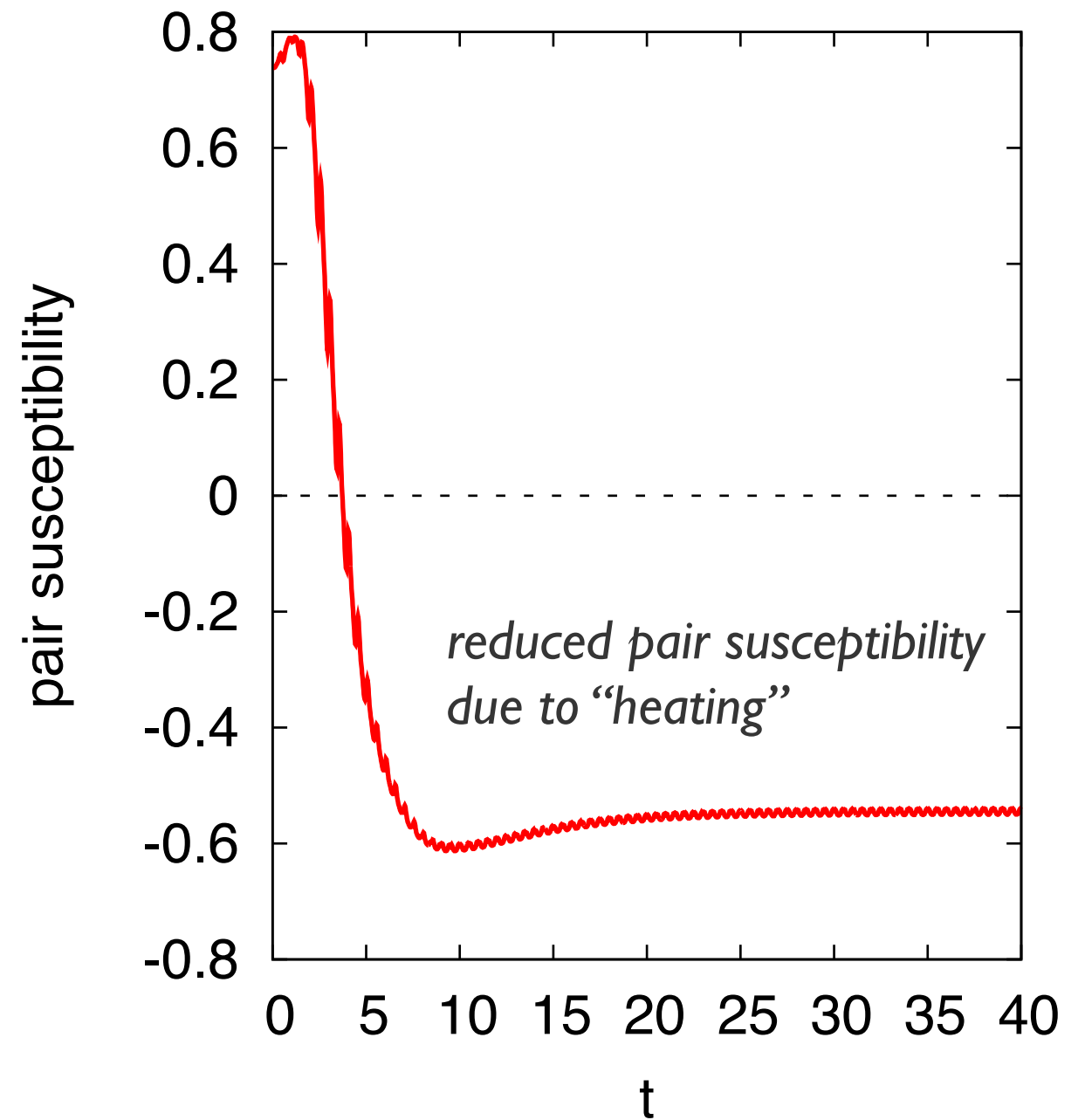
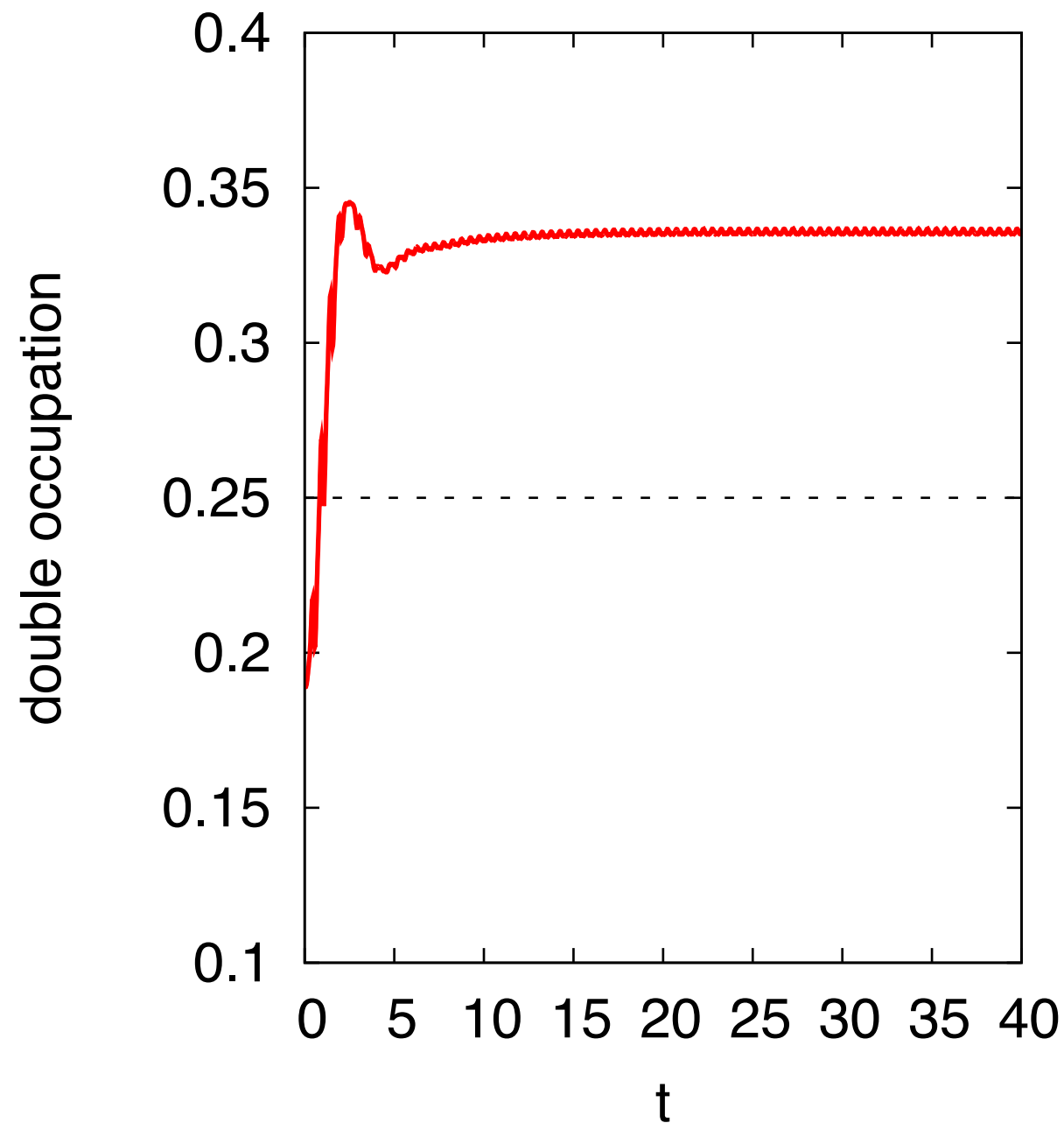
$$\begin{aligned} \tilde{T} < 0, \mathcal{J}_0 < 0 & \quad \rho \propto \exp \left(-\frac{1}{\tilde{T}} \left[\sum_{k\sigma} \mathcal{J}_0 \epsilon_k n_{k\sigma} + U \sum_i n_{i\uparrow} n_{i\downarrow} \right] \right) \\ T_{\text{eff}} = \frac{\tilde{T}}{\mathcal{J}_0} > 0 & \quad = \exp \left(-\frac{1}{T_{\text{eff}}} \left[\sum_{k\sigma} \epsilon_k n_{k\sigma} + \frac{U}{\mathcal{J}_0} \sum_i n_{i\uparrow} n_{i\downarrow} \right] \right) \end{aligned}$$

- Effective interaction of the $T_{\text{eff}} > 0$ state

$$U_{\text{eff}} = \frac{U}{\mathcal{J}_0(E/\Omega)}$$

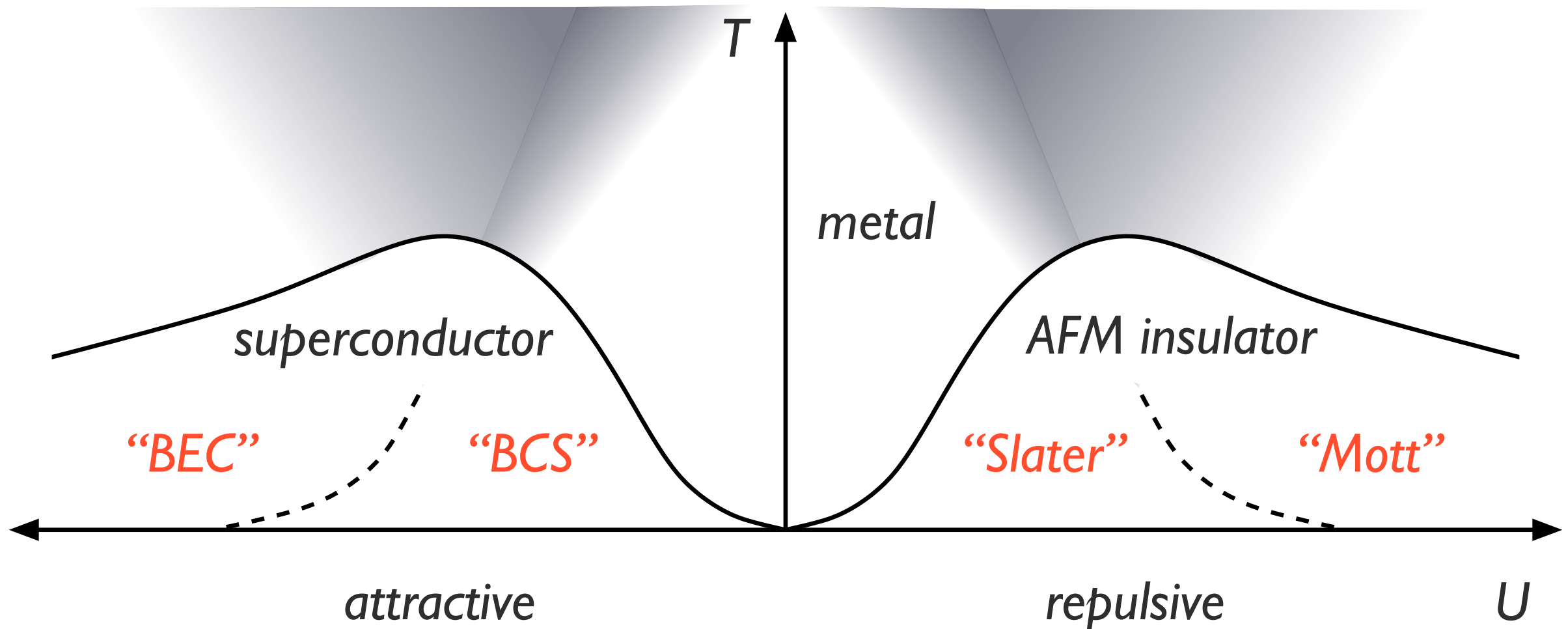
I. Effect on superconductivity

- AC-field quench from $U = 1$ to $U_{\text{eff}} = -2.5$ (NCA solver)



II. Nonthermal symmetry-broken states

- **Equilibrium DMFT phase diagram (half-filling)**
- Half-filling: transformation $c_{i\uparrow} \rightarrow c_{i\uparrow}^\dagger$ ($i \in A$), $c_{i\uparrow} \rightarrow -c_{i\uparrow}^\dagger$ ($i \in B$)
maps repulsive model onto attractive model

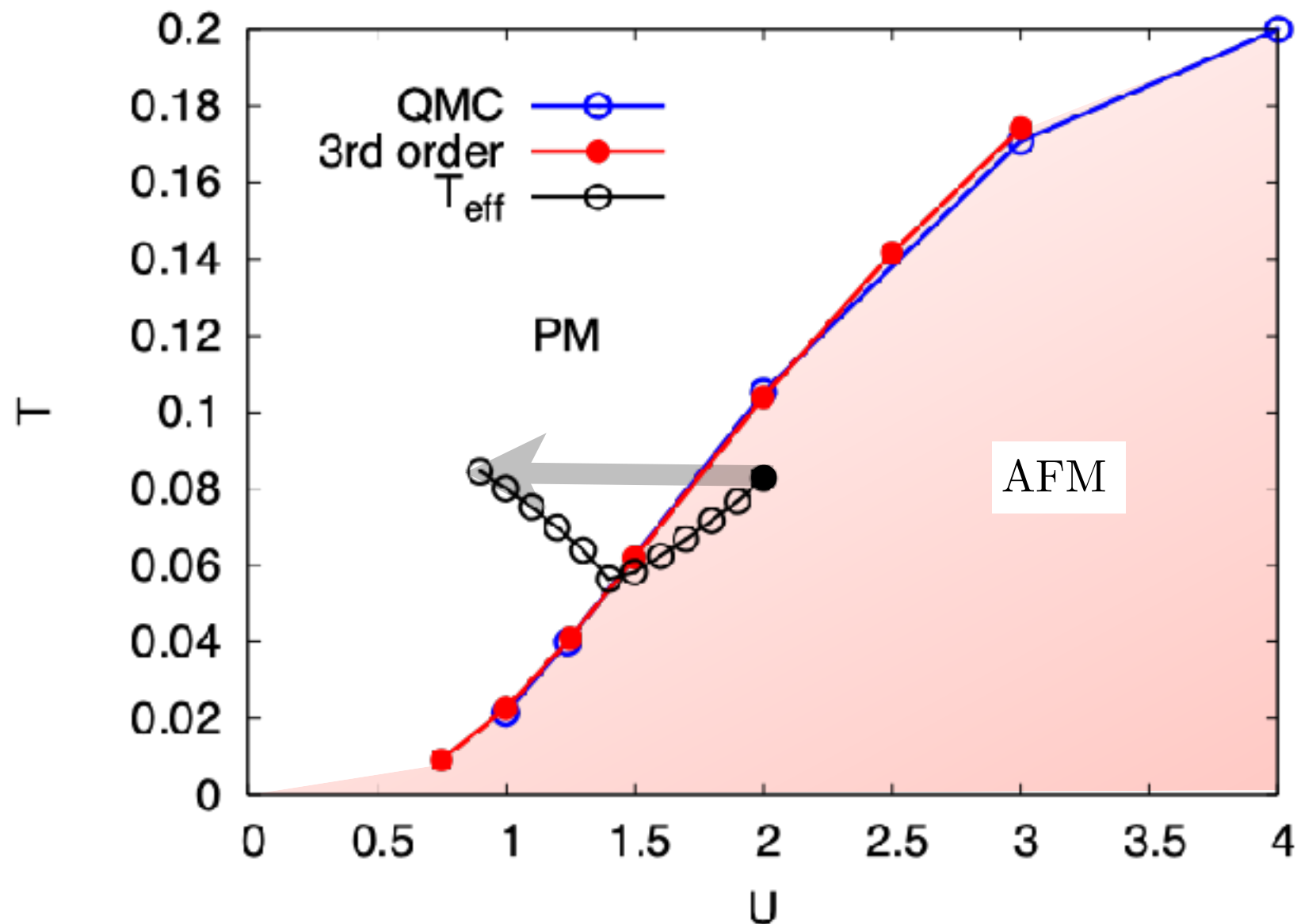


II. Nonthermal symmetry-broken states

- **Weak-coupling regime**

Tsuji, Eckstein & Werner (2012)

- Slow ramp from (Slater-)Antiferromagnet to Paramagnet

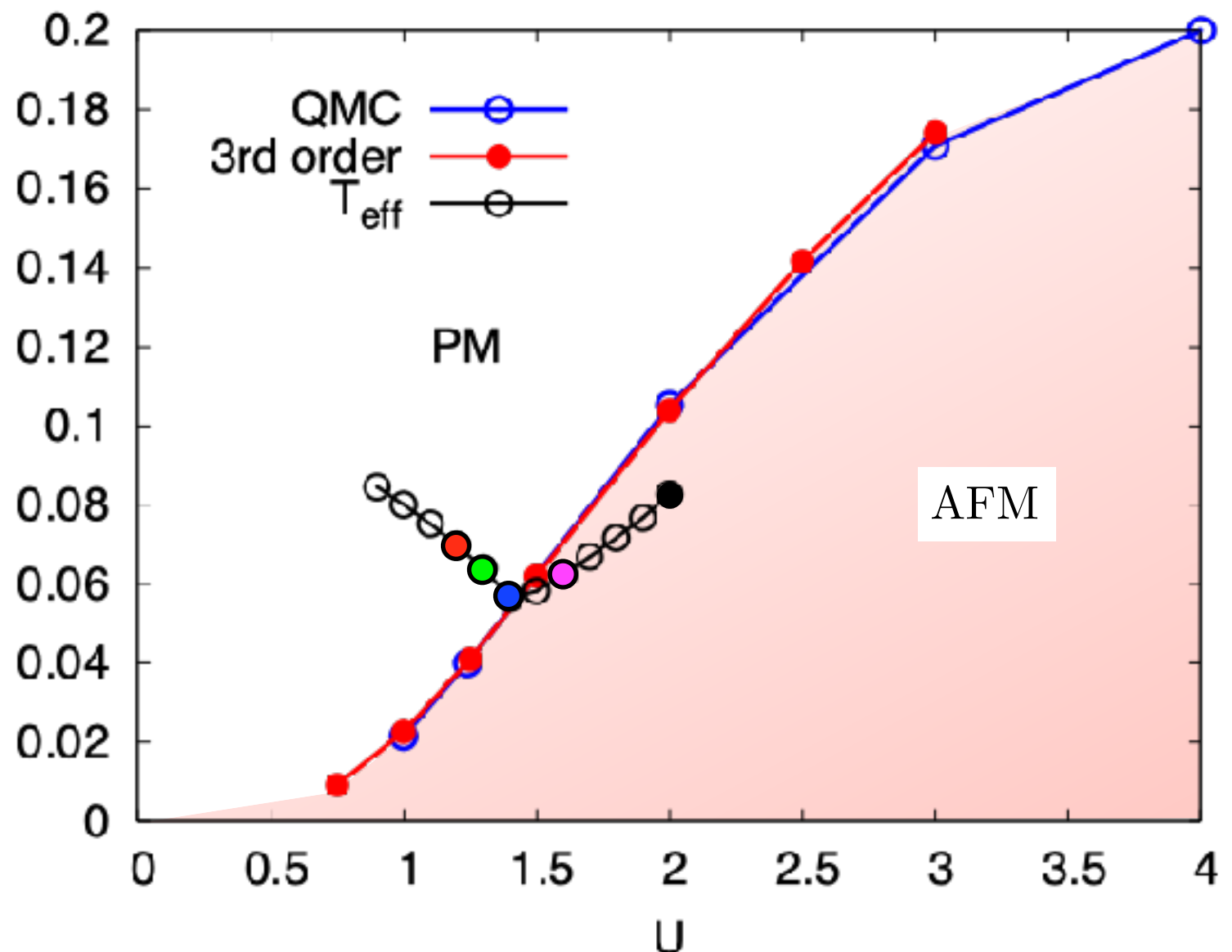
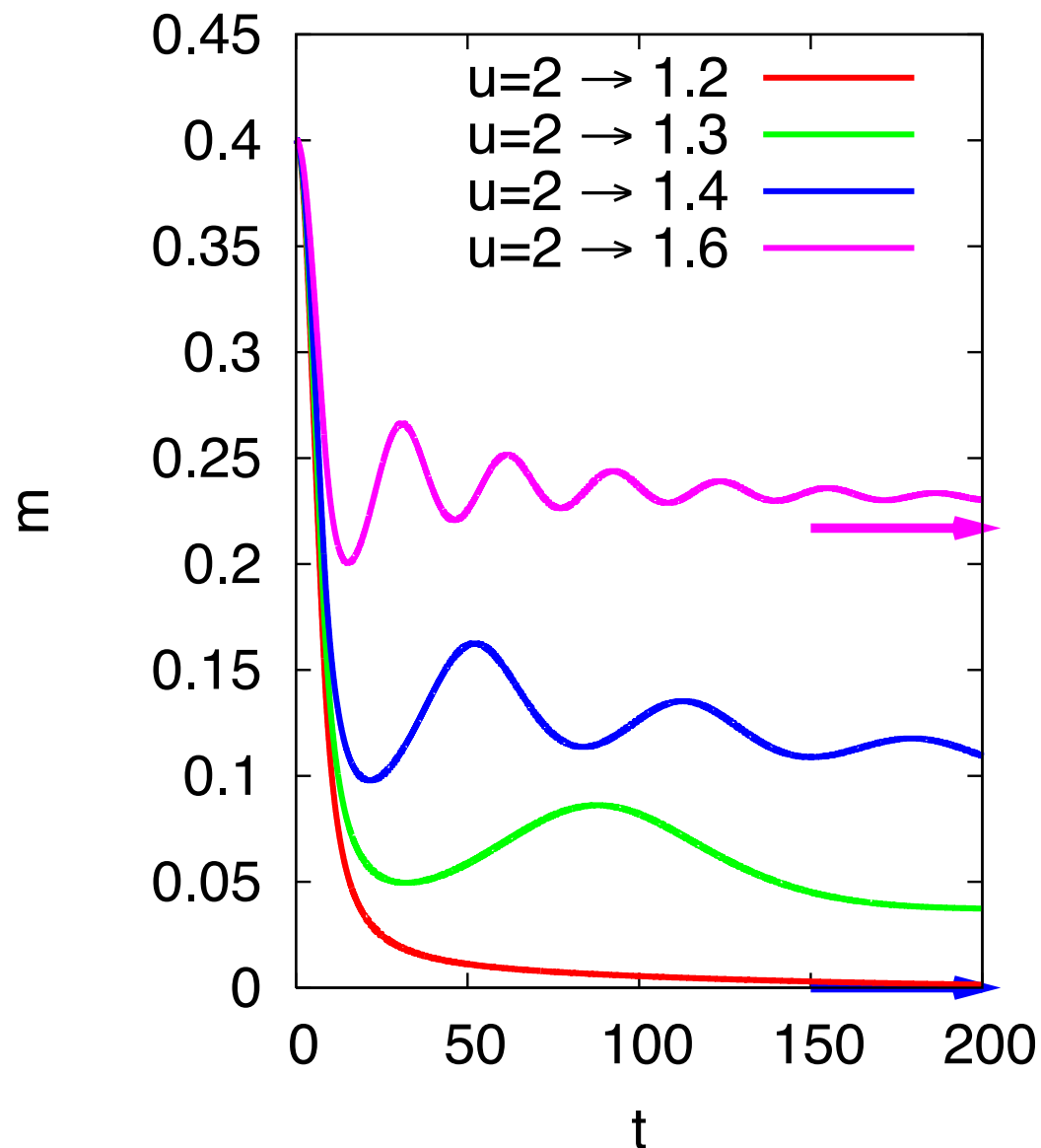


II. Nonthermal symmetry-broken states

- **Weak-coupling regime**

Tsuij, Eckstein & Werner (2012)

- Time-evolution of the magnetization for different final U

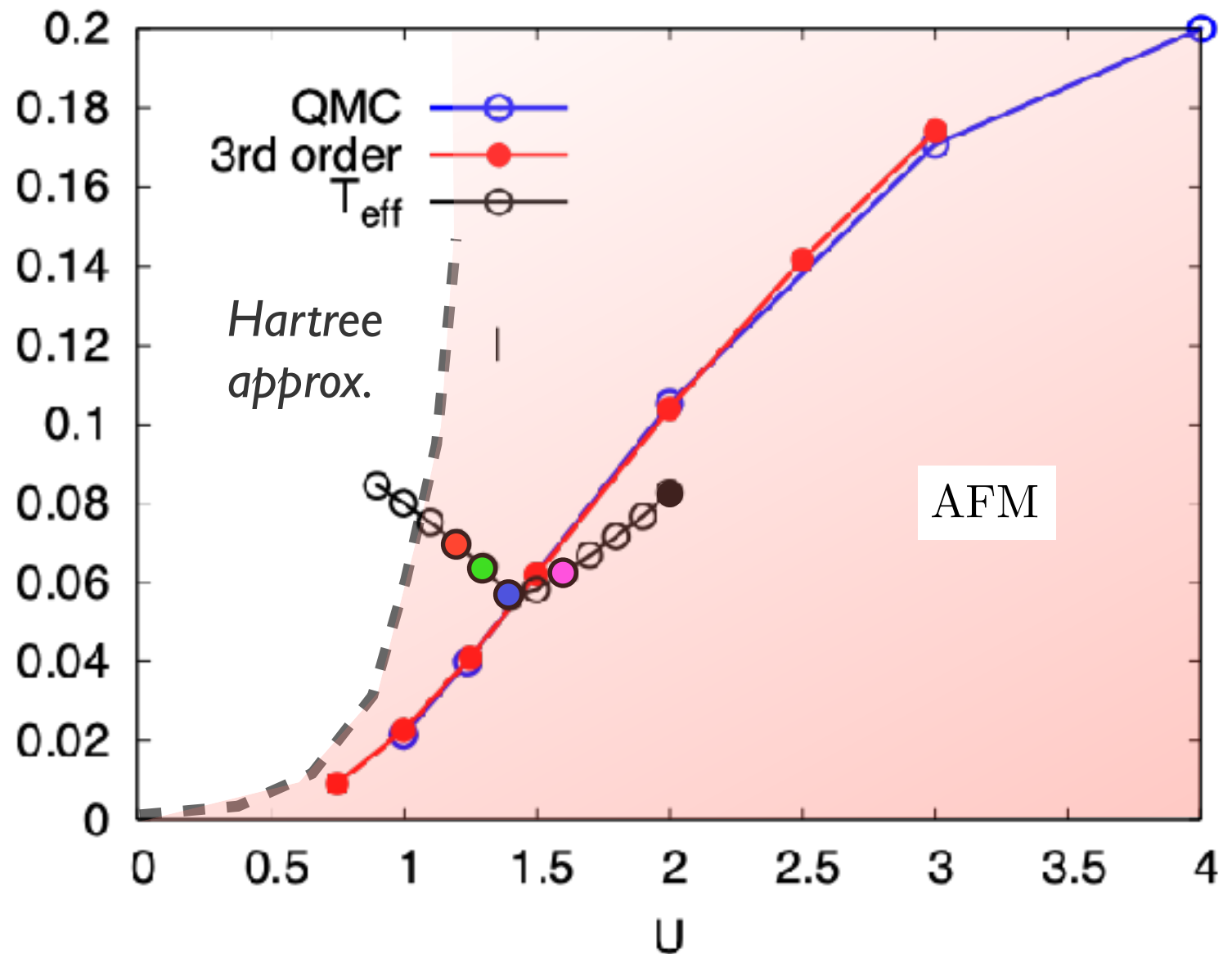
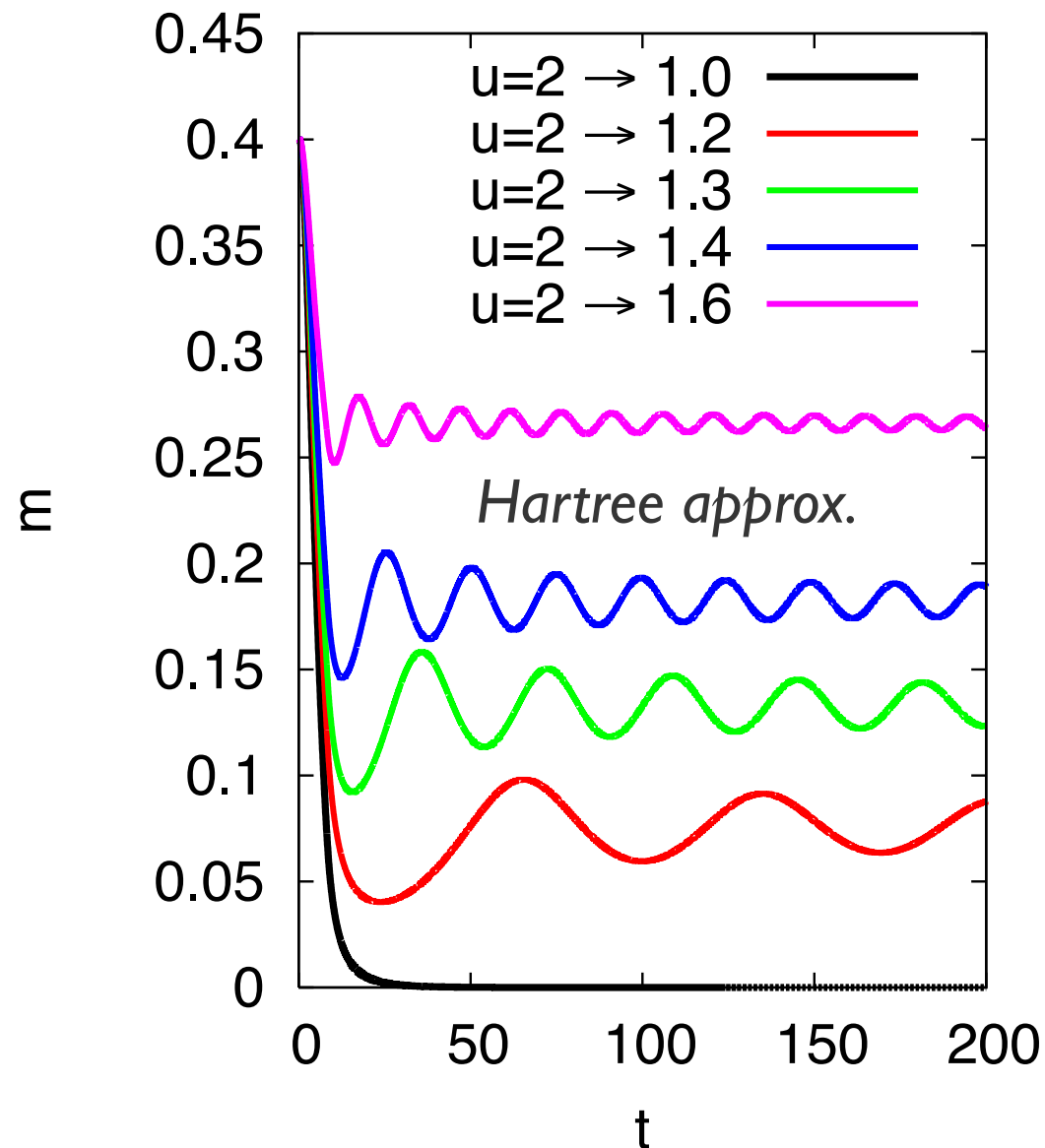


II. Nonthermal symmetry-broken states

- **Weak-coupling regime**

Tsui, Eckstein & Werner (2012)

- Time-evolution of the magnetization for different final U (Hartree)

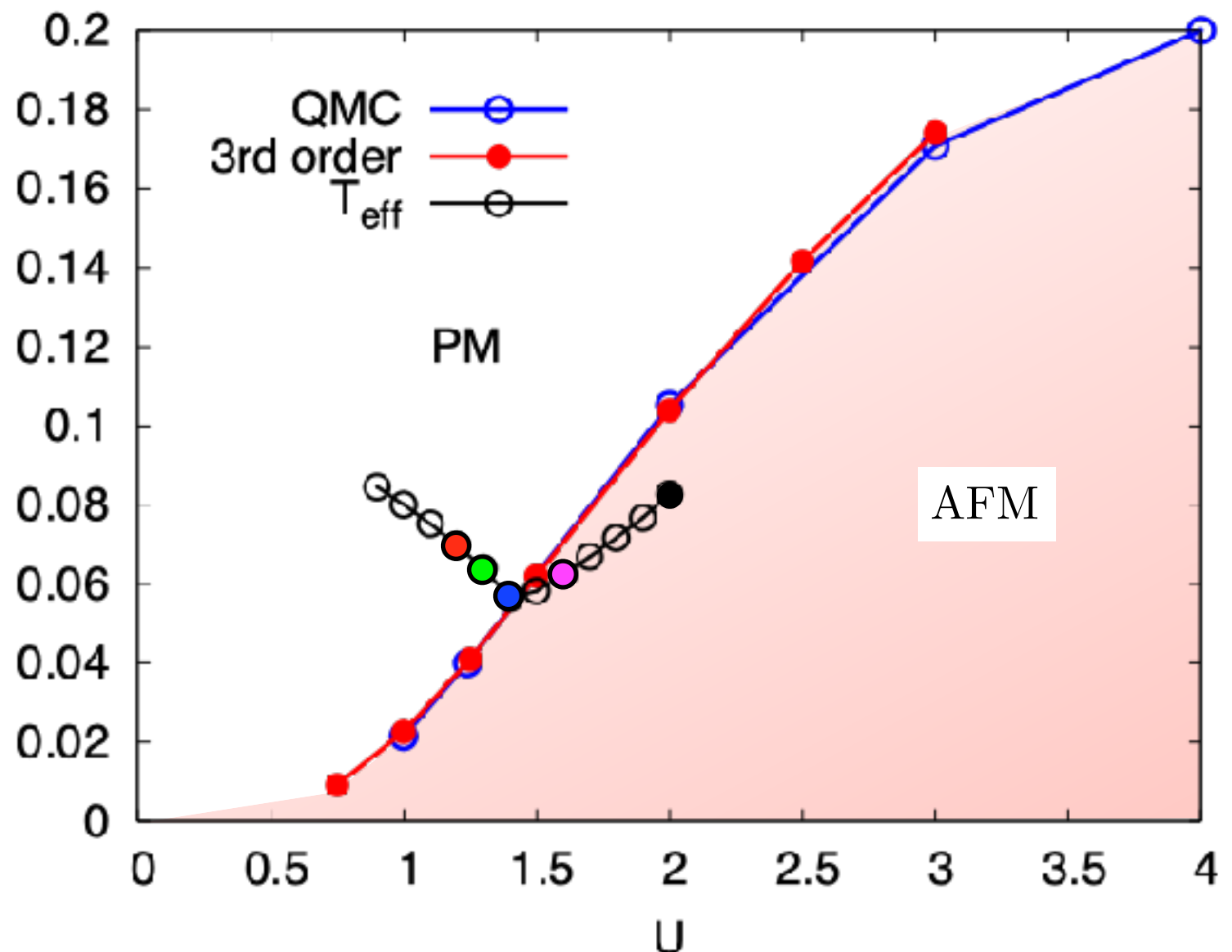
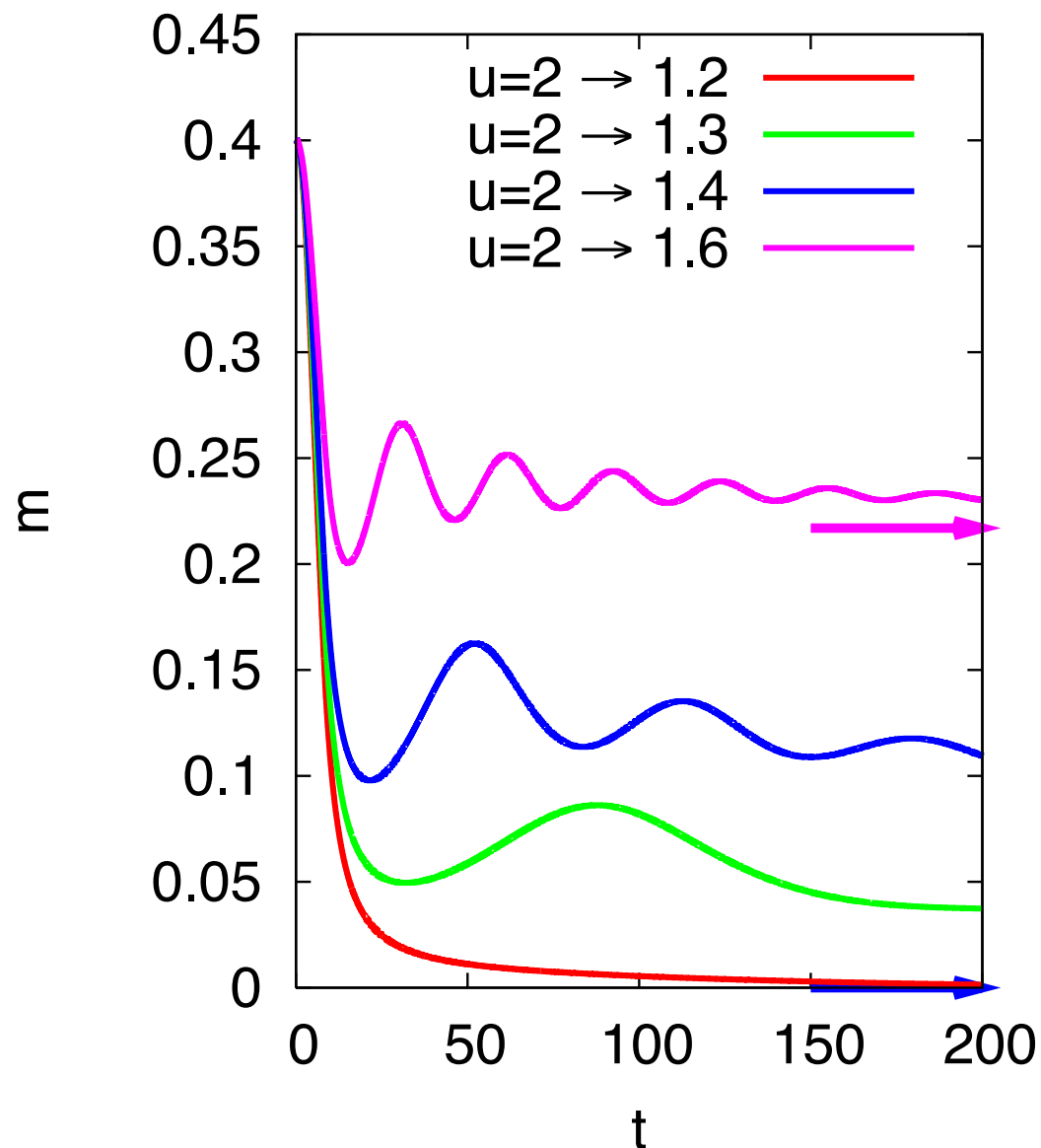


II. Nonthermal symmetry-broken states

- **Weak-coupling regime**

Tsuij, Eckstein & Werner (2012)

- Time-evolution of the magnetization for different final U

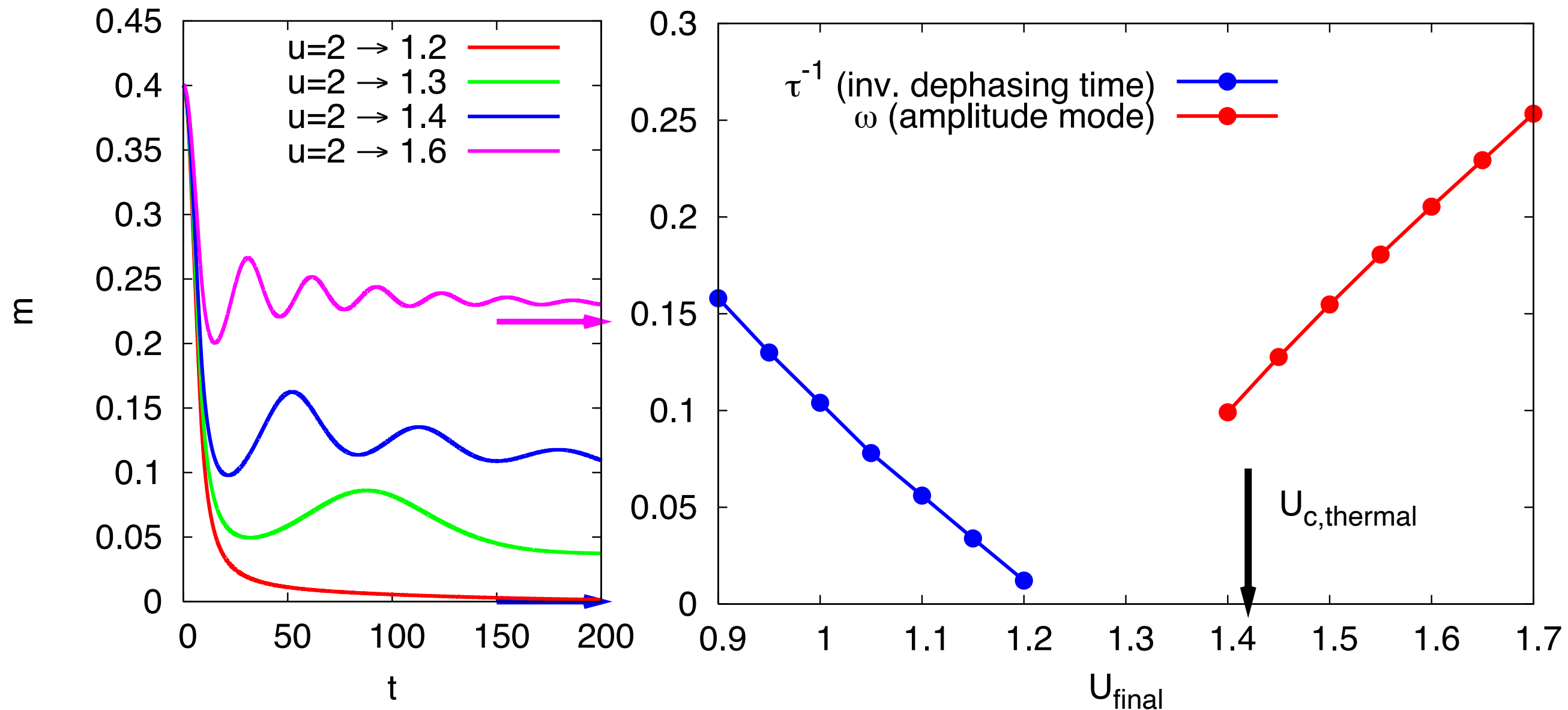


II. Nonthermal symmetry-broken states

- **Weak-coupling regime**

Tsuji, Eckstein & Werner (2012)

- Evidence for a **nonthermal critical point**

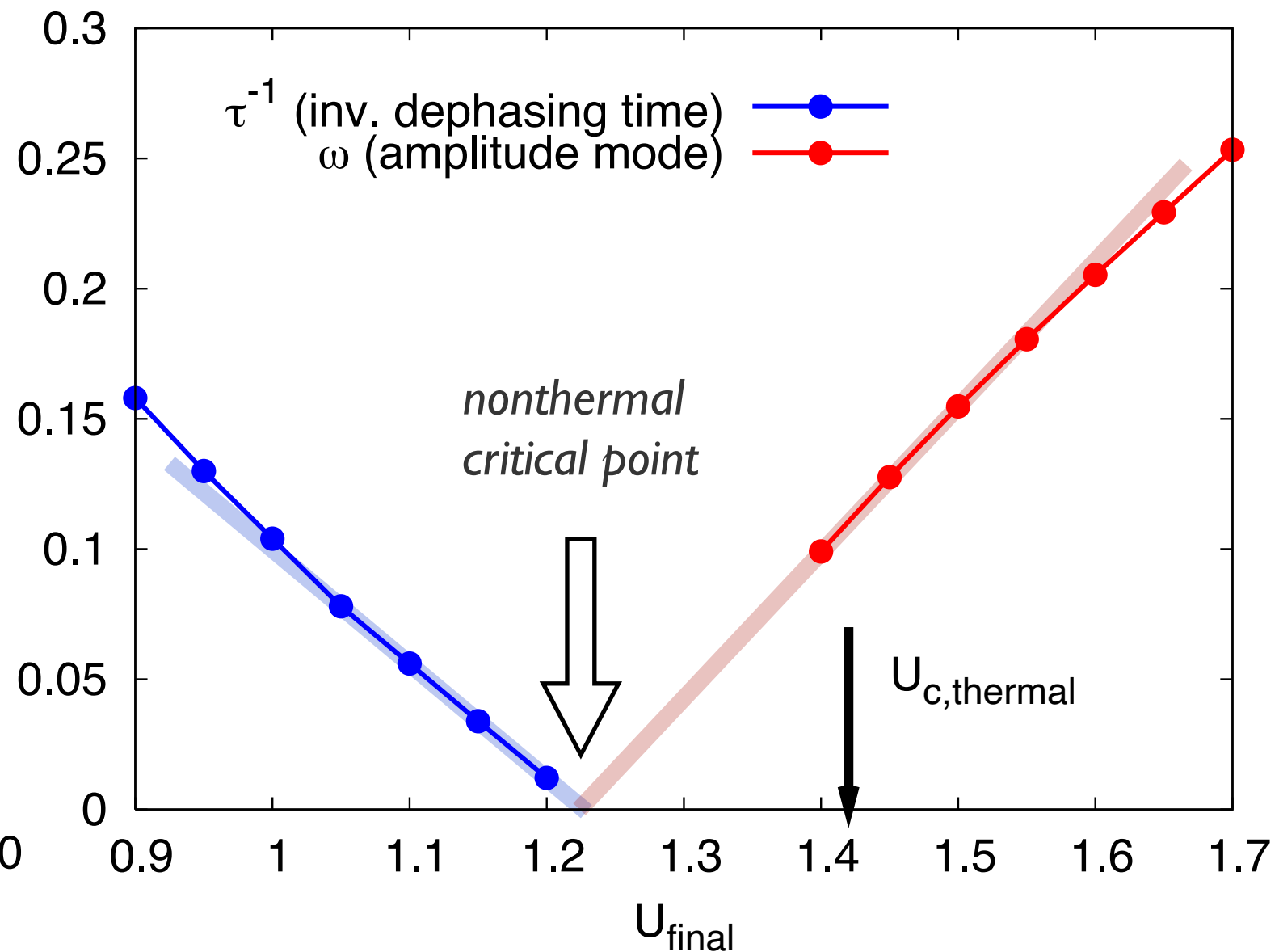
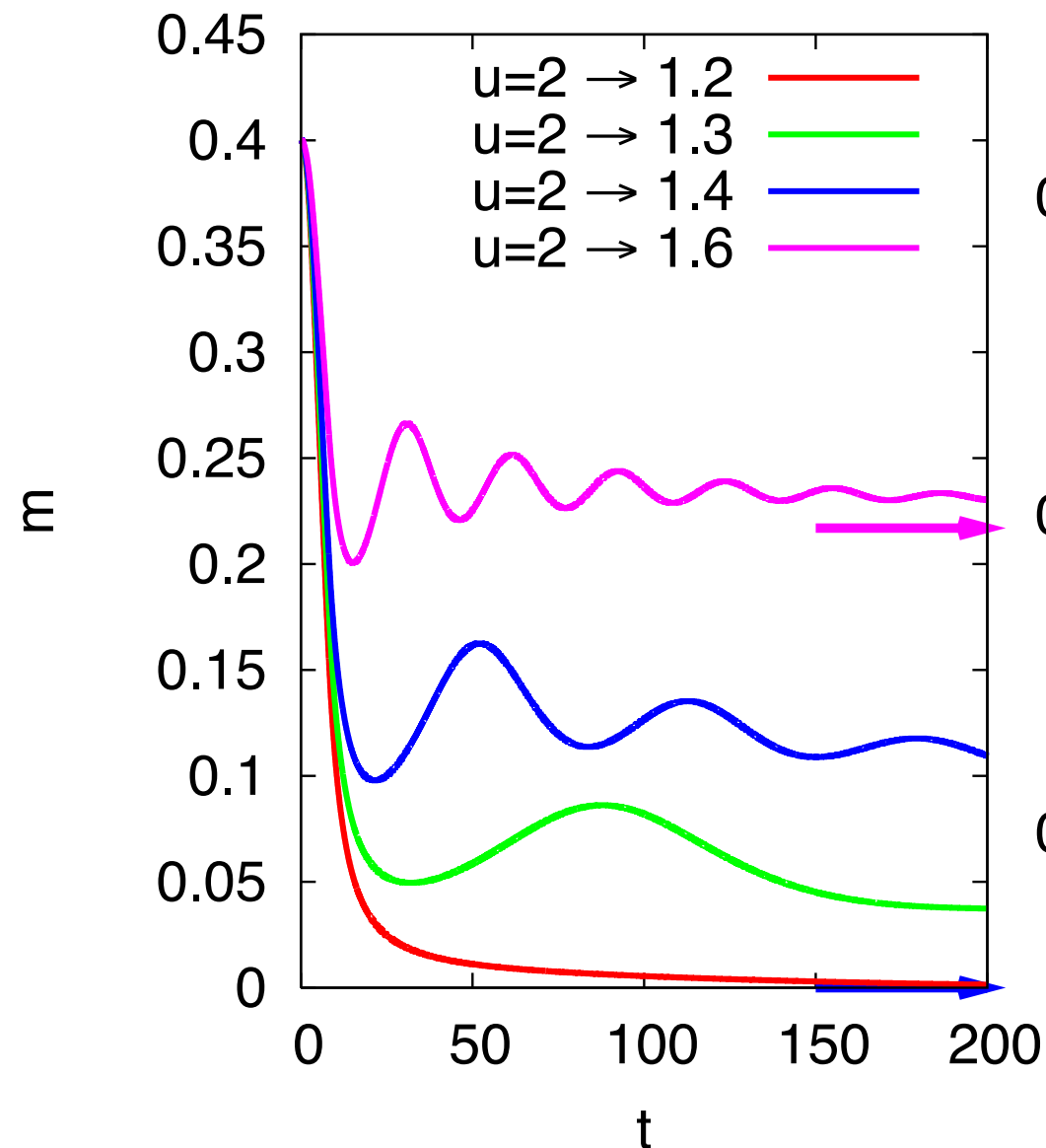


II. Nonthermal symmetry-broken states

- **Weak-coupling regime**

Tsuji, Eckstein & Werner (2012)

- Evidence for a **nonthermal critical point**

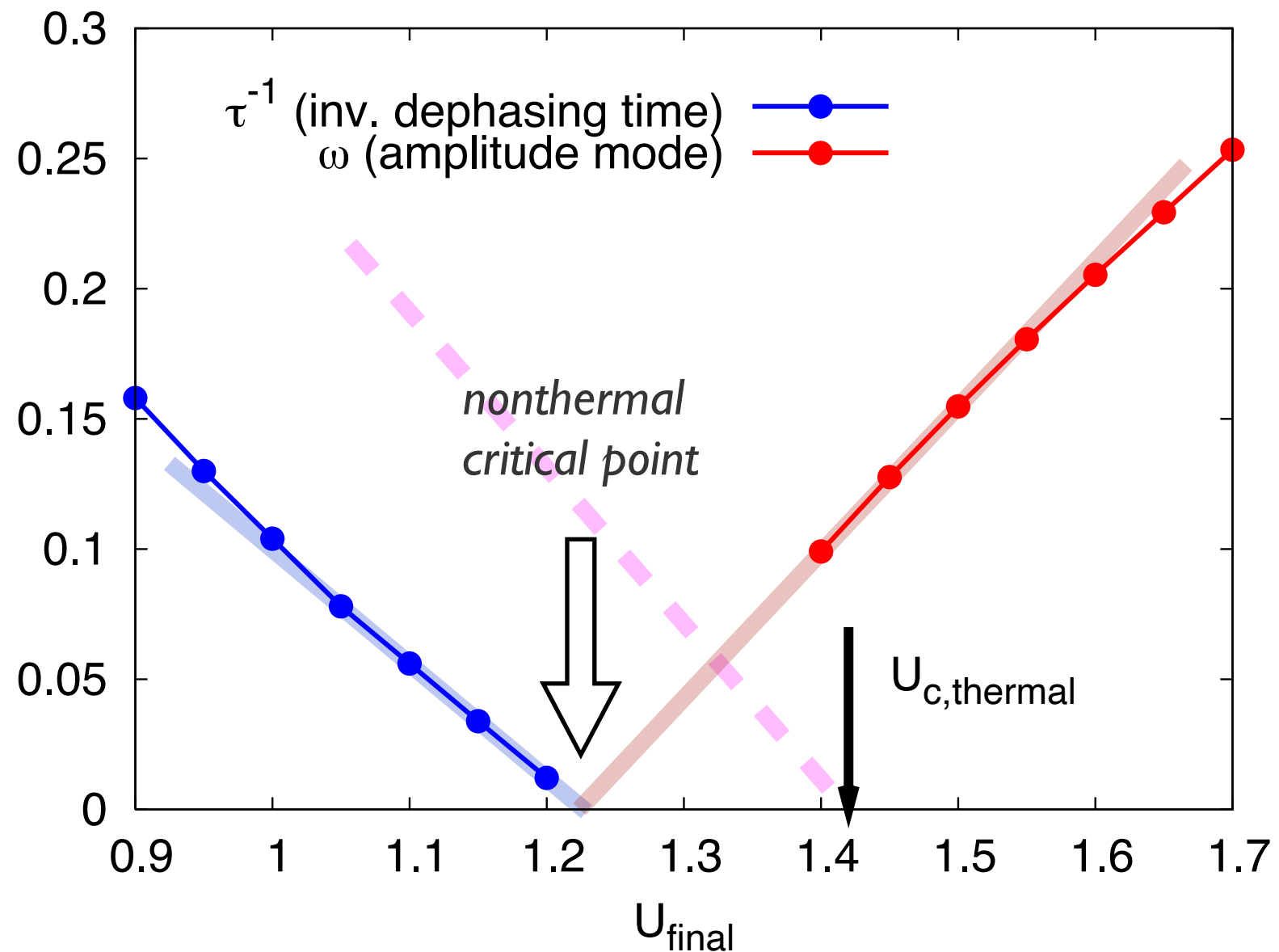
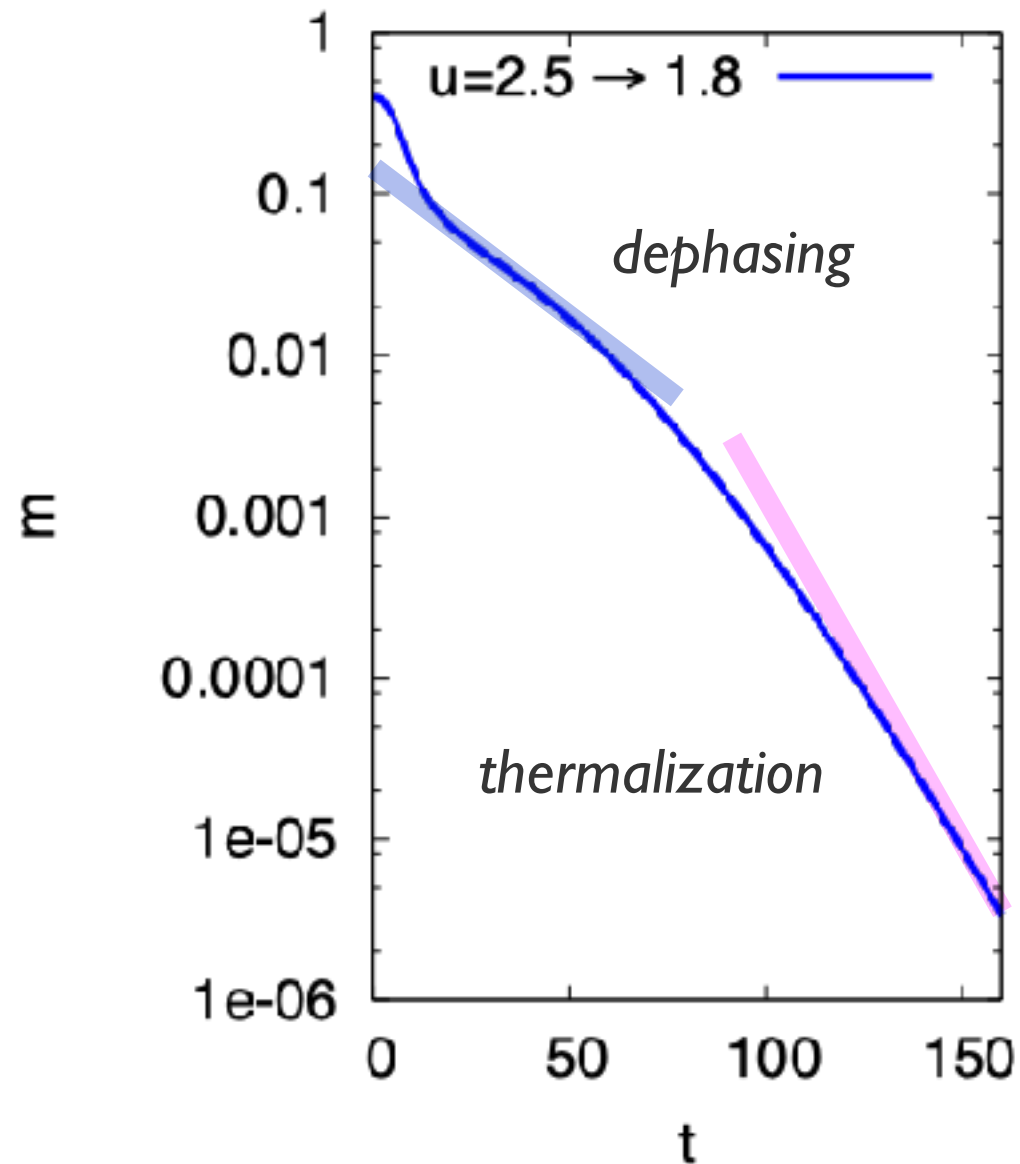


II. Nonthermal symmetry-broken states

- **Weak-coupling regime**

Tsuji, Eckstein & Werner (2012)

- Evidence for a **nonthermal critical point**

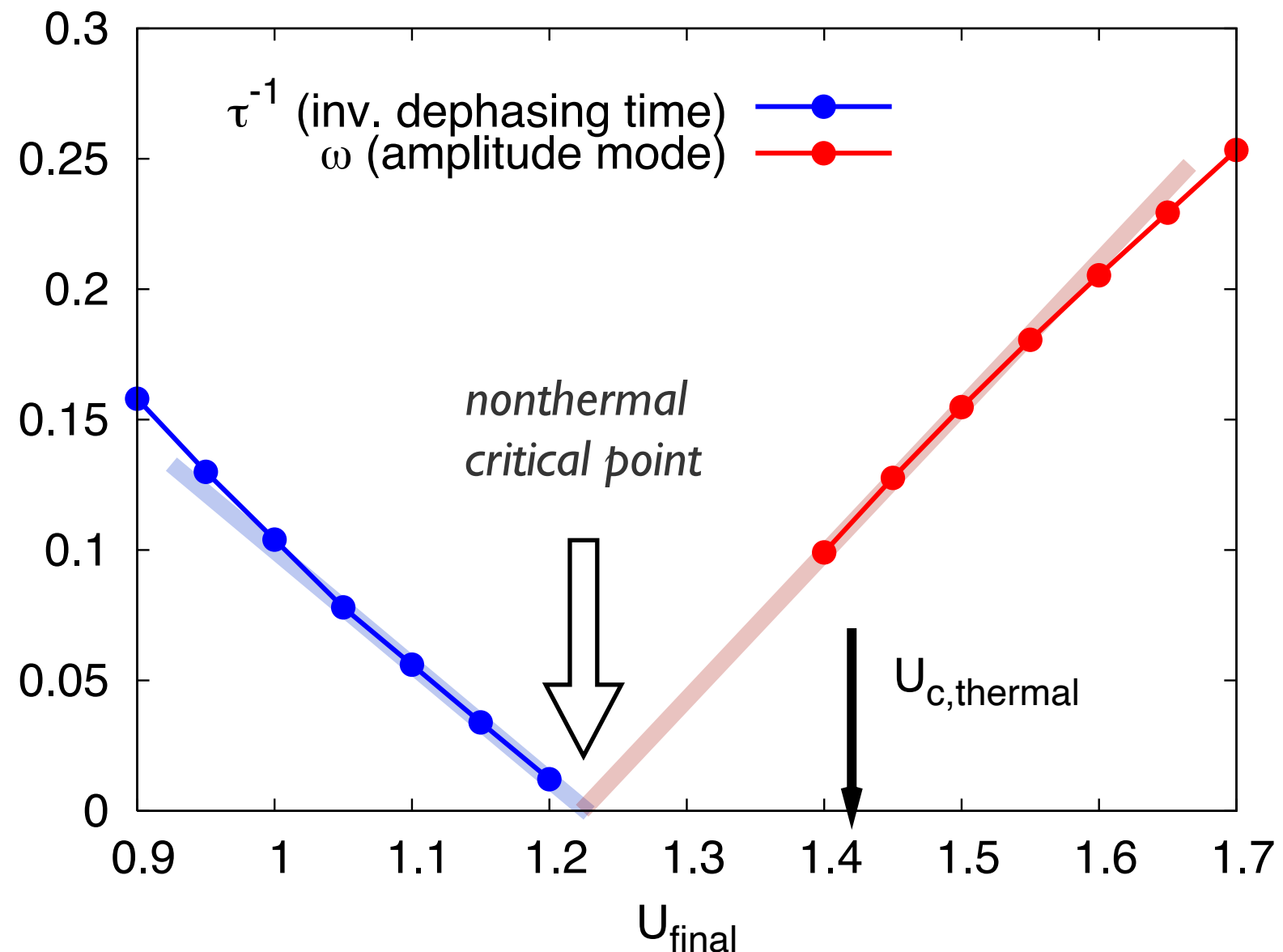
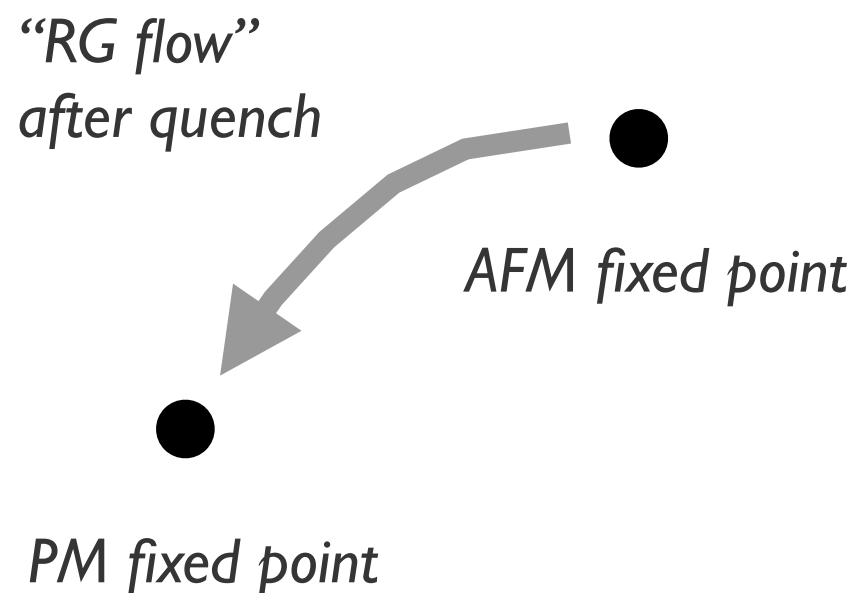


II. Nonthermal symmetry-broken states

- **Weak-coupling regime**

Tsuji, Eckstein & Werner (2012)

- Evidence for a **nonthermal critical point**

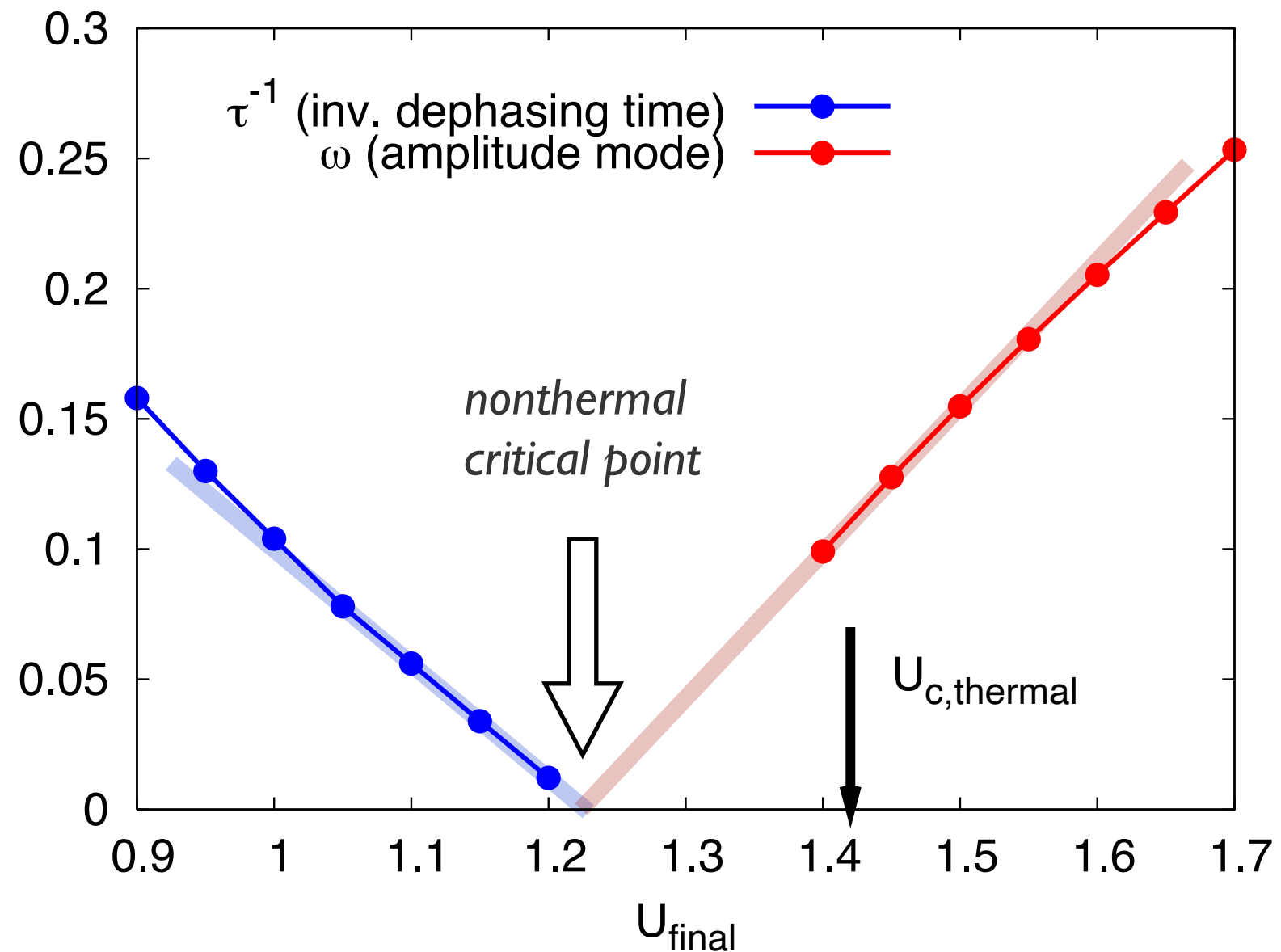
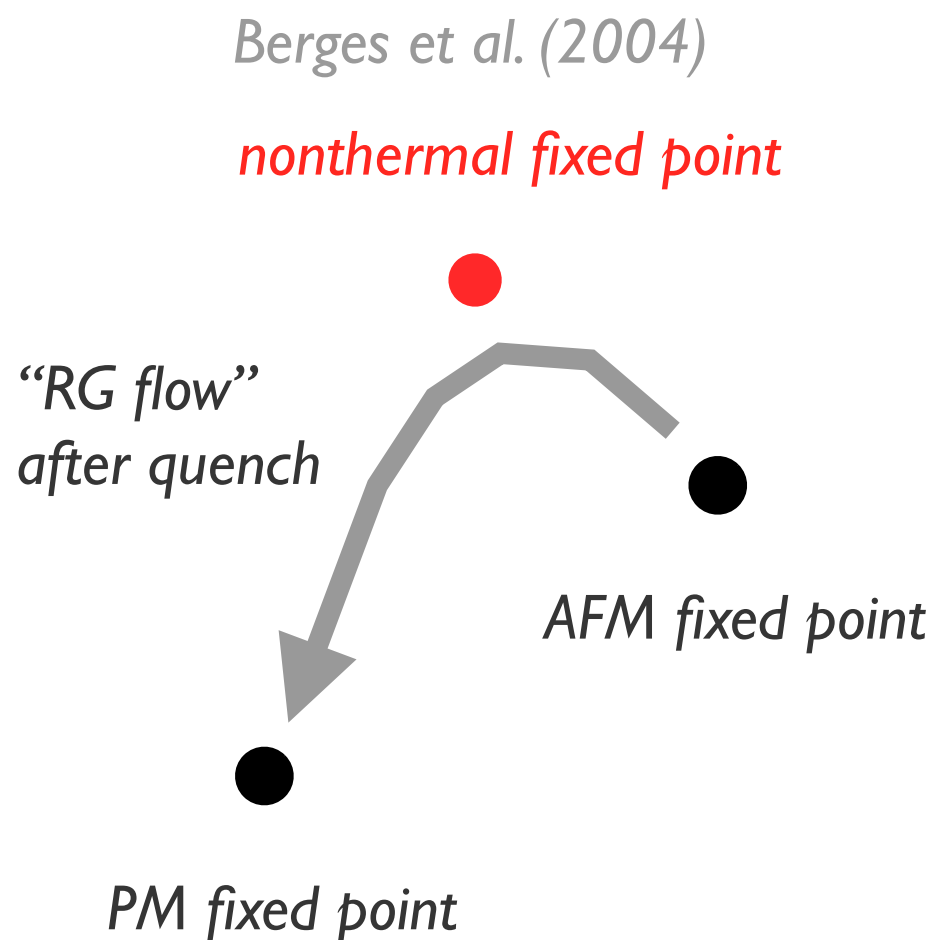


II. Nonthermal symmetry-broken states

- **Weak-coupling regime**

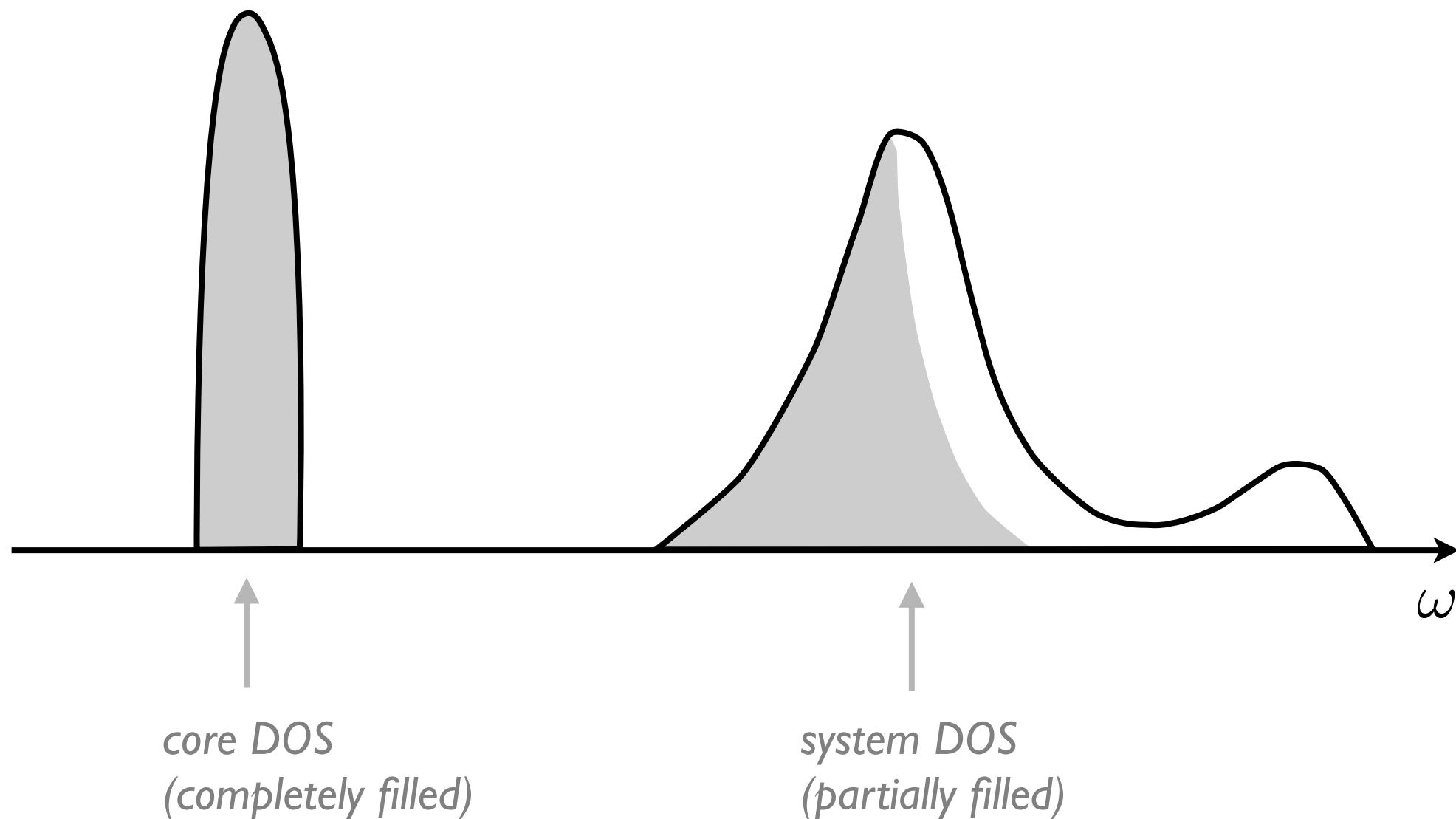
Tsui, Eckstein & Werner (2012)

- Evidence for a **nonthermal critical point**



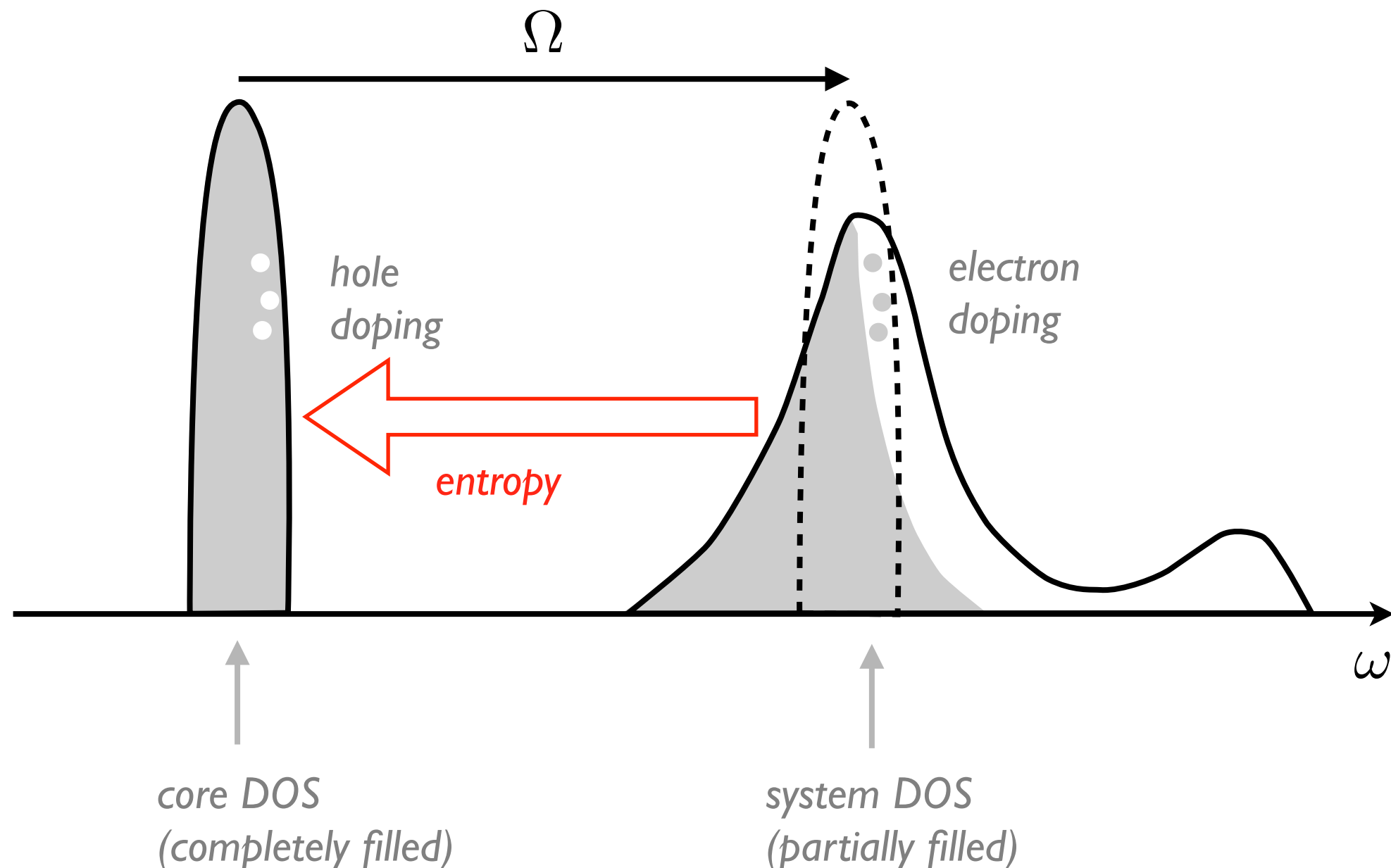
III. Cooling by photo-doping

- **Photo-doping from core levels** *Werner, Eckstein, Mueller & Refael (2019)*
 - Dipolar excitations with appropriate frequency Ω transfer electrons from core to system and **cool down the system**



III. Cooling by photo-doping

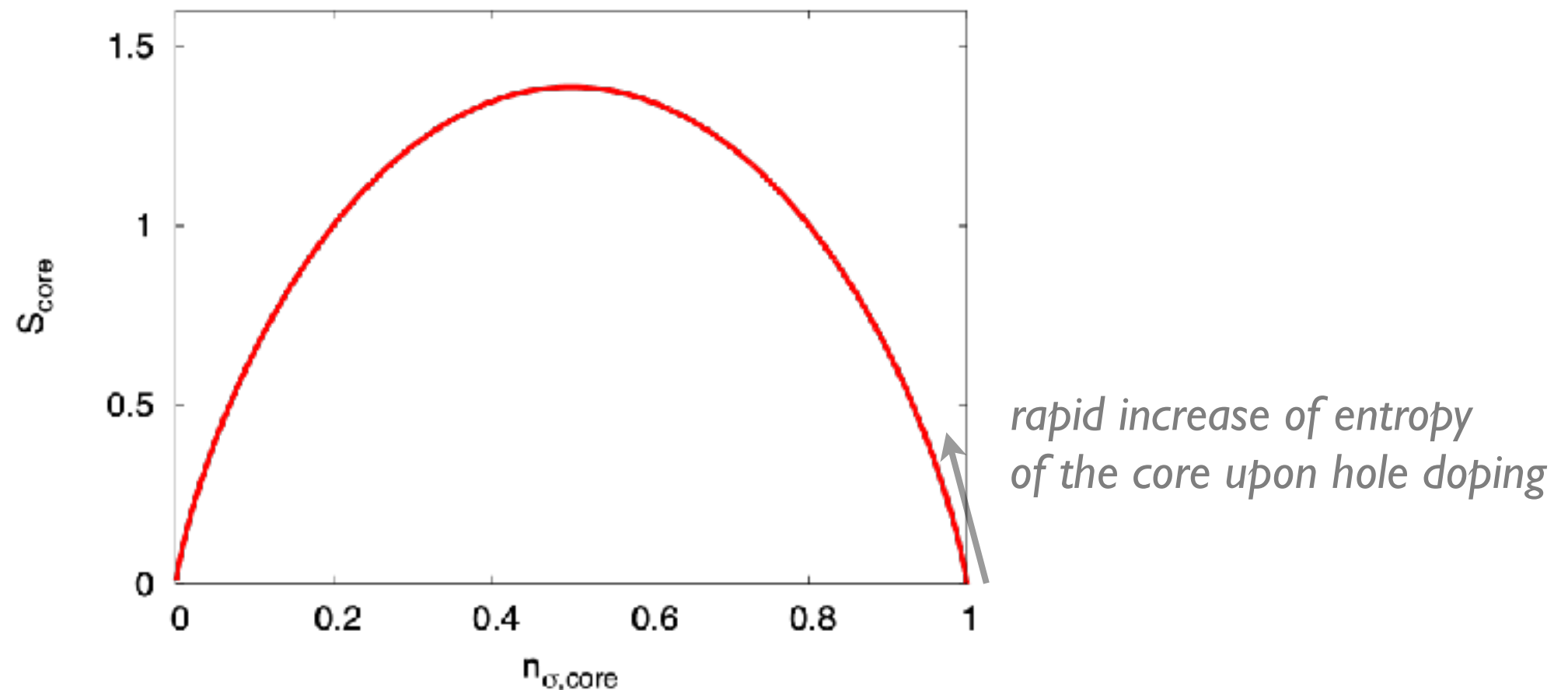
- **Photo-doping from core levels** *Werner, Eckstein, Mueller & Refael (2019)*
 - Dipolar excitations with appropriate frequency Ω transfer electrons from core to system and **cool down the system**



III. Cooling by photo-doping

- **Photo-doping from core levels** *Werner, Eckstein, Mueller & Refael (2019)*
 - Entropy of the core band in the narrow band (atomic) limit:

$$S_{\text{core}} = -2n_{\sigma} \ln(n_{\sigma}) - 2(1 - n_{\sigma}) \ln(1 - n_{\sigma})$$

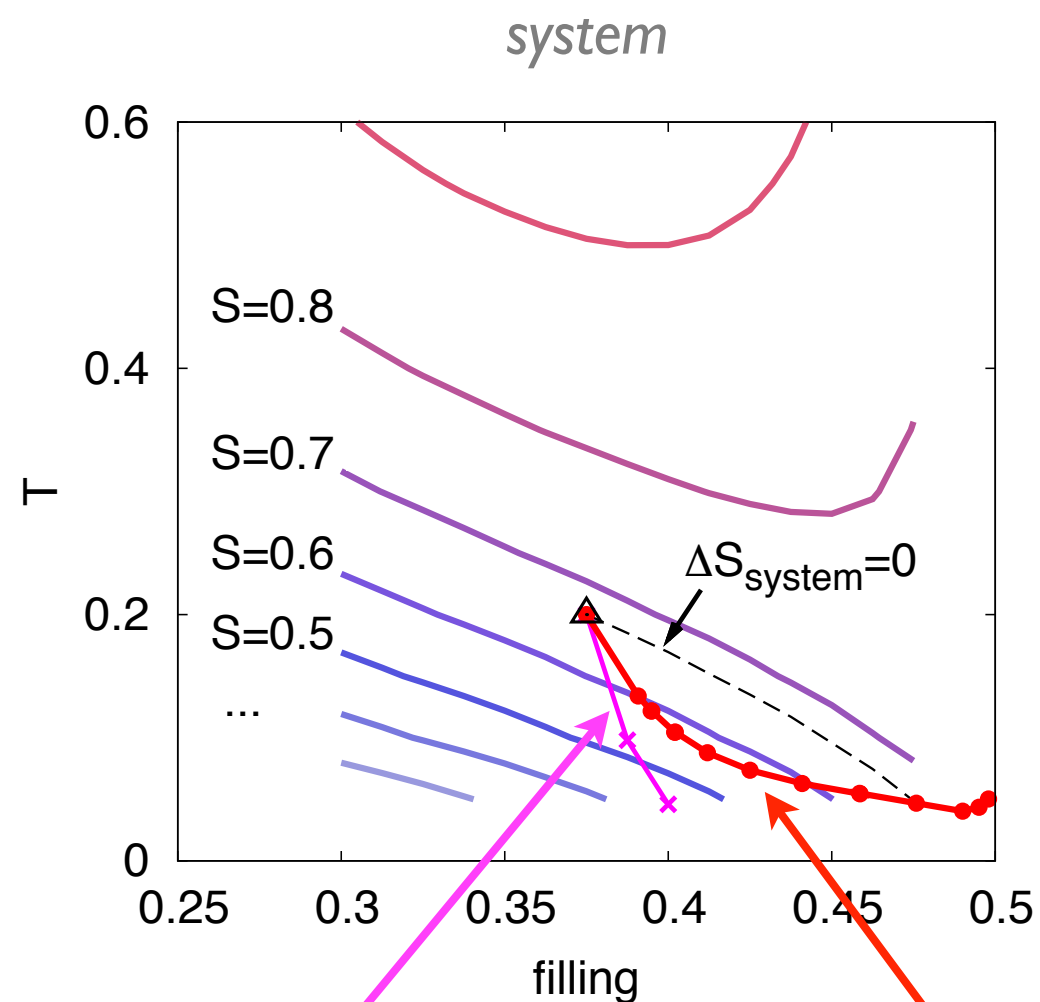


- In case of isentropic doping process:

$$\Delta S_{\text{core}} \nearrow \Rightarrow \Delta S_{\text{system}} \searrow \quad \text{cooling of system due to entropy reshuffling}$$

III. Cooling by photo-doping

- **Photo-doping from core levels** *Werner, Eckstein, Mueller & Refael (2019)*
 - Constant entropy contours in the filling-temperature plane

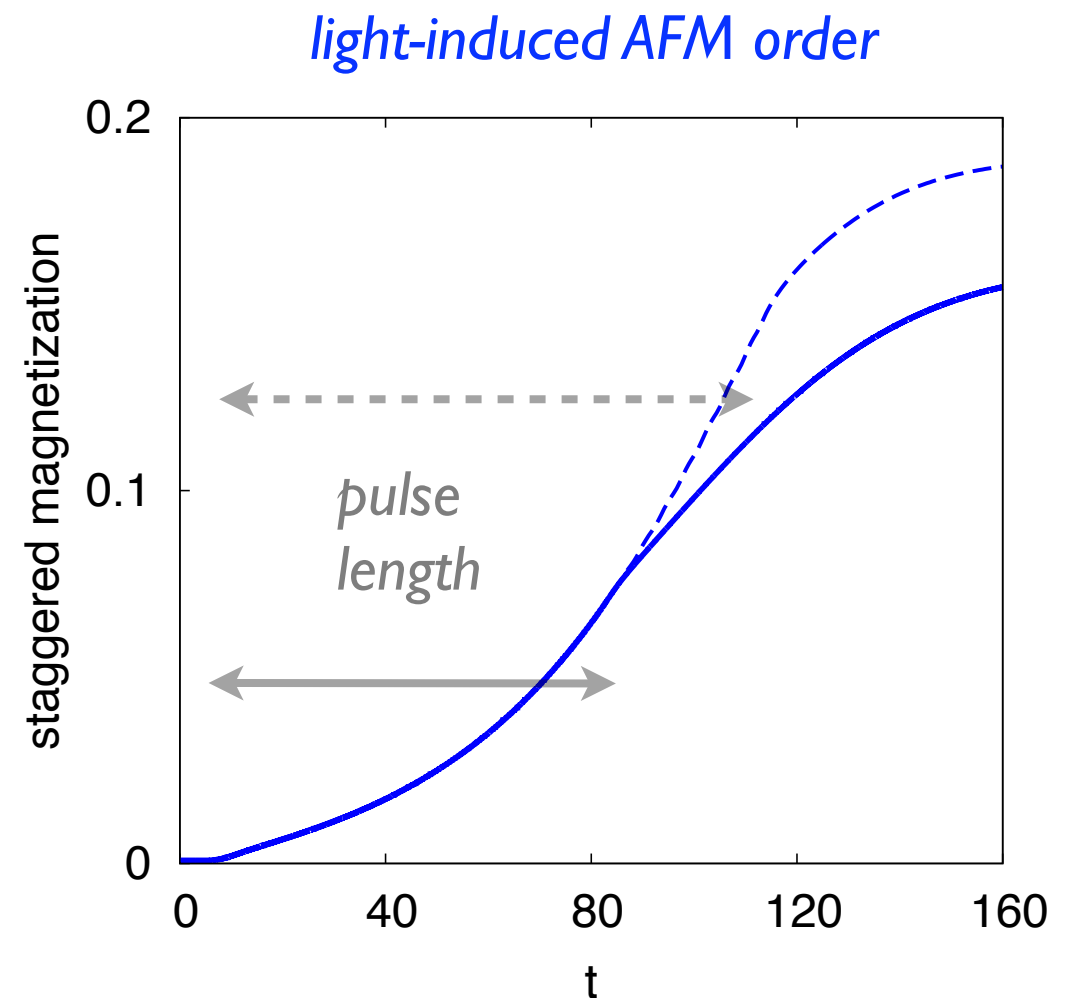
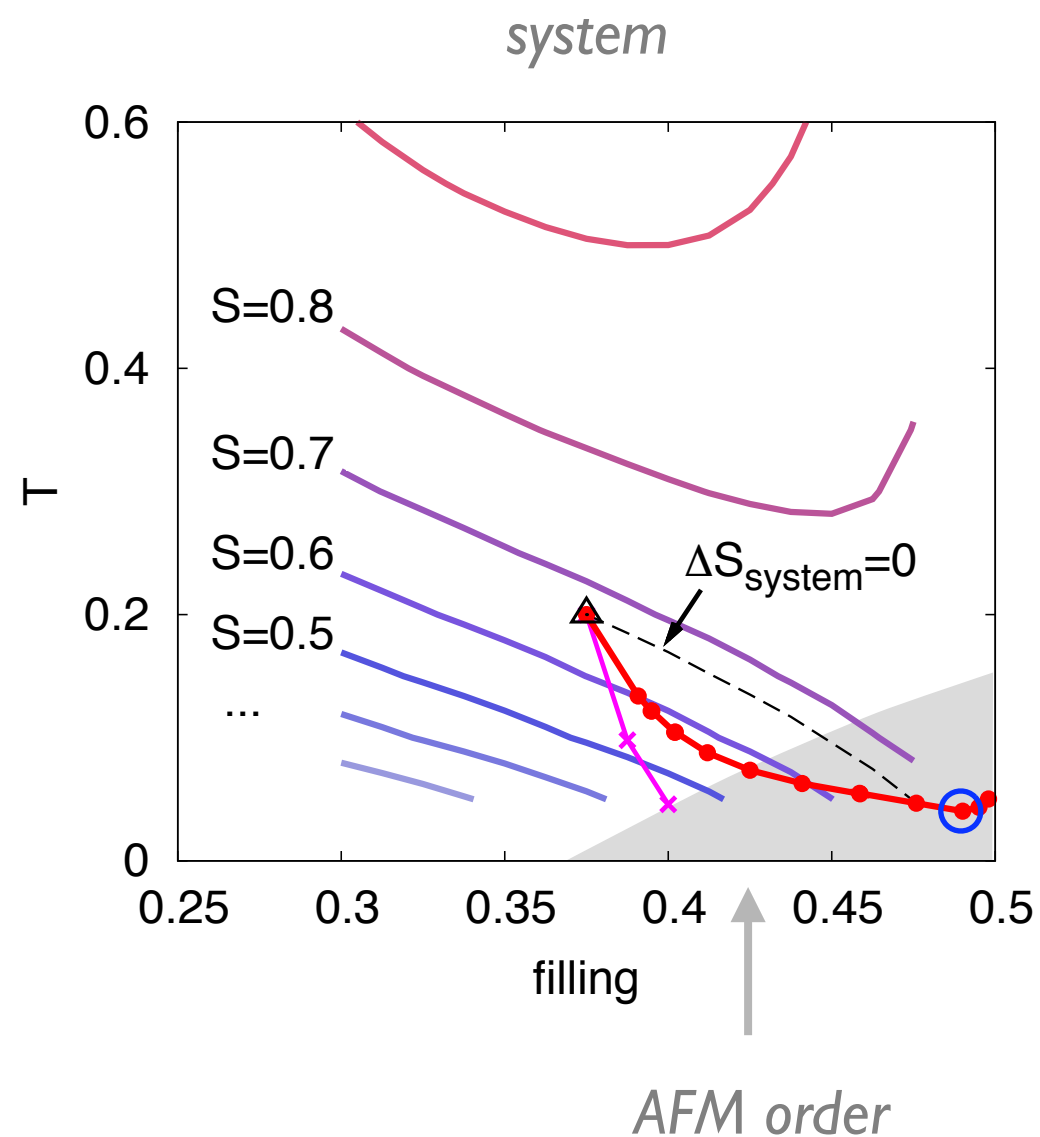


isentropic case

quasi-particle temperature and fillings
realized by chirped pulses

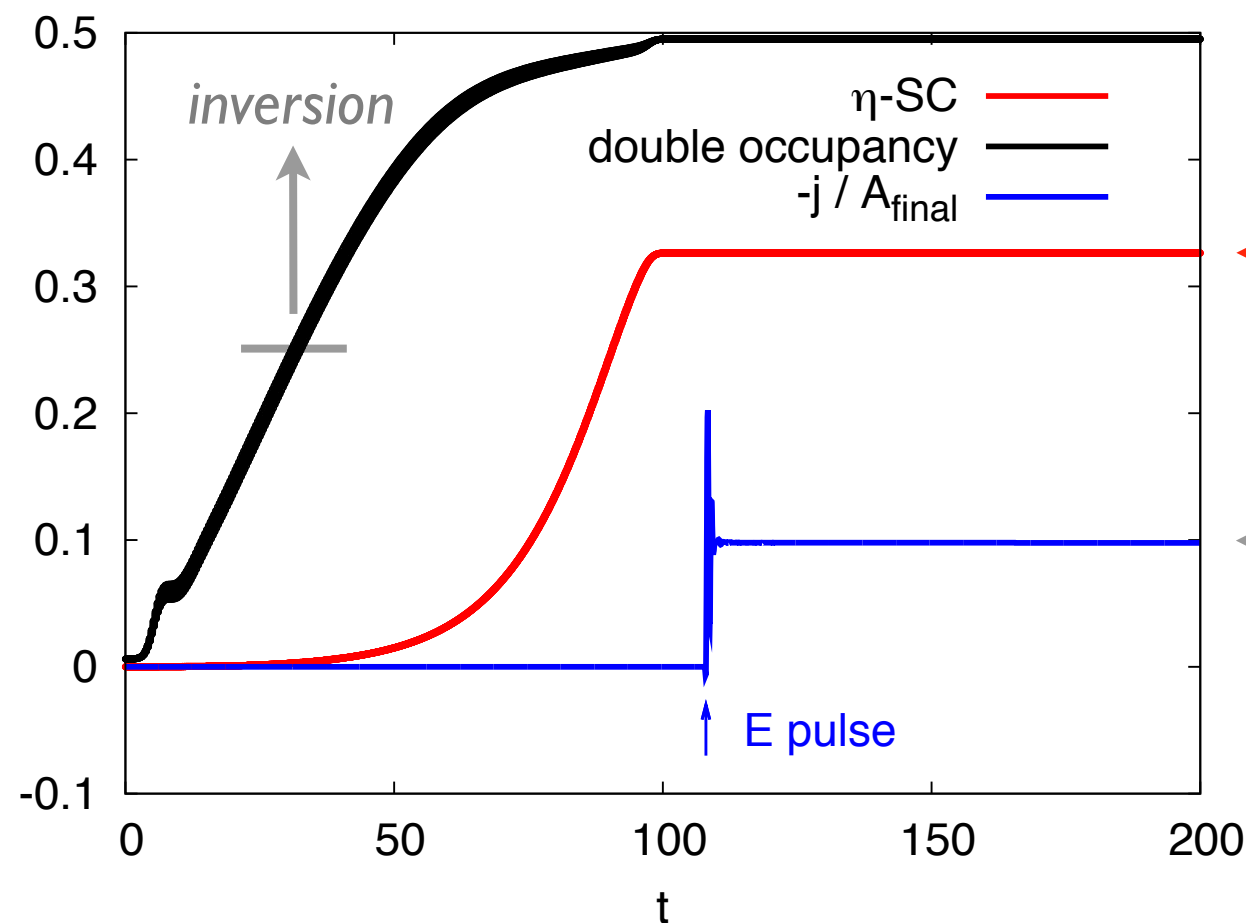
III. Cooling by photo-doping

- **Photo-doping from core levels** *Werner, Eckstein, Mueller & Refael (2019)*
 - Constant entropy contours in the filling-temperature plane



III. Cooling by photo-doping

- **Related example of a nonthermal superconducting state**
 - η -pairing in a repulsive Hubbard model with inverted population
Rosch, Rasch, Binz & Vojta (2008); Kaneko et al. (2019); Werner, Li, Golez & Eckstein (2019)

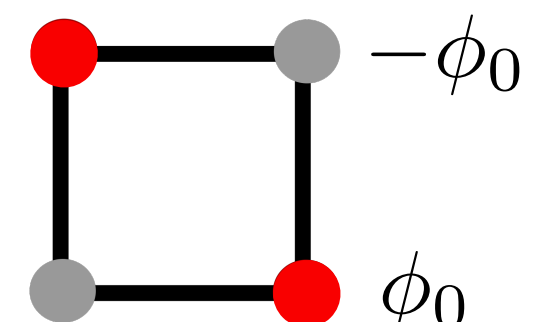
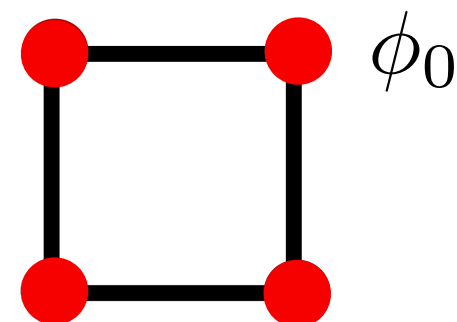


← *light-induced η -pairing*

← *non-decaying current consistent with superconductivity*

uniform pairing

staggered η -pairing



References

- **Dynamical mean field theory of strongly correlated fermion systems and the limit of infinite dimensions**

A. Georges *et al.*, Rev. Mod. Phys. 68, 13 (1996)

- **Nonequilibrium dynamical mean field theory and its applications**

H. Aoki *et al.*, Rev. Mod Phys. 86, 779 (2014)

- Acknowledgments:

Martin Eckstein (Erlangen), **Marcus Kollar** (Augsburg), **Naoto Tsuji** (Tokyo University), **Takashi Oka** (Tokyo University), **Hideo Aoki** (Tsukuba), **Hugo Strand** (Oerebro), **Denis Golez** (Ljubljana), **Yuta Murakami** (RIKEN), **Michael Schueler** (PSI), **Nikolaj Bittner** (Zeiss)